University of Stavanger

Faculty of Science and Technology

MASTER'S THESIS

Study Program/Specialization: MSc Petroleum Engineering/Drilling and Well	Spring semester, 2018 Open
Writer: Steinar Aarnes	Steinar Aarnes (Writer's signature) Mesfin Belayneh (Supervisor's signature)
Faculty supervisors: Mesfin Belayneh Agonafir External Supervisor(s): N/A	
Title of thesis: ***A comprehensive experimental investigation of MWCNTs in oil-well cementing and the development of a new empirical model for UCS estimation***	
Credits (ECTS): 30	
Keywords: Portland Cement Nanotechnology Synthetic Brine MWCNT SiO_2 UCS Tensile Strength UCS Modelling Rheology Heat of Hydration Rubber Silicone Leakage Nanoparticles Bond Strength	Pages: 129 + enclosure: 40 Stavanger, June 2018

Acknowledgements

First and foremost, it is my honor to thank the highly knowledgeable professor, Mesfin Belayneh Agonafir, for his mentoring and counselling of this thesis work. His office doors are always open, and he wholeheartedly invites me to engage in discussions with him from the earliest of mornings to the latest of evenings. His enthusiasm and dedication for his students is beyond measure and is quite invigorating.

Additionally, I want to thank the generous senior engineer, Samdar Kakay for instructing me in the use of the compressive strength testing apparatus in his laboratory, which allowed me to perform destructive tests on my tests specimens. If not for him, the experimental work of this thesis would have been significantly reduced and more theory-based.

I also would like to thank Mona Minde and Wakshum Mekonnen Tucho for assisting me with performing Scanning Electron Microscopy and Energy-dispersive X-ray Spectroscopy analysis of my test specimen.

Gratitude also extend to my friends who contributed to the idea behind this thesis and helped to keep me motivated throughout the semester.

Lastly, I would like to thank my girlfriend whose love and patience has made it possible for me to spend most of my time at school, ensuring that the work required by this thesis reached its satisfactory conclusion.

Preface

This thesis was completed at the Department of Petroleum Technology at the University of Stavanger in accordance with the rules and regulations set by the university, spring 2018.

I hereby declare that all copyrighted information has been properly referenced and cited to the best of my abilities, but should you be a copyright holder and feel in some way that I am violating your rights, please do not hesitate to contact me at aarnes90@gmail.com and I will rectify it at my earliest convenience.

General information considered to be common knowledge or under no one's ownership has not been cited, but sources can still be found in the reference list.

Abstract

Cement is the primary barrier in oil and gas wells and the NORSOK D-010 Standard have very specific requirements for said cement. Amongst others, it states that cement should be impermeable, ductile, strong and resistant to chemically erosive fluids and substances. However, a survey from 2001 states that about 15% of all primary cement jobs fail, [1, p. 14] and data released by the Petroleum Safety Authority (PSA) from the Norwegian Continental Shelf (NCS), in 2006, concluded that at least 11% of the well integrity issues originated from faulty cementing [2, p. 145]. This reveals that the conventional oil-well cement used today does not fulfill the requirements imposed by the NORSOK D-010 Standard. Nanotechnology has seen great developments within academics and applied research over the last decades, enticing the oil companies world-wide due to the viable and cost-effective solutions it offers. Carbon nanotubes, characterized as "the wonder material of the 21st century" [3], are renowned for their exceptional physical properties like its flexibility, strength and thermal conductivity and therefore possess a huge potential in cementitious composites that aims to improve one or more properties of hardened cement. In this thesis, a total of nine test matrices were designed and a number of cement slurries formulated using different water systems and adding varying concentrations of MWCNTs and rubber silicones. It was found that the addition of small amounts of MWCNTs (<0.08wt%) could increase the compressive and tensile strength of cement by 67% and 37% respectively and reduce the heat of hydration by 5% and experienced only 1% leakage after extensive thermal loading. Additionally, it was shown that an increasing concentration of MWCNTs (0-0.26wt%) can reduce the viscosity and shear stress of the cement slurry by 26.7% and 13.3% respectively. Salt water and synthetic brines have also shown promising effects on cement strength when used together with MWCNTs, increasing the UCS of at least 26%. In addition, the new empirical model developed to accurately predict the UCS of cement, shows approximately 90% precision compared to the old model that displayed up to 54% deviances. To further experiment with additives in cement, three rubber silicone elements were used (acid-treated and untreated) as cement replacements, and it was shown that when used in lower concentrations (1.5wt%) the UCS of cement experienced an increase ranging from 22%-40%.

Table of Content

Table of Figures

List of Tables

List of Acronyms

Acronym	Meaning
OPC	Ordinary Portland Cement
SW	Sea Water
DIW	De-ionized Water
SYW	Synthetic Water (brine)
SSW	Single-salt Synthetic Water
HOH	Heat of Hydration
UCS	Uniaxial Compressive Strength
WAG	Water Alternating Gas
ROP	Rate of Penetration
UIS	University of Stavanger
BHA	Bottom Hole Assembly
SCP	Sustained Casing Pressure
DEP	Department of Environmental Protection
WOC	Wait on Cement
ASV	Annular Safety Valve
PSA	Petroleum Safety Authority
NCS	Norwegian Continental Shelf
P&A	Plug & Abandonment
MWCNT	Multi Walled Carbon Nanotubes
DHSV	Downhole Safety Valve
GLV	Gas Lift Valve
ASV	Annular Safety Valve
TRSV	Tubing-Retrievable Safety Valve
WI	Well Integrity
Wt%	Weight % of Cement Content
SEM	Scanning Electron Microscopy
EDS	Energy Dispersive X-ray Spectroscopy

1 Introduction

This MSc thesis presents two main parts, namely experimental investigation and review of the literature. The experimental study investigates the effect of the addition of MWCNTs (mainly) and SiO_2 in cement treated with a new synthetic brine system, seawater, freshwater and single salt brines, with the objective of enhancing the performance of Ordinary Portland Cement (OPC) and thus improving well integrity. Moreover, the effect of acid-treated and untreated rubber on cement are also investigated. The slurry systems have been characterized through non-destructive (Sonic, heat development, deboning/leakage) and destructive (Uniaxial compressive strength, Tensile strength) methods. The modeling part deals with the development of a new uniaxial compressive strength (UCS)-compressional wave velocity (V_p) based empirical model. The literature review base itself on providing the reader and author with background knowledge of nanotechnology applied in the oil industry.

1.1 Background

Cementing is an integral part of the well construction process. Amongst many others, the main functions of the primary cementing job are: (1) seal the annular spacing to prevent the borehole from caving in and causing a collapse; (2) provide a good structural integrity of the casing; (3) provide zonal isolation in order to prevent any migration of gas or fluids between the zones and thus maintain pressure control. It also provides a seal for thief zones and protects the casing from corrosion and shock loads from deeper drilling [4]. The secondary cementing job is mainly used as remedial cementing of any defects associated with a poor primary cement job or the plug and abandonment (P&A) of wells. **Figure 1-1a** shows a completed well, which illustrates the cement placement in a well.

After many years of production, once a well is not producing in a profitable manner, the final fate of the well is to be plugged and abandoned. Moreover, due to a poor cementing job, fluid communication with casing may result in corrosion. This, as result, produces uncontrolled leaks to the surface. If cement-remedial action does not handle the undesired leakage, the well will be plugged and abandoned. For these operations, cement is the key element as illustrated in **figure 1-1b.**

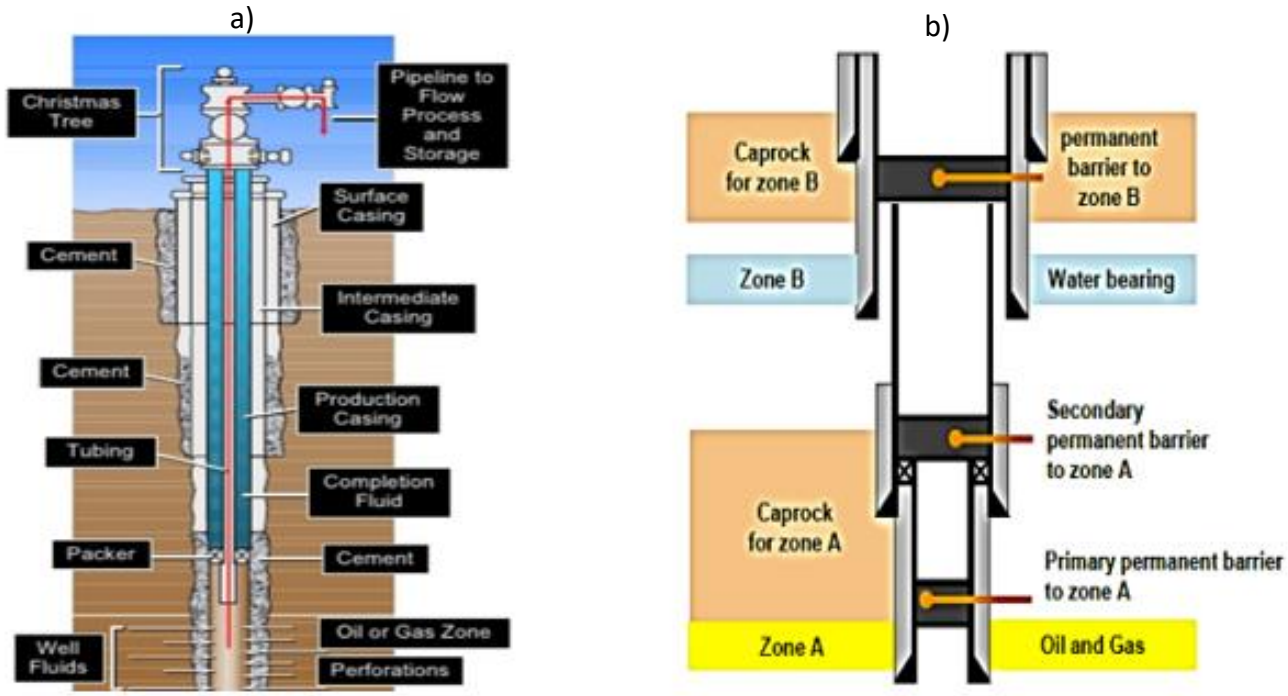

Figure 1-1: a) *A* completed well [1] and b) an illustration of a plugged well

However, properly designed cement slurry and cement jobs are a key factor for a long-term well integrity. Cement in general, as shown in the **figure 1-1a**, experiences several dynamic loadings during its life cycle, such as:

- Pressure decrease, as the natural pressure in the reservoir is reduced due to depletion
- Casing movement because of subsidence
- Fluctuations in pressure and temperature
- Gradual shrinkage over time

Some consequences of such loadings can result in cracking or de-bonding, which will lower the integrity of the well**.** The term “de-bonding” is used to describe the case when cement-rock or pipe-cement interface fails. This can be due to different reasons, one of them being subsidence, which a good cement job would be able to withstand, whereas a poor job would likely collapse along with the casing, as illustrated in **figure 1-2a.** This condition will create fractures (micro-annuli) in the cement [1, p. 14], illustrated in **figure 1-2b** for a P&A scenario, with a cement plug in place (but the same goes for primary cementing). The figure shows six

possible leak paths, which all depends on the quality of the cement. The leak paths are along an existing well: (a, b) between cement and casing; (c) through the cement; (d) through the casing; (e) through fractures; (f) between cement and formation [5].

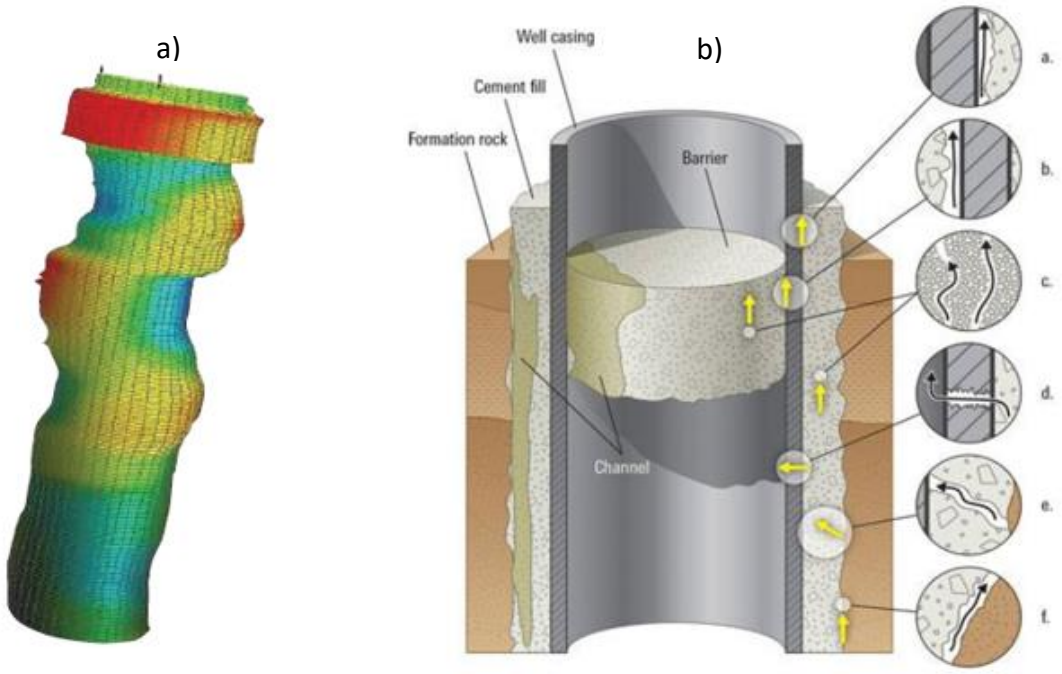

Figure 1-2: a) Formation movement causing casing damage where the cementing was poor *[1]* and b) possible leak paths through cement *[5]*

According to NORSOK D-10, the well integrity issue deals with the application of three solutions (technical, operational and organizational) in order to reduce the risk of uncontrollable leakage during the life of a well [6, p. 4].

Moreover, NORSOK D-010, Rev.4 clearly states the cement should [6, p. 63]:

- Be non-shrinking
- Have a very low permeability or impermeable
- Provide long-term durability with downhole conditions
- Be able to withstand mechanical loads/impact (ductile or non-brittle)
- Be chemically resistant to downhole fluids and gases (H_2S, CO_2)
- Have good bonding to casing or formation

However, well integrity surveys performed around the world has documented that failure in conventional cement integrity is one of the constituents of major well integrity failure. In general, reduced well integrity is likely to be associated with high remedial costs, or even worse, costs of human lives and a severe impact on the environment and wildlife. A survey from 2001 states that about 15% of all primary cement jobs fail, and that the subsequent costs associated to remedial actions amounts to roughly USD 450 million, annually. **Figure 1-3** shows the percentage of wells that experienced shut-in casing pressure (SCP) versus age in the U.S. Gulf of Mexico. By the time of this study, there were 22 000 wells in the U.S. Gulf of Mexico which means that between 8000 and 11 000 wells experienced SCP. [1, p. 14]. Sustained casing pressure, or shut-in casing pressure, is the term the industry utilizes when there is a registered build-up of pressure after first being bled down. This means that the cement integrity is not satisfactory, as it is highly likely (if not always the case) that there is a leak through the poor cement bond between the casing and formation (or the cement itself). The detection of SCP triggers the need for well intervention operations and consequent shut-in(s), losing revenue in the form of reduced production time as well as expenditures related to the intervention operations [7, p. 131].

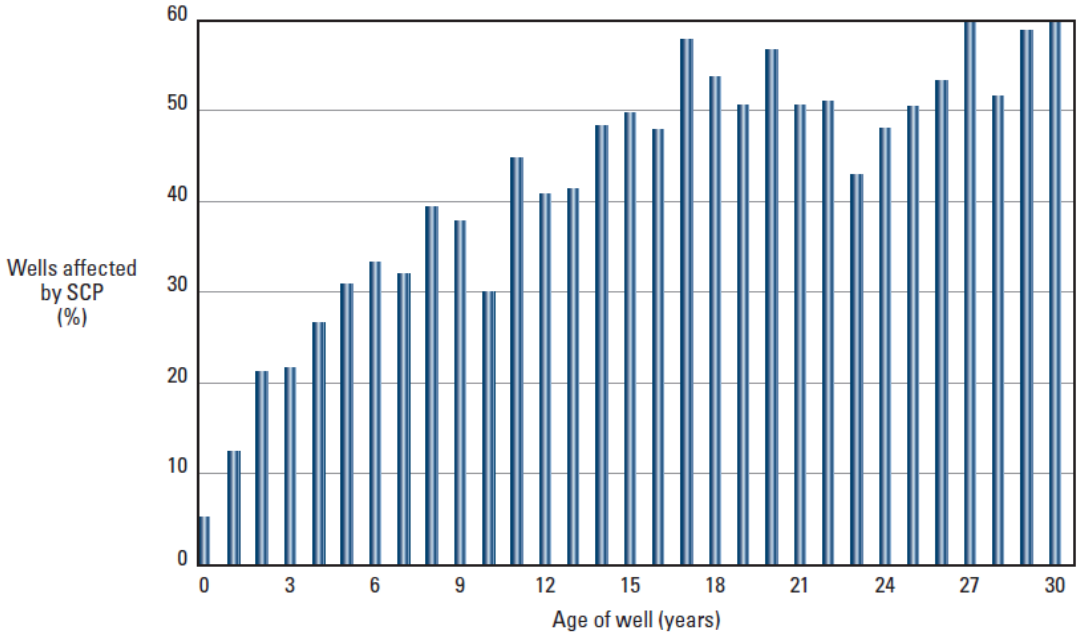

Figure 1-3: SCP vs. age in wells U.S. Gulf of Mexico *[1, p. 13]*

A similar study of well integrity field reports was carried out on the Norwegian Continental Shelf (NCS) in 2006, by the Petroleum Safety Authority (PSA) [2, p. 145]. The study was based on four-hundred and six production and injection wells from seven different operators. **Figure 1-4** shows the number of wells along with the barrier element failure type. The integrity study revealed that 75 (18.5%) of those wells exhibited integrity issues. Out of the 75 wells, 29 (38.6%) of wells reported integrity troubles attributed to the tubing, which could be the result of corrosion damages, miscalculation of collapse, burst or tension ratings or general wear and tear throughout its life. The other major integrity issues reported was attributed to the annular safety valve (ASV), casing and cement respectively, 12%, 11% and 11%. [2, p. 147]. The survey report did not mention the reason for each failure. However, one can assume that the troubles related to the cement is likely caused by problems with improper cement jobs or the quality of cement and thus resulted in the leaking of gas/fluid through the cement-filled annulus the primary cement job, and movement of pipe and/or cement, during its life cycle. [1, p. 13].

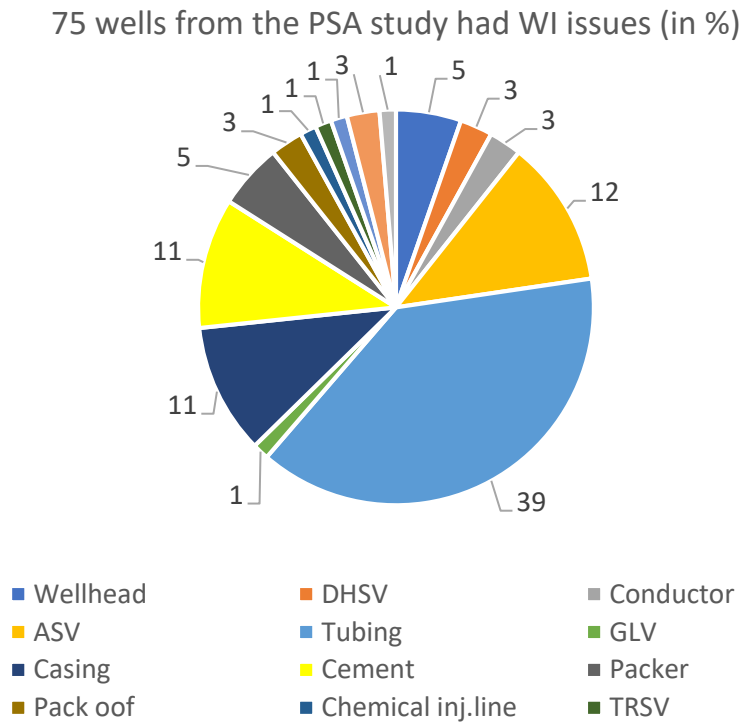

Figure 1-4: The different roots to the well integrity issues in wells in PSA's study on the NCS *[2, p. 147]*(Aarnes2018)

Another data collation was performed by the Department of Environmental Protection (DEP) in the U.S. state of Pennsylvania, where they collected data from 3533 individual wells monitored between 2008 and 2011, where it became apparent that there were 85 examples of cement or casing failure. That is roughly 3% of the total numbers of wells with integrity issues, with 2.41% being cement or casing failure [8, p. 243].

To summarize; these cases strongly advocate the need for a more optimal cement slurry formulation as there is a growing concern regarding economic and environmental ramifications of cement sheath integrity failures. Although some of the cases are likely affected by random course of events and poor execution of procedures, one can, however, argue that there is likely a fault within the standard cement formulation utilized today.

1.2 Problem Statement

Recently, the application of nanotechnology has improved performances in the oil and gas industry. It is believed that nanotechnology can solve several engineering problems in a more efficient and cost-efficient manner compared to conventional technology mostly utilized today.

In literature, the multiwalled carbon nanotubes (MWCNTs) already has a documented effect on the compressive strength of cement. However, those case studies are limited to cement treated with simply one water system and are also limited by focusing solely on strength development of the concrete, without considering the effect it might have on other major factors such as **heat development, elasticity**, **rheology**, **leakage** and **bonding**. With this in mind, the main objective in this thesis is to perform a comprehensive experimental study of MWCNTs in cement treated with various water systems that fulfill the NORSOK D10 cement requirements and will address issues such as:

- What are the effect of salt water and MWCNTs on properties of cement?
- What is the significance of varying concentrations of MWCNTs in cement?
- How does MWCNTs perform in a MWCNT-SiO_2-composite compared to the single effect of MWCNT or SiO_2?
- Will the addition of MWCNTs increase or reduce the heat of hydration?
- Does the addition of MWCNTs in cement make it more or less prone to leaking?
- Are rubber-additives more effective than MWCNTs in terms of mechanical properties of cement?
- Does rubber replacement of cement make it more or less prone to leaking?
- Does it help treating the surfaces of the rubber elements with acid with regards to cement properties?
- Does the addition of MWCNTs affect the rheological properties of cement slurry in a negative way?

1.2.1 Specific Objectives

1. Literature Review of…

- Portland cement in general
- Hydration process of cement
- Applications of cement in the petroleum industry
- The nanoparticles; SiO_2 and MWCNT
- Nanomaterials in oil-well applications

2. To test the effect of MWCNTs on...

Destructive:

- Uniaxial compressive strength of cement treated with: (1) multi-salt synthetic brine (SYW); (2) single-salt synthetic brines (SSW); (3) seawater (SW) and freshwater (FW) (4)
- Splitting tensile strength of cement
- Leakage after excessive heating and rapid cooling of cased cement

Non-destructive:

- Development of the elasticity modulus (M) in cement
- Heat of Hydration (HOH) from cement
- Permeability and pore structure through observation of FW absorption
- SiO_2 and MWCNT nanocomposite on the development of the UCS
- Rheology of cement slurry
- Modelling to correlate empirical UCS with destructive UCS

3. To test the effect of Silicone rubber on...

Destructive:

- Uniaxial compressive strength of cement
- Leakage after excessive heating and rapid cooling of cased cement

Non-destructive:

- Development of the elasticity modulus (M) in cement
- Permeability and pore structure through observation of FW absorption

1.3 Research methods and thesis layout

Figure 1-5 provides an overview of the theoretical work that will be done in this thesis while **figure 1-6** illustrates an overview of the experimental work plan.

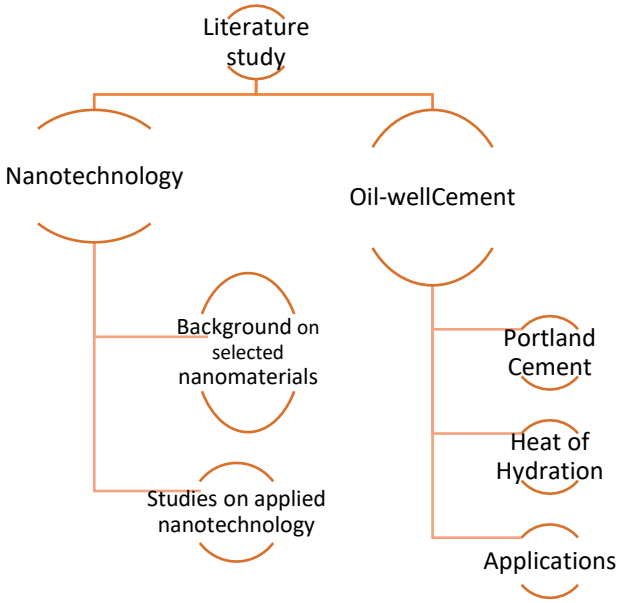

Figure 1-5: Scope of theoretical work

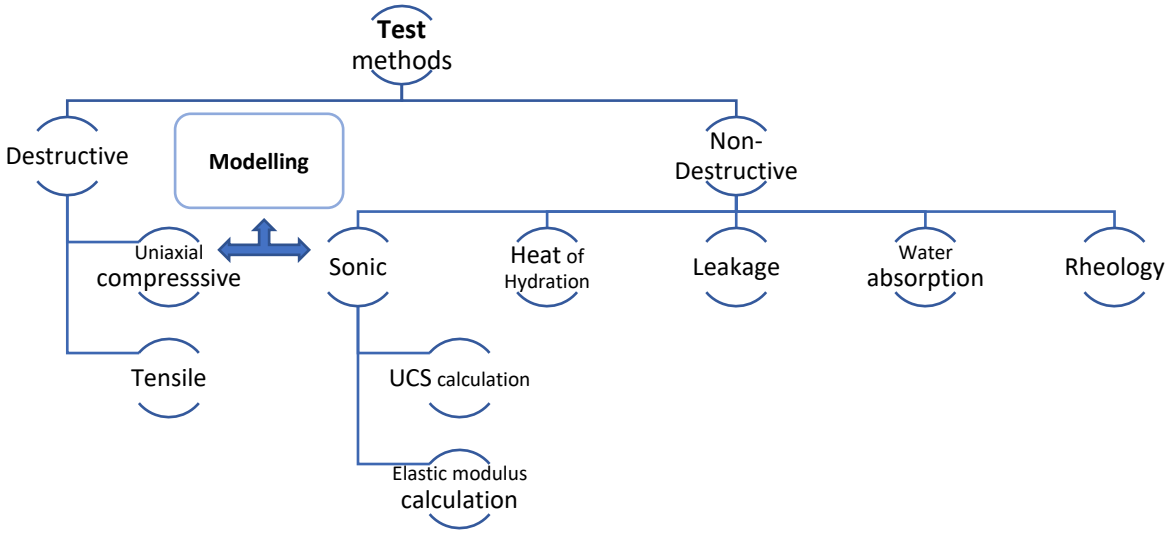

Figure 1-6: Scope of experimental work

2 Literature study

The following chapter presents a literature review of nanotechnology, some applications in the petroleum industry and a description of the nanoparticles selected for use in this thesis' work. Chapter 2.2 is a review of cement, some significant properties, its manufacturing and two of the most important applications in the oil & gas industry.

2.1 Nanotechnology

A nanomaterial is defined as a material with one of its dimensions being less than 100nm ($x10^{-9}$m. One-billionth of a meter). **Figure 2-1a** shows a larger bulk material compared with the much smaller nanoparticles. Nano-sized materials can be prepared by using a method referred to as "top-down" (1) or "bottom-up" (2). (1) Is a mechanical crushing of a solid material into fine grains using a milling process (e. g., hand grinding, ball milling, etc.) whilst (2) on the other hand is a chemical process which involves synthesizing nanoparticles based on physiochemical principles of atomic self-organization [9]. Basically, this translates into; allowing molecules to form novel particles through chemical processes (e. g., chemical vapor deposition, plasma arcing, sol-gel synthesis and electrodeposition). The surface area to volume ratio of nanoparticles are significantly higher than that of microparticles illustrated in **figure 2-1b**. Due to the ultra-small size and high surface area to volume ratio, nanomaterials create materials with a more satisfactory degree of chemical and physical properties compared to its micron-sized (or larger) particles of the same material [10, p. 1].

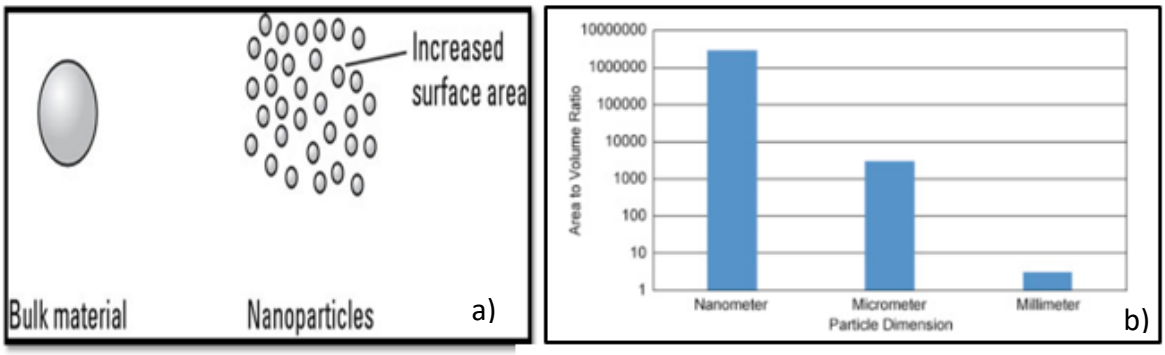

Figure 2-1: a) Increased surface area of nanomaterials compared to bulk materials [11, p. 2] *and b) graphical illustration of nano-sized particles' advantages over other sized materials; Area to Volume Ratio* [12, p. 392]

Many elements and compounds have been successfully produced in a nano-sized scale: metals (e.g. iron, copper, gold, aluminum, etc.), metal oxides (e.g. iron oxide, aluminum oxide, zinc oxide, etc.) and carbon compounds (e.g. fullerene, nanotubes, carbon fibers, etc.), to name some [13]. An important factor in the world of advanced nanomaterials is the cost and availability of the desired product, however, due to the benefits they offer, the cost is often neglected since nanomaterials can succeed where conventional materials do not. Usually, nanoparticles are expensive; so, it will be cost beneficial to use the lowest nanoparticles concentration possible while still achieving an acceptable level of desired performance [12, p. 391]. Nanotechnology have also gained a large momentum within in modern science over the last decade, in both academics and applied research with its demonstrated good results in several industries, for example electronics and biomedicine, and will continue to do so in the future. Because the world continues to see an increase in global energy consumption and a fast-growing demand for fossil fuels as the main source of energy, one can expect a steady improvement of nano-technical solutions. Research results have also shown that nanotechnology entices the oil companies due to their major role in the improvement of many petroleum disciplines, as **figure 2-2** illustrates.

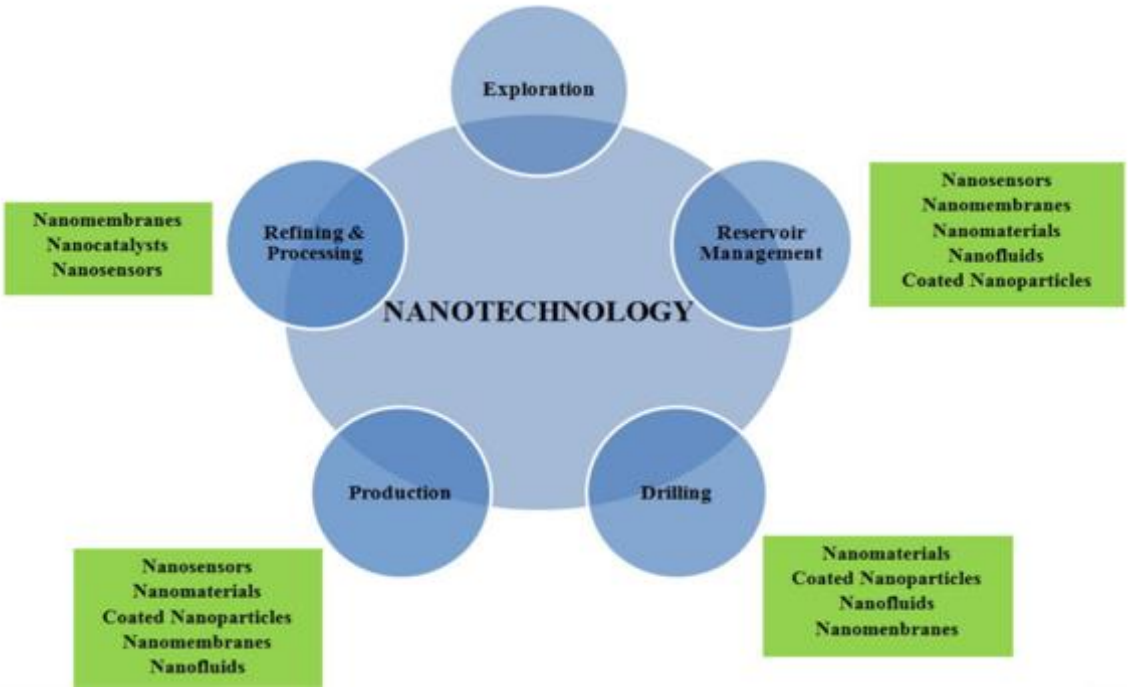

Figure 2-2: Illustration of which disciplines nanotechnology is applied to *[14, p. 288]*

2.1.1 Description of Nanomaterials

This section contains only the descriptions of nanomaterials applied in the experimental parts of this thesis, MWCNT and SiO_2.

2.1.1.1 Carbon Nanotubes

Carbon Nano Tube (CNT) is a cylindrical molecule composed of carbon atoms and has hexagonal patterns that repeat itself periodically in space. CNT is a fiber is much stronger than other conventional fibers. Thus, this material may improve the mechanical properties of cement slurry and is as such used as a highly acclaimed reinforcing material with distinct advantages over many other fibers. The measured tensile strength of a single layer can be as high as 100 times that of steel, with the same diameter [15, p. 100]. CNTs are produced in three common forms: **SWCNT** (single-walled), **MWCNT** (multiwalled) and **DWCNT** (double-walled). Based on the nature of their applications and characteristics (length, diameter, number of walls, density, etc.) they all have their own advantages and disadvantages.

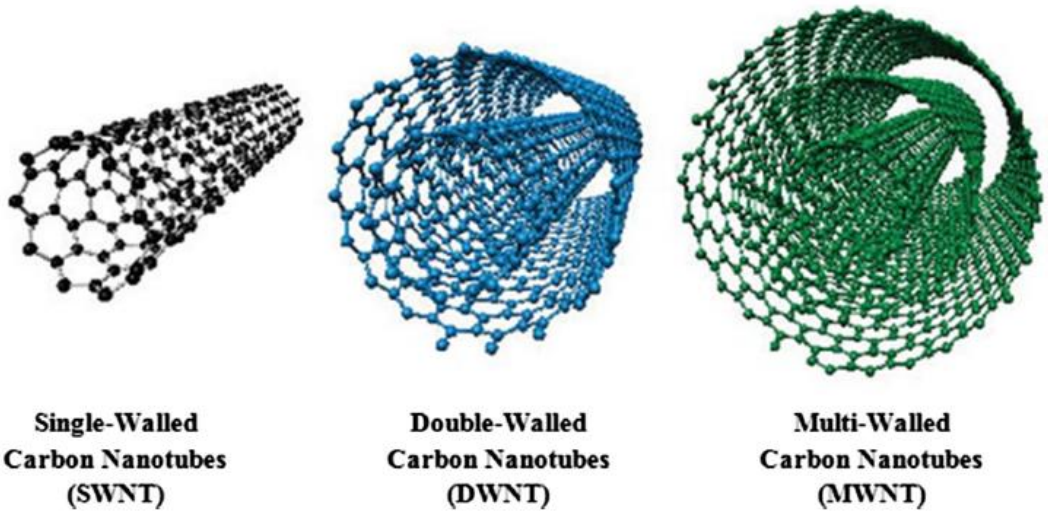

Figure 2-3: Three most common types of structure for carbon nanotubes *[14, p. 292]*

Due to CNTs extraordinary thermal conductivity, mechanical and electrical properties, CNTs are applied in many disciplines and fields of material science (e. g., nanotechnology, electronics and optics) in addition to being added in structural materials (e. g., car parts or golf clubs) for its high tensile strength. Due to these unique physical, chemical and electrical properties, the petroleum industry has also applied it to suit their needs.

Examples of petroleum applications are: CNTs as; emulsion/foam stabilizer in EOR, contrast agent in rock matrix, composite cables and electronics for the extreme conditions of an ultra-deep-water field, wettability alteration agent, cement reinforcement, oil spilled remediation and additive in drilling fluid [14, p. 291].

In this thesis' work, the effect of MWCNT on cement is investigated. **Figure 2-4** presents a SEM picture of MWNT particles and **figure 2-5** as present MWCNT as seen in the laboratory. Section 3.2.3 presents the chemical composition and particle properties of this nanomaterial.

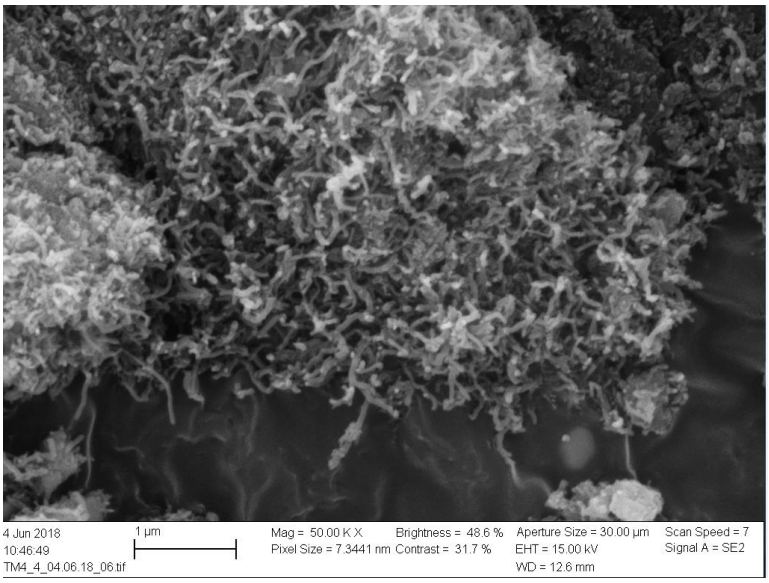

Figure 2-4: A SEM image of MWCNT from TM#4 (Aarnes 2018*)*

Figure 2-5: MWCNT (Aarnes 2018)

2.1.1.2 Nano-Silica

Silica, or silicon dioxide, is a compound of silicon and oxygen with the following chemical formula: SiO_2. It is a very hard substance that is resistant to chemicals and alterations. It exists in abundance in nature and most commonly associated with being one of the major constituents in sand (in certain parts of the world) and is also commonly found in crystalline forms, like quartz and amorphous forms (non-crystalline forms). Unlike MWCNT, silica nanoparticles have a poor thermal conductivity (poor conductor of both electrons and heat) and as such can be used to create temperature resistant equipment [16].

Nano-silica particles are quite small (typically 5-30nm in size) and visually it is a fine white powder and is attributed by researchers to be a very versatile and shapeable material. In the petroleum industry alone, it has several areas of application; some of which are included, but not limited to: oil well cementing (e. g., reduced setting time, increase in compressive and flexural strength, lower permeability and better pore distribution) [17], EOR, fluid dynamics, scale inhibition, corrosion prevention and fluid loss improvement.

In this thesis' work, the performance of nano-SiO_2 has been evaluated only for its effect on cement sheath strength and is tested for single effect and combined effect together with MWCNT. **Figure 2-6** presents a SEM picture and the nanomaterial and **figure 2-7** presents its visage when utilized in the laboratory.

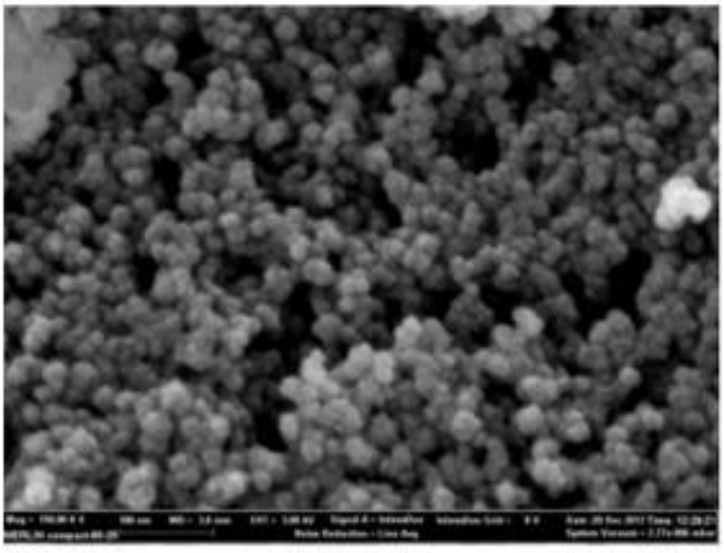

Figure 2-6: A SEM image of nano-SiO_2 *[18]*

Figure 2-7: A picture of the white-powdered nano SiO_2 (Aarnes 2018)

2.1.2 General Areas of Application of Nanotechnology in the field of Petroleum

The application nanotechnology has achieved prodigious effects within the oil and gas industry. For instance, within imaging and measuring tools to help characterize potential fields in oil exploration [19], or development of sophisticated nanosensors that are compatible with the hostile deep well environments for reservoir management [20].

Additionally, using polymeric nanoparticles, oxide nanoparticles, nanosheets and nanoemulsions have progressed the field of the always-popular enhanced oil recovery to a significant extent [21], [22]. Nanoparticles can create an improved and cost-effective EOR process through for example improved wettability alterations, viscosity alterations and sand consolidation [23], [24], [25]. In addition, nanoparticles have a proven effect on drilling fluids, fluid loss, lubrication and tool longevity [10], [26]. Similarly, for common problems such as scale depositions, nanoparticles can reduce the chance of its occurrence [27]. Operations like acid picking, oil well cleaning and descaling are known to cause corrosion to metallic mediums, however, with the aid of nanotechnology this potentially costly problem can be reduced [28].

Nanotechnology has gained a momentum within cementing processes where the goal is to improve its quality (e. g., setting time, compressive and tensile strength), like for instance applying nanotechnology to accelerate hydration and early age strength development of cement, in order to reduce the associated costs of waiting on cement (WOC) [29], [10], potentially saving the industry fortunes. Using nano-spacers formulated from nano-emulsions one can achieve an optimal bond between casing-cement-formation [30], ensuring higher integrity of the cement job. From a cement sheath perspective, some of the issues with concrete in its unaltered form, is that it is quite brittle, display a low tensile strength, produces large exothermic reactions when setting and is a victim to bulk shrinkage which leads to reduced zonal isolation (potential gas migration) thus reducing the concrete's overall quality and uses in the oil and gas industry. The addition of some nanoparticles have proved that the heat conductivity can be reduced [3], tensile and flexural strength of the cement, can be increased [31], [32] and its similar for compressive strength of cement [33], [31], [34], [10], and not to mention controlling fluid loss and preventing gas migration [35], potentially reducing costly remedial operations and poor performance in bottom-hole conditions, poor production capacity, environmental issues, or worse, the loss of the well, like the Macondo accident.

2.1.3 Specific Application of Nanotechnology in Oil-well Cementing

Compiled below are some studies performed by researchers using nanoparticles as additives in cement to achieve certain desirable properties. Such properties can be an increase in cement strength, better cement-steel bond and cement-formation, acceleration of strength development and reduction of WOC (wait on cement).

2.1.3.1 MWCNT on Cement Strength

Gillani et al. (2017) [32] studied the effect of adding MWCNT into cement mortar and expose the concrete specimens to splitting tensile test, flexure and compressive strength tests after 3, 7, 28 and 56 days. The successful dispersion of the MWCNT in the composite matrix is a key element in unlocking the ultimate potential of MWCNT in performance improvement. They used a high energy sonication device to achieve a uniform dispersion

Using ordinary Portland cement (ASTM Type 1, which is classified as a general-purpose Portland cement with a relatively high content of C_3S for early strength development [36]) and crushed lime aggregates conforming to ASTM C33 (which is a standard that specifies requirements for grading and quality of fine and coarse aggregates utilized in concrete [37]), with a fineness modulus of 2.13, specific density of 3.10 and water absorption of 2.87%.

Figure 2-8 present the results they found after 3, 7, 28 and 56 days. Some words of explanation: Modulus of rupture is, in fact, flexural strength.

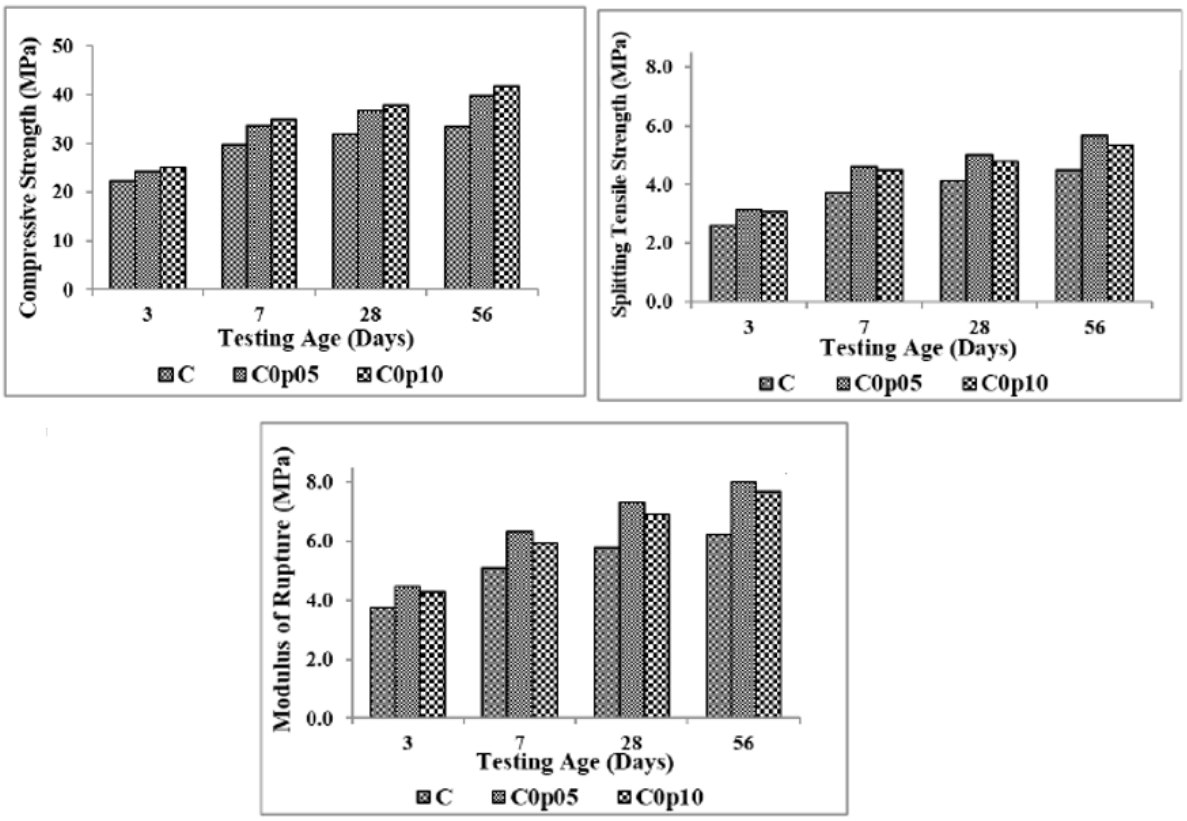

Figure 2-8: Compressive, tensile and flexural strength of the concrete mixes *[32].*

After adding 0.05 wt. % of MWCNT into the cement mortar, they reported an increase in splitting tensile strength by 20.58%, flexural strength by 26.96% and compressive strength by 15.60% after 28 days of curing, when compared with the control mix. In other words, adding even the slightest amount of MWCNT in the concrete cement mix improved the mechanical strengths and behavior to a remarkable extent. An interesting observation is that they concluded that small amounts of MWCNT in the mix could enhance the tensile and flexural

strength whilst a larger fraction of said nanoparticle was more effective in terms of compressive strength.

2.1.3.2 Nano-Silica on Accelerated Strength Development of Cement

Patil et al. (2012) [10] knew that waiting on cement (WOC) translates into substantial potential profit loss and therefore performed experiments on how nano-SiO_2 could be used in cement formulation to obtain high early strength development and how it could enhance final compressive strength and aiding in controlling fluid losses, while keeping a low rheology and good mechanical properties.

Latex, a finer-sized elastomer, is commonly added to cement mortars to help improve challenges with fluid loss and gas migration, but at a cost, as said elastomer can hamper the development of early-stage strength. By adding nano-silica, this problem could be circumvented. The Latex elastomer was a commercial product and had a particle size of roughly 150nm, whilst the nano-silica particle was approximately 5-7nm.

The cement utilized was Premium Class H Cement. All dry additives were mixed with cement and liquid additives with water (Latex dispersed in water). The cement blend was added to the fluid system which contained Latex, water and Nano-silica to create the slurry. The tests were performed at a relatively high temperature of 88 °C.

TABLE 1—EFFECT OF NANOSILICA ON COMPRESSIVE STRENGTH[a]

Latex (gal/sk)	Silica	Retarder (gal/sk)	Time to 500 psi (hr:min)	UCA Strength Rate of Strength Development (psi/hr)	24-hr Strength (psi)
1.5	0	0.05	23:05	172	690
1.5	Micron sized silica	0.05	21:45	160	610
1.5	Nanosilica	0.05	13:29	460	2203

[a]Premium Class H cement, defoamer 0.05 gal/sk, stabilizer 0.2 gal/sk, dispersant 0.143 gal/sk, density 16.4 lbm/gal, Yield 1.1 ft^3/sk.

Figure 2-9: Effect of Nano-silica on compressive strength *[10]*

From the table above, it is evident that adding 0.2 gal/sk. of nano-silica, the rate of strength development increased from 172 to 460 psi/hr. In addition to increasing the early-age strength development, the ultimate strength was also improved by as much as 3x the strength of the control sample (where nano-silica was absent). And to prove the effect of “nano” silica compared to “micro” silica a control sample containing micro-sized silica was also created.

The ultimate strength was 3x times that of the control sample containing micro-sized silica particles. In section 2.2.4 the chemical reason for this strength development will be discussed.

2.1.3.3 Iron-oxide on Compressive Strength of Cement

Vipulandan et al. (2015) [34] recognized the importance of a strong cement sheath in light of the Macondo accident**,** and investigated the effect of nano-sized iron oxide (Fe_2O_3) on modified smart cement, Portland Class H. Modulus of elasticity, compressive strength of cement and piezoresistive behavior was monitored and documented.

The cement, Class H, was mixed with water by a ratio of 0.38 and the cement specimens were prepared in accordance with API standards. To achieve uniform and proper distribution of elements a speed propeller-type mixer was used. By adding varying amounts of nano iron oxide (up to 1.0 wt% of cement) the cement was tested up to 28 days of curing.

$NanoFe_2O_3$ (%)	Curing time (days)	σ_f (MPa)	ϵ_f (%)	Ei (MPa)	p_o
0	1	10.9 ± 2	0.28 ± 0.01	967 ± 21	0.034 ± 0.01
	28	19.3 ± 3.5	0.21 ± 0.02	1936 ± 20	0.160 ± 0.03
1	1	13.7 ± 2.6	0.20 ± 0.01	1239 ± 28	0.095 ± 0.001
	28	27.0 ± 3.2	0.20 ± 0.01	2479 ± 38	0.097 ± 0.002

Figure 2-10: Compressive stress-strain model parameters for NanoFe2O3 modified smart cement *[34]*

After 1 day of curing, initial modulus of elasticity in smart cement had increased by 28% after addition 1.0 % nano Fe_2O_3 and the compressive strength of smart cement (σ_f) after adding 0.5% and 1.0 % nano Fe_2O_3 experienced in a 7 % and 26 % increase, respectively.

After 28 days of curing, initial modulus of elasticity (Ei) in smart cement after addition 1.0 % nano Fe_2O_3, experienced a 28% increase (same as for 1 day of curing) and compressive

strength of smart cement (σ_f) after adding 0.5 % and 1.0 % nano Fe_2O_3 experienced in a 32 % and 40 % increase, respectively.

2.1.3.4 Nano-Graphene on cement

Basically, soft cement paste undergoes a transformation and becomes a hard solid during its hardening process and a combination of flexural and compressive strength of the cement determines its durability and longevity. However, the flexural strength is a bit low, and that is why **Lv et al. (2014)** [31] investigated the effect of graphene oxide nanosheets with different sizes and dosages on cement hydration and mechanical strength of cement paste.

The cement used was Portland cement (42,5R) and the cement slurry was created by mixing cement, water, polycarboxylate superplasticizer (admixture to avoid particle agglomeration) and graphene. The cement/water ratio remained at 0.3. After 24 hours, the specimens were removed from the molds and cured at 20 °C ± 1 °C and 90% relative humidity until a destructive strength test was performed.

GO dosage (%)	Flexural strength (MPa)/increase (%)	Compressive strength (MPa)/increase (%)
0 (control sample)	8.84/100	59.31/100
0.01	10.36/117.2	67.46/113.7
0.02	12.33/139.5	76.51/129.0
0.03	13.47/152.4	79.64/134.3
0.04	13.52/152.9	81.56/137.5
0.05	13.46/152.3	81.89/138.1
0.06	13.43/151.9	81.95/138.2

a w/c was 0.3 and PCs was 0.2% bwoc.

b GO nanosheets size: average thickness was 3.1 nm and average size was 72 nm.

Figure 2-11: Flexural and compressive strengths of cement paste with GO nanosheets at 28 days *[31]*

The conclusion found because of this investigation was that GO nanosheets, added in small dosages, had a large effect on the formation of cement hydration crystals, which in turn

corresponds to the hardened cement paste and thus exhibited remarkable increases in flexural and compressive strengths. By adding 0.03 wt% and 0.04 wt%, they reported an increase in the flexural and compressive strength of the concrete by 152.4% and 137.5% respectively when compared to the control. The flexural strength saw a greater degree of improvement relative to the compressive strength.

2.1.4 Other Interesting Applications

2.1.4.1 Nano-Silica on EOR

One example of nano-EOR is **Moradi et al. (2015)** [23] who studied the effect of nano-WAG (water alternating gas-injection) process by different core flooding tests in carbonate samples and compared results with the conventional approach of WAG injection. He found that adding nano-silica changed the wettability process of the rock from oil wet to strongly water-wet due to the adsorption of SiO_2 nanoparticles on the rock surface, which will affect the oil recovery. His research concluded that a nano-WAG process compared to conventional WAG-process showed a 20% increase in incremental recovery factor.

2.1.4.2 Metal-Oxides Nano on EOR

Ogolo et al. (2012) [24] studied the potential increase in recovery from a sandstone reservoir and identified the better agent for EOR. He used nine different metal oxides and silica in different combinations to study the effects on recovery. He found aluminum oxide to improve oil recovery when dispersed in distilled water and brine because the Al_2O_3 nanoparticles reduced the oil viscosity, thereby increasing EOR. Whilst Silica dispersed in ethanol changed the wettability of the rock and thus enhanced the recovery.

2.1.4.3 Nano-Silica on Scale Deposition

Kumar et al. (2012) [27] have done research into the field of scale deposition. This is a challenging and serious field and the problems scale can cause are great and potential costs of remedial actions of removing tubing, even greater. The highlighted challenge of scale deposition is that it changes the roughness of the surface of the production tubing and thereby increasing the friction the producing fluid experiences on the way up (frictional pressure drop), resulting in a lower production rate. By creating a micro, - and nano-silica coating (adhesive) to apply on the inside of the tubing, they effectively made the tubing

superhydrophobic and thereby reducing the contact angle of water with the surface of the tubing. Scale formation is directly related to the contact surface.

2.1.4.4 Nano-Graphene on Drilling Fluids

Taha and Lee (2015) [26], used graphene, a material with respectable electrical and heat conductivity, in water-based drilling fluid and ascertained it to have several significant beneficial effects on the system. Graphene, by penetrating the microscopic pores of the tubular metal, crystallized in layers under high pressure, formed a protective film by chemically bonding to the surface of the tubular metal and thus improved lubricity, torque reduction (70-80%), helped prevent bit bailing, improved the BHAs (bottom-hole-assembly) lifespan (>75%), improved the ROP (rate of penetration) (125% increase) and most importantly: the fluid's thermal stability.

2.1.4.5 Ferromagnetic Nanoparticles (Fe_3O_4) on Corrosion

Jauhari et al. (2011) [28]**,** recognized the inherent hazards of petroleum-related corrosion of metallic structures (e. g., casing strings, production platform, tools, etc.), which essentially leads to its devastation or at best, deterioration over time. Some operations expose their own materials and equipment for an acidic solution (e. g., acid cleaning, descaling, oil well cleaning, etc.) and for most of these operations the acid is propelled through metallic conduits. The authors turned to nanotechnology to inhibit corrosion and as such, in their experimental work, a novel nanomagnetic fluid comprising ferromagnetic nanoparticles (3-15nm) was formulated and it demonstrated abilities to reduce the corrosion rate of carbon steel in an acidic medium by serving as a coating on the metallic surface. The effectiveness was measured to be proportional with the amount of ferromagnetic material used, up to a certain optimal maximum.

2.1.4.6 Nano-emulsions as Cement Spacer

Maserati et al. (2010) [30], stated that to avoid cement job failure a proper spacer with high cleaning properties had to be designed. Spacers, due to their density, gel strength and viscosity are fluids meant to separate the cement from drilling fluids during a cementing operation to avoid possible contamination. They formulated a new innovative spacer, called nano-spacer, from nano-emulsions with droplets being the size of <500nm. The nano-spacer

compared to conventional spacers, exhibited improved mud removal, wettability reverse and better casing-bore adhesion of the concrete.

2.2 Cement, its Properties, Hydration and Applications in an Oil Well

2.2.1 Portland Cement

Ordinary Portland cement, or OPC as it is abbreviated, is one of the most produced construction materials in the world today and sees an extensive use in many fields and especially in the construction of carparks and infrastructure to huge skyscrapers and everything in-between. OPC is also currently the most important binding material in oil-well applications in terms of quantities used.

It is used to this extent because it is simply a remarkably good building material with its vast availability, good binding property, predictable and uniform strength development, low permeability and is almost insoluble in water. However, it's not without faults as it is said that cement-based materials have relatively poor mechanical properties (e. g., flexural strength, ductility and toughness) and often a low resistance to chemical compounds. Most of these flaws can be rectified by shaping and molding nanomaterials as needed and adding them to the material production mixtures to create a hybrid material.

It is manufactured in cement plants by pulverizing the so-called *clinker* (hydraulic calcium silicates, calcium aluminates and calcium aluminoferrites), which is the burned, or calcined, material that exits the rotary kiln in the cement plant. The rotary kiln is a large cylindrical vessel, or a pyroprocessing device used to expose a material to high temperatures. The term "ordinary" in OPC just refers to the cement being factory-made in said rotary kiln.

2.2.2 API Classification of Portland Cement

The US has through ASTM C150 designed several types of Portland cement to suit various constructional needs. The API class cement specification designs, however, takes into the consideration the severe temperature and pressure conditions that exist in a well and are classified as A through H, with G and H being the most commonly utilized. API Classes A through C is similar to ASTM C150 Type I through Type III. The main difference (physically and

chemically) between the kinds of cement is primarily the content of C_3A (essential for early strength development), fineness and resistance to sulfates.

Table 2-1: API classes for Portland cement *[38]*.

API Class	Purpose	Characteristics	Corresponding ASTM C150
A	When no special requirements are needed	Only ordinary type available, T.T (90 mins)	Type I
B	When moderate sulfate resistance is needed	Available in HSR or MSR, T.T (90 mins)	Type II
C	When conditions require high early strength development	Available in MSR, HES, fine, T.T (90 mins)	Type III
D	For uses under conditions with moderate pressures and temperatures	Available in HSR or MSR, coarse, T.T (120 mins)	
E	For uses under conditions with higher pressures and temperatures	Available in HSR or MSR, T.T (154 mins)	
F	For uses under conditions with extreme pressures and temperatures	Only available in HSR, T.T (180 mins)	
G	Intended use as basic well cement	Available in HSR or MSR, fine	
H	Intended use as basic well cement	Available in OSR or MSR, coarse	

Explanation: T.T: thickening time, H: high, S: sulfate, R: resistance, M: moderate, E: early, O: ordinary

2.2.3 Properties of Portland cement

The properties of Portland cement are determined by the mineralogical composition of the clinker, and generally two families of raw materials are required to formulate Portland cement clinker: calcareous materials (lime from: limestone, coral, shell deposits or artificial types like calcium carbonate) and argillaceous materials (alumina, silica and iron oxide from: clay, shale, marl, mudstone, slate, volcanic ashes and alluvial slit) [1, p. 24].

Table 2-2: Basic mineralogical composition of classic Portland cement clinker *[1, p. 24]*

Common Name	Cement Notation	Oxide Composition	Concentration (wt %)
Alite	C_3S	$3CaO \cdot SiO_2$	55-65
Belite	C_2S	$2CaO \cdot SiO_2$	15-25
Aluminate	C_3A	$3CaO \cdot Al_2O_3$	8-14
Ferrite phase	C_3AF	$4CaO \cdot Al_2O_3 \cdot Fe_2O_3$	8-12

The total content of minor compounds (CaO, MgO, K_2O, Na_2O, Mn_2O_3, SO_3) is usually <5%

2.2.4 Traditional Cement Hydration Process

When a cement slurry is prepared, water is mixed with fine cement powder and the result is a paste-like substance. Said paste is then, through chemical reactions, transduced into a solid hardened concrete. Responsible for the cement strength formation is the hydration process which produces complex chemical fusions that is necessary to bind together the fine and coarse aggregate. The most significant cement compounds this process are, in addition to gypsum, some alkali sulphates and lime, C_3A (aluminate), C_4AF (ferrite phase), C_3S (alite) and C_2S (belite) two of which controls rheology and gelation processes (C_3A and C_4AF) and the two others are responsible for strength development (C_3S and C_2S), early and long-term strength respectively [10].

$$2C_3S + 6H \longrightarrow C\text{-}S\text{-}H + 3\,CH$$
$$2C_2S + 4H \longrightarrow C\text{-}S\text{-}H + CH$$

Figure 2-12: Formation C-S-H gel *[10]*

Figure 2-12 shows that when C_2S and C_3S interact with water, they form calcium silicate hydrate gel (C-S-H) and calcium hydroxide (CH). The C-S-H gel acts as a binder for the cement and consolidates the cement matrix and provides strength to the cement. Also owing to the fact that the C−S−H gel diameter is approximately 10 nm, potentially dispersed nanoparticles (e. g., nano-silica) can fill the voids between cement grains, resulting in denser and stronger material [10]. It is noted, however, that when used in excessive amounts, the nanoparticles might aggregate to generate weak zones and voids that actually serves to deteriorate the overall durability and strength of cement.

When the hydration process takes place, one can observe that heat is being liberated. This is a result of the compounds reacting with water and the subsequent decomposing.

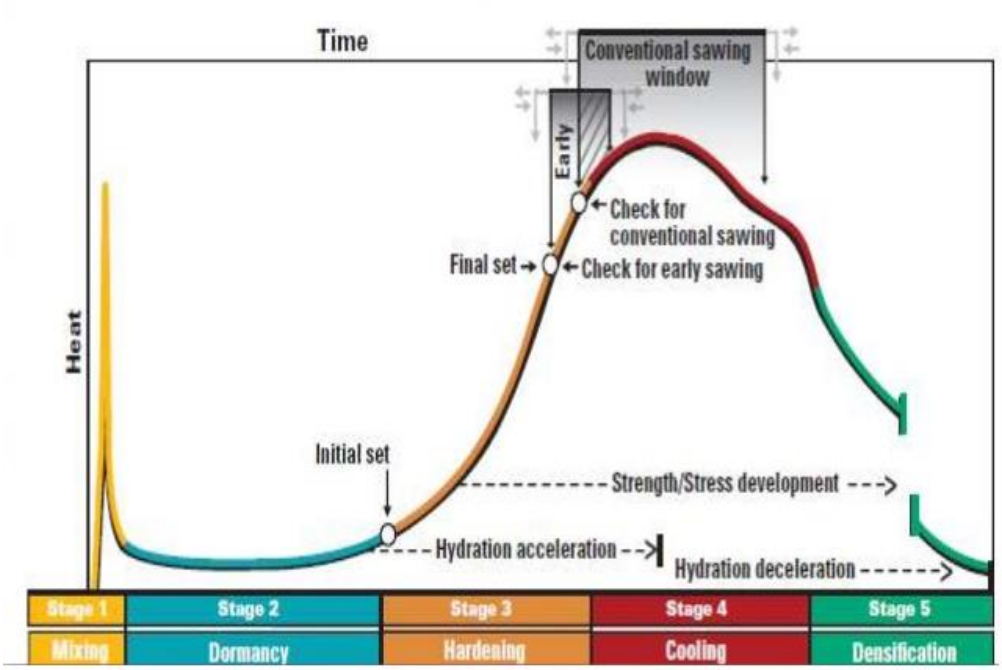

Figure 2-13: Cement hydration mapped on a heat vs. time curve *[39]*

This reaction is termed “heat of hydration” and is a chemical reaction between cement and water. It has a significant impact on the quality of cement as it contributes to increase the chance of for example thermal fracturing. Consider a case where the wellbore is thermally insulated to a sufficient degree, the hydration of cement can increase the temperature of the cement, casing and the surroundings by as much as 27 ^oC - 33 ^oC, after the placement [1, p. 52]. This will impact the casing, potentially causing thermal expansion.

Also, there is an issue regarding the dissipation of heat which might result in something called “thermal micro-annulus” which is the term used when the liberated heat from the hydration process finally dissipates and results in the casing shrinking away from the cement due to different thermal expansion coefficients and thus compromising the integrity of the zonal isolation.

Another case where it would be unwise to have a large exothermic reaction is in arctic environments (e. g., Alaska, northern Canada, Siberia, etc.) with temperatures as low as – 3 ^{o}C, where it is expected that the subsurface formation is permanently frozen. Such permafrost formations can possibly reach depths up to 600 meters. [1, p. 237]. This permafrost must not be allowed to thaw, potentially causing the upper earth to subside and thus reducing the integrity of the well. The cement system should therefore exhibit a low or at least a severely reduced exothermic reaction to avoid such a problem.

2.2.4.1 Five Stages of the Traditional Cement Hydration [39]:

Stage 1: Mixing, or pre-induction period:

It begins during mixing and is a short stage, only some minutes long (<15 minutes), and happens when the cement powder comes in contact with water. A fast hydration reaction occurs between C_3S and water and a large exothermic reaction can be observed at this point.

Stage 2: Dormant, or induction period:

It is observed in **figure 2-13,** that this is a period of relatively low hydration activity, as the heat liberated drastically falls compared to Stage 1. The silicates alite and belite slowly dissolves and C-S-H phase begins to precipitate slowly when at a critical supersaturation. The viscosity is gradually increasing. Compared to stage 1 (that lasts minutes), Stage 2 lasts hours (approx. 2-4).

Stage 3: Hardening, or acceleration period:

The system develops strength and is solidified as well as experience a decrease in porosity due to hydrate deposition. C-S-H and CH forms fully and deposits into the available water-filled space. They intergrow and form cohesive networks that provides the strength to

concrete. Heat is generated, causing thermal expansion. This phase is also some hours long (approx. 2-4)

Stage 4: Cooling, or deceleration period:

In this phase the heat development peaks and gradually begins to drop, meaning the concrete will cool and contract (possible resulting in cracking). The buildup of C-S-H and CH at this point limit the access of water to undisclosed cement. Porosity continues to drop.

Stage 5: Densification, or diffusion period:

Hydration continues at a very slow pace due to the ever-decreasing porosity. The hydrated products become more and more dense and strength continues to rise. This phase can linger for many years or even indefinitely.

2.2.5 Application of Cement in an Oil Well

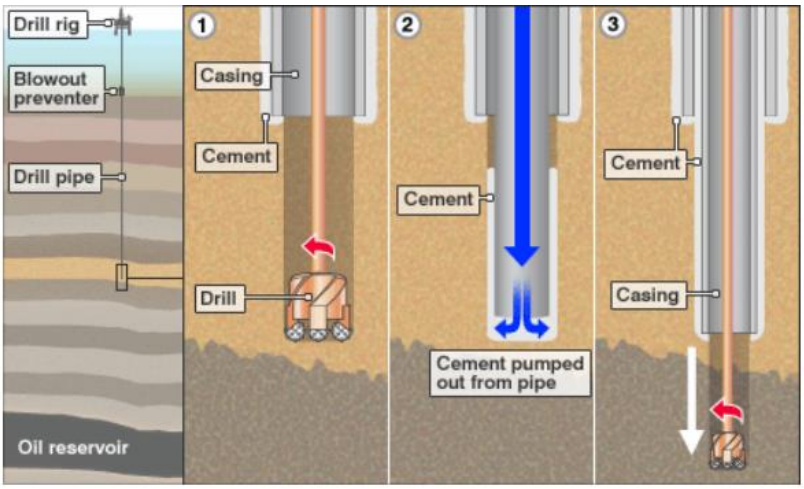

Figure 2-14: How cement and casing is placed in drilling borehole *[40]*

Before the cementing operation can commence, a thorough analysis of the well parameters must be performed (e. g., depth, wellbore geometry, temperature, and formation pressure and formation characteristics) [41]. Following that, necessary calculations to evaluate the amount of required cement slurry is carried out. The cement crew pumps the suspension consisting mainly of water, cement and chemicals down the casing and up the annulus at the cementing interval between the casing and formation, as illustrated in **figure 2-14** above. The well is always filled with drilling fluid to balance the pressure (constant hydrostatic pressure)

to avoid a collapse or an unwanted production of formation fluids. When the cement is pumped down, it displaces said drilling fluid which is the critical part of the cement job due to its role in achieving a suitable casing-cement-formation bond and thus a high degree of well integrity and subsequent production performances [30], [3].

The cement then hydrates or solidifies, anchoring the casing in place. Then the drilling continues, and this process is repeated until all necessary casings are in place and the well is completed, illustrated in **figure 2-15** below.

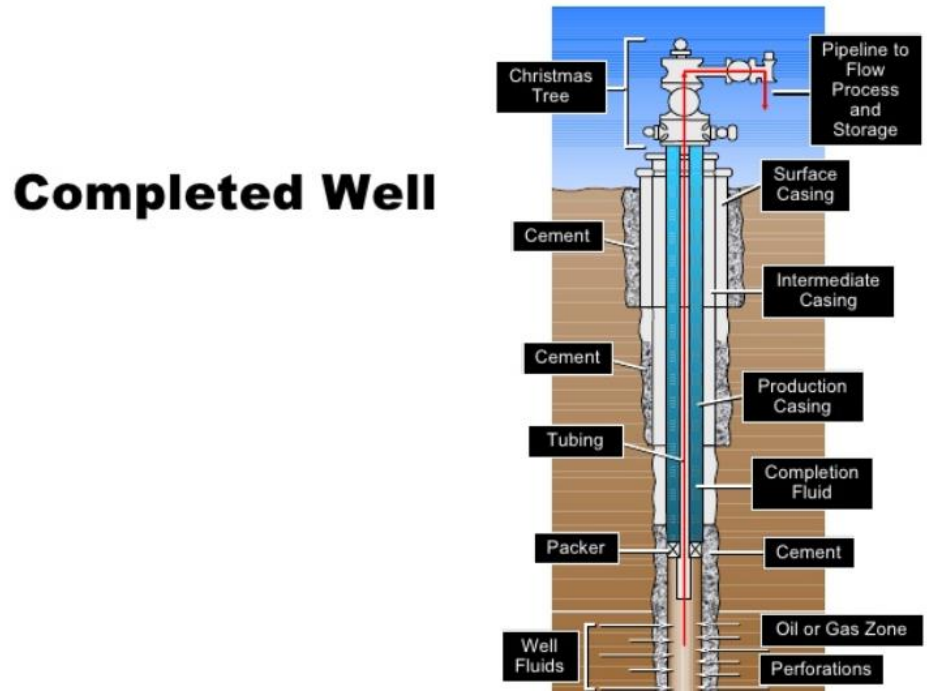

Figure 2-15: A completed well, will all casing strings cemented in place *[42]*

One of the most important operations in an oil and gas well is the primary cement job. The main purpose of cement is to bond and support the casing, which keeps the hole open and prevents the borehole from caving in, causing a collapse, but the foremost purpose of cementing is achieving complete and total zonal isolation, which basically means prevention of any migration of gas or fluids between the zones thus protecting the casing from corrosion and preventing blowouts by facilitating quality pressure control. It also provides a seal for thief zones and protects the casing from shock loads from deeper drilling [4]. From **figure 1-2b** in the introduction of this thesis, it is observed that despite the cement being in place many potential leak paths might exist or occur. In other words, anchoring the casing

is not the challenge, achieving zonal isolation is. The success of zonal isolation depends largely on the hydraulic seal between casing and cement and formation and cement, in the same interval and a better bond might be achieved by a more thorough displacement of drilling fluid by cement. Secondary cementing, referred to as remedial cementing is more related to rectifying hitches resulting from the primary cement job (e. g., alter formation characteristics, repairing casing problems and P&A (plug and abandonment) of wells.

3 Experimental Program

This chapter comprises the physical and theoretical labor required to reach the desired objectives of this thesis.

3.1 Experimental Program Overview

Section 3.2 presents the materials utilized

Section 3.3 presents plug preparation and design background for each matrix

Section 3.4 presents the experimental test setup and theoretical background for each test

Chapter 4 present the results and relevant discussion for the experiments

Chapter 5 presents the formulation of a new model to estimate UCS with higher accuracy

Chapter 6 comprise the conclusions drawn from the experimental results

Chapter 7 comprise a list of ideas for future work

3.2 Materials

All materials have been provided by the University of Stavanger or its representatives unless otherwise specified.

3.2.1 Cement

Portland cement (API class G) was purchased and retrieved from *Norcem A.S, Breivik*. Class G oil-well cement and its major compounds are described in section 2.2.3.

3.2.2 Water Systems

The water utilized for the preparation of the different cement slurries are locally available tap water, seawater and synthetic brines and it is assumed that they are pure and relatively free of contamination, such as oil, alkali, acid, etc.

3.2.2.1 Freshwater

Freshwater, abbreviated as FW, was procured from the readily available tap water located in the laboratory.

3.2.2.2 Seawater

Seawater (SW) was fetched from the harbor in central Stavanger, which is part of the North Sea. The ionic composition of seawater is 31.1g/l and the chemical composition of the North Sea is presented in **table 3-1** and is based on info from **Paramour et al. (2009)** [43]**.**

Table 3-1: Chemical composition of North Sea seawater *[43]*

Name	Chemical Formula	Salinity (ppm)
Chloride	Cl^-	18.980
Sulphate	SO_4^{2-}	2.649
Bicarbonate	HCO_3^-	0.140
Bromide	Br^-	0.065
Borate	$H_2BO_3^-$	0.026
Fluoride	F^-	0.001
Sodium	Na^+	10.556
Magnesium	Mg^{2+}	1.272
Calcium	Ca^{2+}	0.400
Potassium	K^+	0.380
Strontium	Sr^{2+}	0.013

3.2.2.3 Synthetic Brines

3.2.2.3.1 Multi-Salt Synthetic water

Based on the formation water properties obtained from Pierre II shale formation pore fluid from **Tare et al. (2002)** [44], in this thesis work, a synthetic water system is developed (SYW), which is a brine with a 10% salt concentration (3.11 g/l). Higher concentrations of salt

generally have negative effects (e. g., rust, pitting, crevice, etc.) on certain metallic materials. For this reason, it was decided to use 10% of the formation brine (**table 3-2**).

Table 3-2: Multi-salt synthetic brine with 10% salt concentration (Aarnes2018)

Salt	Salt content (g/l)
$NaHCO_3$	1.56
Na_2SO_4	0.730
NaCl	0.386
Na_2CO_3	0.33
$MgSO_4$	0.062
$CaSO_4$	0.042
Total	**3.11**

3.2.2.3.2 Single-Salt Synthetic Water

Single-salt synthetic water (SSW) is a collective term for four separate brines, each containing a salt concentration of 100% (31.1g/l) and consists of a single salt as its only salt-constituent. Due to a limitation of access to 1.0-liter bottles, it was decided to use 0.5-liter bottles with 15.55 grams salt in each brine, thus achieving 100% salt concentration.

Table 3-3: Singe-salt synthetic brine with 100% salt concentration (Aarnes 2018)

Salt	Salt content (g/0.5l)
$NaHCO_3$	15.55
Na_2SO_4	15.55
NaCl	15.55
$MgSO_4$	15.55

3.2.3 Description of Nanomaterials used in this thesis work

The nanomaterials utilized was purchased in powdered form from *EPRUI Nanoparticles & Microspheres Co. Ltd.* The tables below are based on their specification of the respective products.

3.2.3.1 Multiwalled Carbon Nanotubes (MWCNT)

A description of the material has been provided as part of the literature study in chapter 2.

Table 3-4: Properties of MWCNT *[45]*

Item	Specification
Purity	99.50%
Color	Black
Morphology	Hexagonal
Carbon	99.5-99.9
APS (approximation of size)	20-50nm
SSA (specific surface area)	500m^2/g
True density	3.02-3.30g/cm^3

3.2.3.2 Nano Silica Oxide (SiO_2)

A description of the material has been provided as part of the literature study in chapter 2

Table 3-5: Properties of nano-SiO_2 *[46]*

Item	Specification
Purity	99.5 % +
Color	White
Morphology	Amorphous
APS (approximation of size)	15-30nm
True density	2.00-2.40g/cm^3
Oxygen	53.33
Silicon	46.83

3.2.4 Rubber

To further test the possible improvement of cement by way of additives, an idea was formulated in which a rubber element would be included in the cement slurry mix and be tested in the same fashion as the with the cement plugs containing nano-additives. Three types of rubber were used: grey silicone rubber, purchased in the form of a silicone water bottle. Red silicone rubber purchased as a red silicone seal cup. Tyre rubber, purchased in the form of cut pieces of tyre rubber (vehicles). The exact specifications of their elemental composition are not known, unfortunately.

Figure 3-1: Rubber elements utilized as additives in cement (Aarnes 2018)

Said rubbers were utilized in both their natural form and acid-treated form. A guide to perform acid treatment of a rubber element was provided by **Colom et al. (2007)** [47] from which the following steps were taken:

1. Immerse specimen in a 95-97% sulphuric acid (H_2SO_4) for one minute.
2. Retrieve specimen from the acid and leave to air dry for 2 minutes to allow for further reaction.
3. Use hot distilled water (approx. 50^oC) to wash the specimen and ammonium hydroxide (NH_4OH) (15% ammonia) to neutralize the remaining acid.
4. Wash the specimen with distilled water again, but at room temperature.

Three types of acid solutions were tested by **Colom et al**.; H_2SO_4, HNO_3, and $HClO_4$, and sulphuric acid (H_2SO_4) came out on top.

Figure 3-2 and **figure 3-3** below illustrate the change in surface structure of the red silicone cup before and after acid treatment, respectively. Treating the rubber with acid aims to provide a rougher surface of the rubber specimens and thus potentially achieving improved bonding with the cement particles.

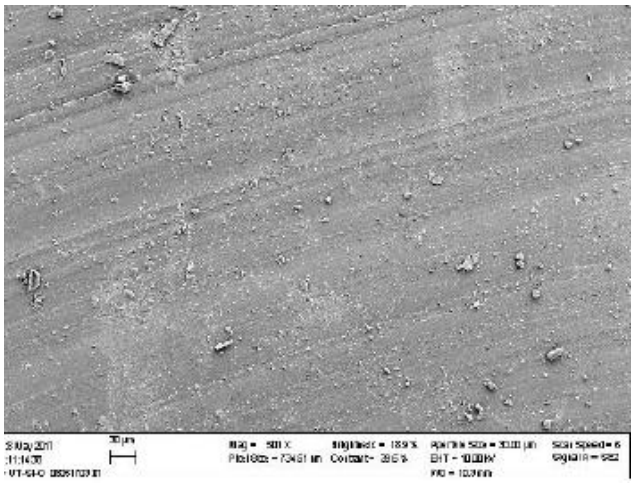

Figure 3-3: Red silicone cup before acid treatment (Kjærnsmo 2017)

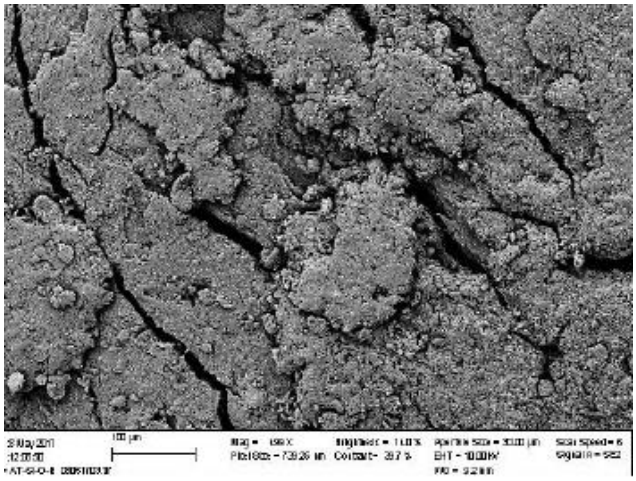

Figure 3-2: After acid treatment of red silicone (Kjærnsmo 2017)

Figure 3-4 shows all the rubber elements cut and prepared for mixing.

Figure 3-4: From top left to bottom right: Grey silicone (treated and untreated), red silicone (treated and untreated), tyre rubber (treated and untreated) & the collective batch of rubber specimens (Aarnes 2018)

3.2.5 Cement Molds

3.2.5.1 Plastic Cylinders

Standard cylinder plastic cups with the following dimensions were used as cement molds and are presented in **figure 3-5**:

L = 69.00 mm (≈70 mm)

D = 34.50 mm (≈ 35 mm)

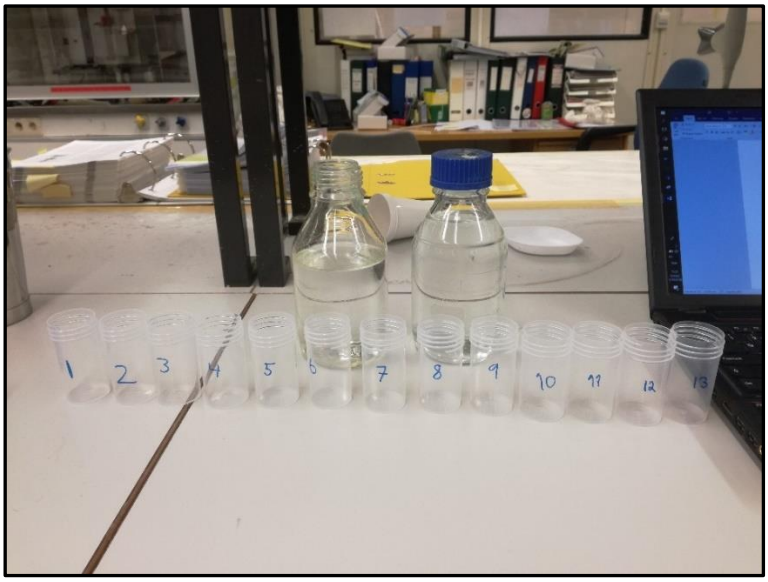

Figure 3-5: Plastic cylinder cups utilized to formulate cement plugs (Aarnes 2018)

Regular oil was used to lubricate the inside of the cylinder molds to ensure the cement plugs, after proper curing, could be safely retrieved.

Figure 3-6: Oil for lubrication (Aarnes 2018).

Figure 3-7: Plastic molds without oil lubrication (left) and with oil lubrication (right) (Aarnes 2018)

3.2.5.2 Metal Cylinders

Steel cylinders were purchased from *Biltema* in the form of table legs and repurposed to act as "casings" for the leakage tests. The exact composition of elements within the pipes is unknown. The dimensions are 200mm (length) and 30mm (diameter).

Figure 3-8: From table legs to casings (Aarnes 2018)

3.3 Formulation of Test Specimens

3.3.1 Introduction

The test mixes, or so-called test matrices, presents the respective plug preparation recipes, or compound overview, utilized to create each specific batch. The results from each study are found in chapter 4.

TM#1 investigated the effect of salt and a set concentration of MWCNTs on cement treated with a mix of freshwater (FW) and multi-salt brine (SYW) system, with the intent on screening out the optimal fluid system for cement slurry formulation.

TM#2 investigated the effect of salt and a fixed concentration of MWCNTs on cement treated with four individual single-salt brines (SSW).

TM#3 studied the effects of salt and various concentrations of MWCNTs on cement treated with seawater (SW).

TM#4 investigated the effect of various concentrations of MWCNTs on cement treated with SYW.

TM#5 investigated the effect of various concentrations of MWCNTs on cement treated with a 20/80 SYW/FW water system (which was the optimal fluid system from **TM#1**).

TM#6 studied the single and combined effect of MWCNTs and nano-SiO_2 on cement treated with the optimal water system from **TM#1.**

TM#7 investigated the effect of various concentrations MWCNTs on heat development during cement hydration.

TM#8 further investigated the effect of MWCNTs on heat development using a larger volume of cement slurry. Leftover slurry was used to perform **leakage** and **UCS tests.**

TM#9 investigated the effect of rubber silicones on cement treated with FW. Leftover slurry was used to perform **leakage tests** and **UCS tests**

Rheology testing investigated the effect of MWCNTs on rheological properties of cement slurry.

TM#1, **TM#2**, and **TM#3**: After slurry formulation, the cement plugs were cured in their plastic molds for 24 hours, then retrieved and air dried for 24 more, after which the cement plugs would be cured in freshwater for 28 days. Every 24 hours up to seven days; mass absorption

and sonic travel time were measured and empirical UCS, density and compressional wave velocity were calculated for all matrices. After seven days it was observed that the plugs had reached their saturation, after which no more calculations nor measurements were performed until day 28, when they were subjected to destructive testing. To avoid oversaturating this chapter with data, only results from seven and 28 days are presented.

Please note that the special modulus of elasticity (M-modulus) depends on density, compressional wave velocity, sonic travel time and mass absorption and thus will be the only representative of the non-destructive test results.

TM#4, TM#5, TM#6, TM#8, and **TM#9:** Same conditions as above except these plugs were only cured in freshwater for only seven days due to time constraints. It would not be realistic within the timeframe of a master's thesis to test nine matrices for 28-day results each. However, there are sources stating that a linear relationship exists between strength development of seven, - and 28 – days [48], [49]. In any case, these matrices will only be compared amongst themselves and their respective control samples, not the 28-day samples.

M-modulus is calculated from **equation 3-6** (ref) and is performed in the same way for all matrices, regardless of curing time. It is the only non-destructive test represented in the result-part of this thesis.

Empirical UCS was initially a part of the non-destructive tests, but as Horsrud's model [50] had sever and unacceptable deviances it was discarded from the results and appendix but used as motivation to create a new model, with higher accuracy, instead.

3.3.2 Test Matrices

3.3.2.1 Test Matrix 1: Design Background

The main objective of this design was to test salt and a set concentration of MWCNTs on the final compressive strength and the modulus of elasticity of cement and also, to screen out the optimal water system solution for further investigation. This was done by mixing cement slurry with synthetic water in a reverse proportional relationship with freshwater. Synthetic multi-salt brine, SYW, consists of 3.11 grams of salt per liter of freshwater, which is a salt concentration of 10% (ref). The cement slurry was created with a water/cement ratio of 100/191 ≈ 0.523. **TM#1** is the first matrix created and consists of 13 plugs. Gradually from plug 1 through plug 13, an increasing amount of freshwater is added to the mix, with the total sum of water always being 100 grams. Additionally, in plug 2, through plug 12, 0.5 gr of MWCNT (0.26 wt %) was added. Plug 1 and 13 are control samples (zero nano), each containing a pure water mix of 100 grams of synthetic brine and freshwater, respectively.

Table 3-6: Test matrix no.1

Plug (#)	Synthetic Brine (gr)	Freshwater (gr)	MWCNT (gr)	MWCNT (Wt %)
1	100	0	0	0.0
2	100	0	0.5	0.26
3	90	10		
4	80	20		
5	70	30		
6	60	40		
7	50	50		
8	40	60		
9	30	70		
10	20	80		
11	10	90		
12	0	100		
13	0	100	0	0.0

3.3.2.2 Test Matrix 2: *Design Background*

This matrix was designed to study the effect of salt and MWCNTs on the final compressive strength and the modulus of elasticity of cement. Four different single salt synthetic water systems (SSW) were created using $NaHCO_3$, NaCl, $MgSO_4$ and Na_2SO_4 individually. Each contained a salt content of 31.1 g/l which translates into a 100% salt concentration (ref). The cement slurry was created with a water/cement ratio of 100/191 ≈ 0.523. **TM#2** is the second batch of cement plugs prepared and consists of eight plugs in total. Two plugs for each salt was formulated, one with a set amount of nano (0.26 wt %) and one as a control (zero nano).

Table 3-7: Test matrix no. 2

Salt (formula)	Plug (#)	SSW (gr)	MWCNT (gr)	MWCNT (Wt %)
NaCl (ref.)	S1	100	0	0.0
NaCl	S2		0.5	0.26
$MgSO_4$ (ref.)	S3		0	0.0
$MgSO_4$	S4		0.5	0.26
$NaHCO_3$ (ref.)	S5		0	0.0
$NaHCO_3$	S6		0.5	0.26
Na_2SO_4 (ref.)	S7		0	0.0
Na_2SO_4	S8		0.5	0.26

3.3.2.3 Test Matrix 3: *Design Background*

This design aimed to study the effect of salt and various concentrations of MWCNTs on the final compressive strength and the modulus of elasticity of cement treated with seawater. It is assumed a 100% salt concentration (31.1 g/l) (ref). The cement slurry was formulated with a water/cement ratio of 100/191≈0.523. **TM#**3 is the third and final batch of cement plugs that used a 28-day timeframe. Six plugs were prepared in total, with SW_0 as a control sample (zero nano) and plug SW_1 through plug SW_5 saw a gradual increase (+0.1g per plug) in the amount of MWCNT.

Table 3-8: Test matrix no. 3

Plug (#)	SW (gr)	MWCNT (gr)	MWCNT (Wt %)
SW_0	100	0.0	0
SW_1		0.1	0.05
SW_2		0.2	0.10
SW_3		0.3	0.16
SW_4		0.4	0.21
SW_5		0.5	0.26

3.3.2.4 Test Matrix 4: *Design Background*

The main objective of this design was to investigate how various concentrations of MWCNT affects the development of the elastic modulus and compressive strength of cement treated with SYW and was thus crushed after seven days of curing (compared to 28). The synthetic brine, in this case, is the same type used in **TM#1** but without any FW dilution. It had a salt content of 3.11 g/l. The cement slurry was created with a water/cement ratio of 100/191≈0.523. **TM#4** contained a total of five cement plugs, with TM4_0 being the control sample and the rest having a non-linear increase in MWCNT concentration up to a maximum of 0.5g (0.26wt%).

Table 3-9: Test matrix no.4

Plug (#)	SYW (gr)	MWCNT (gr)	MWCNT (Wt %)
TM4_0	100	0.00	0
TM4_1		0.05	0.03
TM4_2		0.15	0.08
TM4_3		0.35	0.18
TM4_4		0.50	0.26

3.3.2.5 Test Matrix 5: Design Background

The goal was to investigate the effect of various concentrations of MWCNTs the development of the elastic modulus, compressive strength and tensile strength of cement treated with the optimal water system established from **TM#1**. Like **TM#4**, the plugs were crushed after seven days of curing. The cement was treated with SYW mixed with FW in a 20/80 relationship. The salt content was 0.622 g/l which translates into a 2% salt concentration. The cement slurry was created with a water/cement ratio of 100/191≈0.523. A total of 10 cement plugs was formulated with five pairs being identical in their composition. The reason for this was to perform tensile splitting tests on one half and compressive strength tests on the other. MWCNT content follows the same trend as in **TM#4.**

Table 3-10: Test matrix no.5

Plug (#)	SYW/FW (gr)	MWCNT (gr)	MWCNT (Wt %)	Tensile Plug (#)
TM5_0	20/80	0.00	0.00	TM5_0.0
TM5_1		0.05	0.03	TM5_1.1
TM5_2		0.15	0.08	TM5_1.2
TM5_3		0.35	0.18	TM5_1.3
TM5_4		0.50	0.26	TM5_1.4

3.3.2.6 Test Matrix 6: Design Background

This design aimed to investigate the combined and single effects of MWCNT and SiO_2 in a nanocomposite mix with a reverse proportional relationship with each other. Like **TM#4** and **TM#5**, **TM#6** was crushed after seven days of curing since the development of the elasticity modulus and the compressive strength of cement was mainly in focus. The cement was treated with the optimal water system solution established from **TM#1**. The cement slurry was created with a water/cement ratio of 100/191≈0.523. **TM#6** has a total of six cement plugs with a varying degree of nanoparticles dispersed in the slurry. The total content of nanoparticles in each sample always amounts to 0.3g (0.16wt%MWCNTs).

Table 3-11: Test matrix no.6

Plug (#)	SYW/FW (gr)	MWCNT (gr)	SiO_2 (gr)	Nano (Wt %)
TM6_0	20/80	0.0	0.0	0.16
TM6_1		0.05	0.25	
TM6_2		0.15	0.15	
TM6_3		0.25	0.05	
TM6_MWCNT		0.30	0.0	
TM6_SiO_2		0.0	0.30	

3.3.2.7 Test Matrix 7: Design Background

The main goal of this design was to investigate the effect of MWCNTs on heat development during cement hydration and thus no destructive tests were performed on this batch. The cement slurry was treated with the optimal water system from **TM#1** and a higher water/cement ratio of WCR≈0.602. Some plugs from **TM#1** and **TM#3** exhibited remarkable durability when the compressive strength testing machine was unable to break them. This called for either a weaker cement formulation or a reduction in the curing time by 30% (arbitrarily selected) and thus **TM#7** had a higher WCR. It was the original intention to crush a set of plugs from this slurry to better study the effect of MWCNT on the final compressive strength of cement as it is likely that the weaker cement would not be able to carry the compressive loads imposed by the UCS machine, but some unforeseen events made this obsolete and thus the focus was only on the temperature development.

Four cement plugs were formulated in the same fashion as the previous plugs and then stored in polystyrene boxes to measure the heat of hydration. H_1.0 is the reference specimen and plugs H_1.1 through H_1.3 saw an increase in MWCNTs from 0.05g (0.03wt%) to 0.35g (0.18wt%).

Table 3-12: Test matrix no.7

Plug (#)	SYW/FW (gr)	MWCNT (gr)	MWCNT (Wt %)
H_1.0	20/80	0.00	0
H_1.1		0.05	0.03
H_1.2		0.15	0.08
H_1.3		0.35	0.18

3.3.2.8 Test Matrix 8: Design Background

Like **TM#7**, the goal was to further investigate the effect of various concentrations of MWCNTs on the heat of hydration of cement, but unlike **TM#7,** a larger volume of cement slurry was formulated as well as a lower WCR. The cement was treated with FW and created with a water/cement ratio of 500/955≈0.523. Four 0.5-liter containers with cement were formulated and the remaining slurry was used to fill eight additional test specimens; four were poured into steel cylinders (leakage testing) and four were poured into plastic cement molds (destructive compressive strength testing and modulus of elasticity development). To accommodate for the larger volume of cement slurry, the concentration of MWCNT-additive was scaled up accordingly.

Table 3-13: Test matrix no.8

Heat Plug (#)	FW (gr)	MWCNT (gr)	MWCNT (Wt %)	Leak Plug (#)	Strength Plug (#)
Ref	500	0.00	0	Ref	Ref
H_1		0.50	0.05	H_1	H_1
H_2		1.50	0.16	H_2	H_2
H_3		2.50	0.26	H_3	H_3

3.3.2.9 Test Matrix 9: Design Background

In this design, the goal was to investigate the development of strength and elasticity modulus in addition to leaking properties (cement-steel-bond) in cement treated with FW. The cement was treated with a water/cement ratio of 100/191≈0.523. After the slurry containing rubber additives was mixed and poured into steel cylinder pipes, the leftover cement was used to create cement plug specimens to cure for seven days before being subjected to destructive testing. Three different silicone rubbers were used. Each type has two acid-treated samples and two untreated samples, each of which contains a dosage of high concentration of rubber and low concentration of rubber. Low concentration equals to 3.0g (1.5wt%) and high concentration equals to 8.0g (4.0wt%). The rubber materials have been described in subchapter 3.2.4.

Table 3-14: Test matrix no.9

Plug (name)	FW (gr)	Rubber (gr)	Rubber (Wt %)
Tyre-T-L	100	3.0	1.5
Tyre-T-H		8.0	4.0
Tyre-U-L		3.0	1.5
Tyre-U-H		8.0	4.0
GS-T-L		3.0	1.5
GS-T-H		8.0	4.0
GS-U-L		3.0	1.5
GS-U-H		8.0	4.0
RS-T-L		3.0	1.5
RS-T-H		8.0	4.0
RS-U-L		3.0	1.5
RS-U-H		8.0	4.0

T: treated, U: untreated, L: low concentration, H: high concentration

3.4 Theory, Test-Setup and Procedures

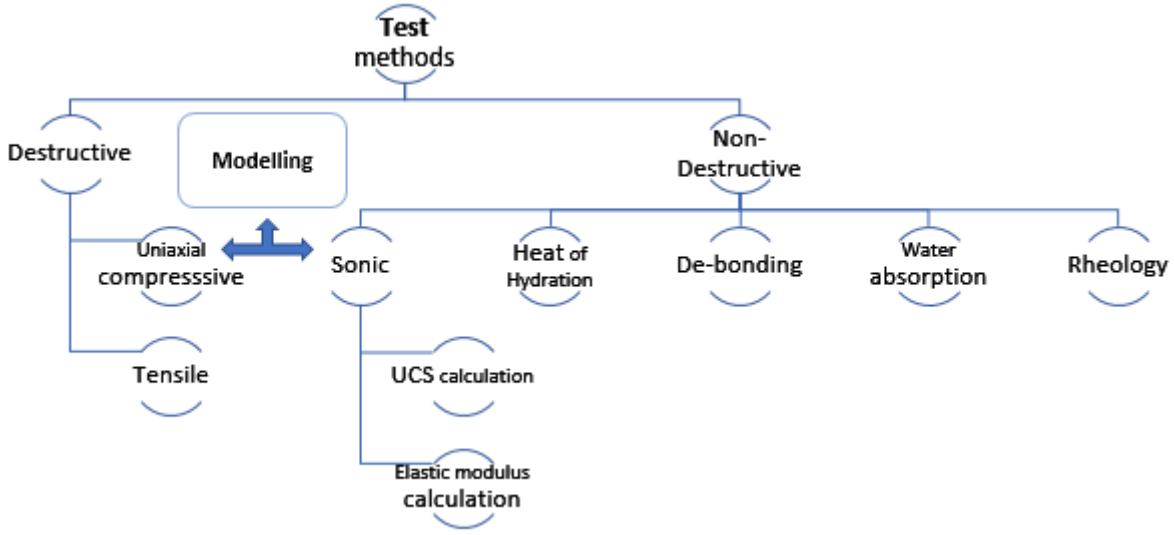

Figure 3-9: Scope of experimental work (Aarnes 2018)

3.4.1 Non-destructive testing

As the name implies, no destructive force is utilized to conduct these experiments. It is more theoretical work and empirical estimations or simple calculations.

3.4.1.1 Ultrasonic measurements

3.4.1.1.1 Theory

The mechanical properties of a material can be determined by measuring the sonic velocity through a solid sample (e. g., concrete or natural rock formation). It works by emitting an ultrasonic pulse through the concrete specimen and record the time for it to reach the receiver on the other side of the bulk material. This test will disclose information about the concrete specimen in terms of strength, homogeneity, trapped air, internal flaws, compaction, cracks, segregation and durability [51].

3.4.1.1.2 Test Setup

Device: *CNS Farnell Pundit 7*, is a sonic velocity meter and is utilized in measuring the sonic travel time through the cement specimen. The value does not have to be calculated as it can be read directly from the display.

Unit: µs ($1 \cdot 10^{-6}$ seconds)

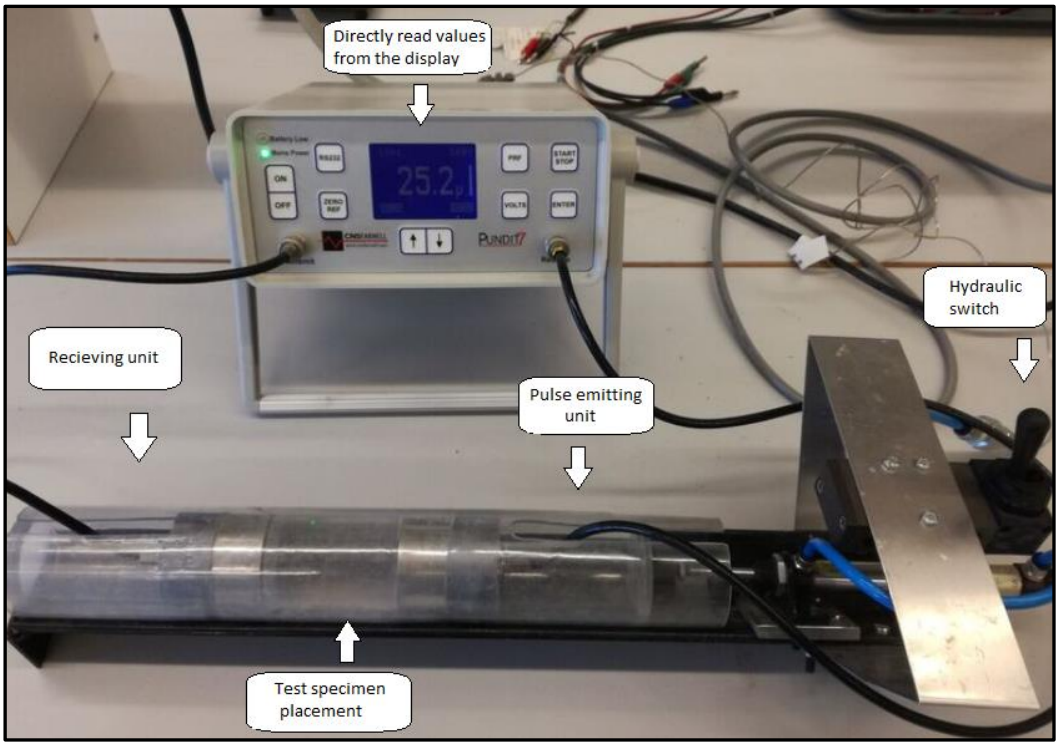

Figure 3-10: Ultrasonic measurement of a test specimen (Aarnes 2018)

The testing equipment consists of an electronic circuit that generates pulses, and a transducer to transform the electrical pulse into a mechanical one, and lastly a pulse reception circuit that receives the signal. The sonic pulses are emitted along the axial direction of the cement plug. **Figure 3-10** shows the assembled apparatus. Calibration of the apparatus is performed by resetting the clock to display 25.2 µs when a pulse is emitted through a plastic test specimen with known properties.

3.4.1.1.3 Procedure

After calibration, the cement plugs are placed inside a plastic ring with the same outer diameter as the inner diameter of the test compartment before sonic measurements are performed. This is to centralize the specimens. To achieve full contact between the surfaces of the receiver-plug-transmitter, a hydraulic press is activated to maintain a light mechanical pressure on the cement plug to ensure that it is firmly and securely placed between the two probes, resulting in a high-quality measurement.

3.4.1.2 Water Absorption

3.4.1.2.1 Theory

Water absorption can tell a lot about the microstructure of the cement plugs in terms of pore volume. Explained shortly, the more absorption of water, the larger the pores and thus a higher likelihood for formation fluids migrating through the cement. These pores can also be a crack or some faulty microstructure which will affect the integrity of the cement at a later stage. Usually, nanoparticles are so small that they are attributed to be able to fill those pores sufficiently and thus reducing the water absorption.

The formula utilized to calculate the increase in weight is presented below:

$$\Delta M = \frac{\mathrm{Mt} - \mathrm{M0}}{\mathrm{M0}} \cdot 100 \qquad (3\text{-}1)$$

Where,

ΔM is the change in mass (%)

$M0$ is the mass after setting

Mt is the mass at time t

3.4.1.3 Empirical Estimation of UCS

3.4.1.3.1 Theory

Uniaxial compressive strength is the measure of the maximum loads (resisting compression) a material can endure before failing. Compressive loads are applied to a test subject in which the subject will be reduced in size until a complete breakdown of the inner structure occurs (failing). It is also called unconfined compressive strength, as with the case for a destructive test to measure UCS of the material, only the top and bottom surface area of the cylindrical cement test specimen has any contact with the compressing apparatus, which means that the confining stress equals to zero. Axial load is the most common load concrete will experience in any industrial appliances and UCS is therefore one of the most important properties in concrete.

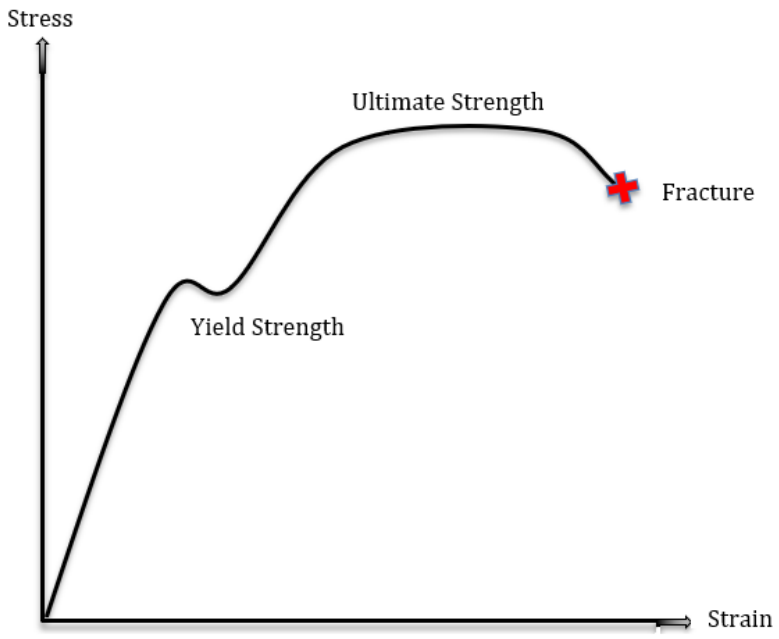

Figure 3-11: Stress vs. strain diagram (Aarnes 2018)

3.4.1.3.2 Procedure

A method for estimating the uniaxial compressive strength of cement, without destroying the sample, was needed for simplicity sake. By having such a model, it is easier to predict the effect of additives in the cement. Per Horsrud, a staff engineer at Statoil, developed a correlation between the UCS of a material and sonic measurements.

Keep in mind that this was a prediction of shale mechanical properties and might be limited by this fact. The experimental work of this thesis utilized this correlation for predicting the UCS of the cement plug specimens prepared in the laboratory [50, p. 70].

$$UCS = 0.77 \cdot {v_p}^{2.92} \tag{3-2}$$

Where:

UCS-is the uniaxial (unconfined) compressive strength, in megaPascals [MPa]

V_p-is the P-wave velocity through matter, in kilometers per second [km/s]

These values were calculated in Microsoft Excel and were dependent on the directly read sonic measurements discussed earlier.

3.4.1.4 Elastic Modulus Calculation

3.4.1.4.1 Theory

M-modulus, or P-wave modulus, is used to describe isotropic homogenous materials. This modulus is not to be confused with the conventional elasticity-module (E-modulus or Young's modulus) with stress versus strain but is, however, defined as the ratio of axial stress vs. strain in a uniaxial state.

3.4.1.4.2 Procedure

To calculate the material's elasticity modulus (axial modulus) (M), a relationship has been developed between the sonic velocity and axial modulus:

$$v_p = \sqrt{\frac{K + \frac{4 \cdot G}{3}}{\rho}} \tag{3-3}$$

After a minor rearrangement:

$$v_p^2 \cdot \rho = (K + \frac{4G}{3}) \quad (3\text{-}4)$$

and from:

$$M = (K + \frac{4G}{3}) \quad (3\text{-}5)$$

the Modulus of elasticity (M) can be calculated as:

$$M = \frac{v_p^2 \cdot \rho}{10^9} \quad (3\text{-}6)$$

Where

M-is the special modulus of elasticity, [GPa] (after dividing with 10^9)

K-is the bulk modulus, [GPa]

G-is the shear modulus, [GPa]

Where:

-K-modulus predicts how much resistance a material will provide when it comes to physical changes to its bulk, or in other words, resistance to uniform compression.

-G-modulus (shear modulus) predicts how a material can handle torsion or resist torsion.

And:

V_p-is the compressional wave velocity, [m/s]

ρ-is the density of cement plug specimen, [kg/m^3]

3.4.1.5 SEM-Sample Analysis

3.4.1.5.1 Theory

SEM or Scanning Electron Microscopy is an electron microscope that provides a large magnification, very high resolution (larger than 1 nm) and can reflect the real micro structure of the specimen surface [52]. It works by bombarding the surface of the solid specimen with intensive high-energy beams which are full of electrons. The specimen that is charged by the electron beam may accumulate the electricity and that will likely result in faulty imaging. A way of redirecting the current is achieved by having a carbon tape used as a conductive adhesive on which the samples rest upon and then spraying the samples with palladium.

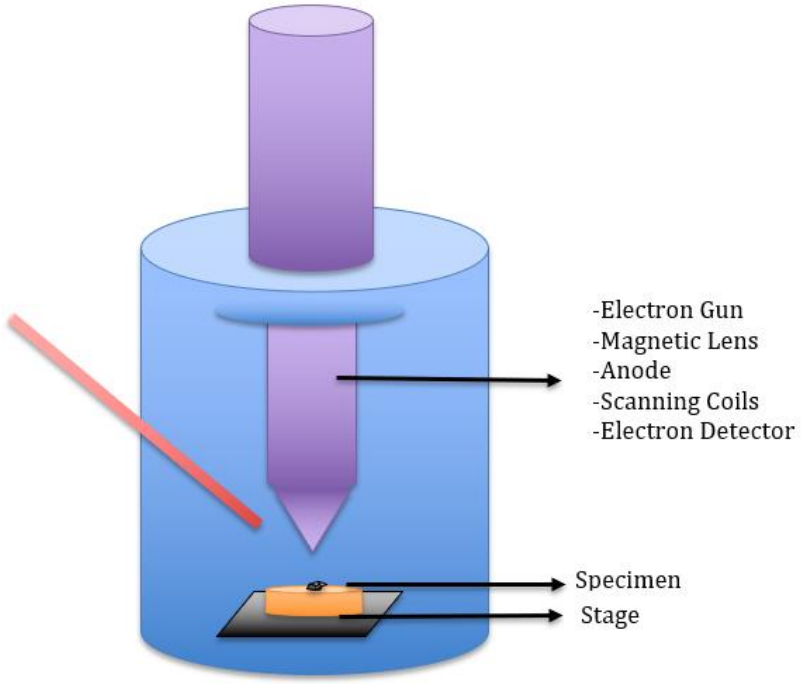

Figure 3-12: A simple sketch illustrating the SEM procedure (Aarnes 2018)

3.4.1.5.2 Procedure

The specimen pieces were plucked from central parts of the destroyed cement plugs. It was adamant that the specimen in the SEM-test did not have any contact with the human body and the various micro bacteria found on it, or any liquid, to avoid contamination or influencing the results by external factors. An EDS-analysis (element analysis) was also performed on the same samples to provide good supporting evidence for any presence of MWCNT embedded in the cement structure.

Device: *Gemini Supra (35VP)* from the producer *Zeiss*

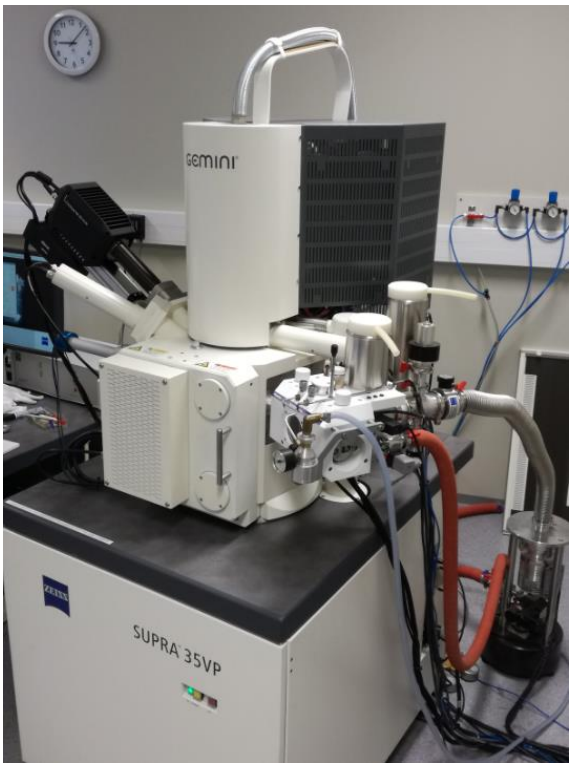

Figure 3-13: Gemini Supra 35VP from Zeiss (Aarnes 2018)

3.4.1.6 Heat Development

3.4.1.6.1 Theory

Heat development, or heat liberation, is the result of cement being mixed with water. It is an exothermic chemical reaction that happens with Portland cement during hydration. This reaction was covered in section 2.2.4. In common appliances, like construction, this heat will disperse into the soil or air and has no significant effect on the quality of the work, but in the field of petroleum this heat development should not be readily released due to the possibility of thermal expansion of casing and cement, and combine that with a rapid non-uniform cooling and structural restraints, it can result in cracking before the cement is adequately set and cooled [53]. It is also a concern for operations in arctic environments that cement exhibits such significant exothermic traits. Therefore, it is of large interest to study how much and how fast heat is liberated when the cement slurry is treated with various water systems and different concentrations of nanoparticles.

Device: Four portable temperature sensors were purchased from *Eskeland Electronics (ESK·EL)* along with the software *Easy Log* to depict the heat development in graph form.

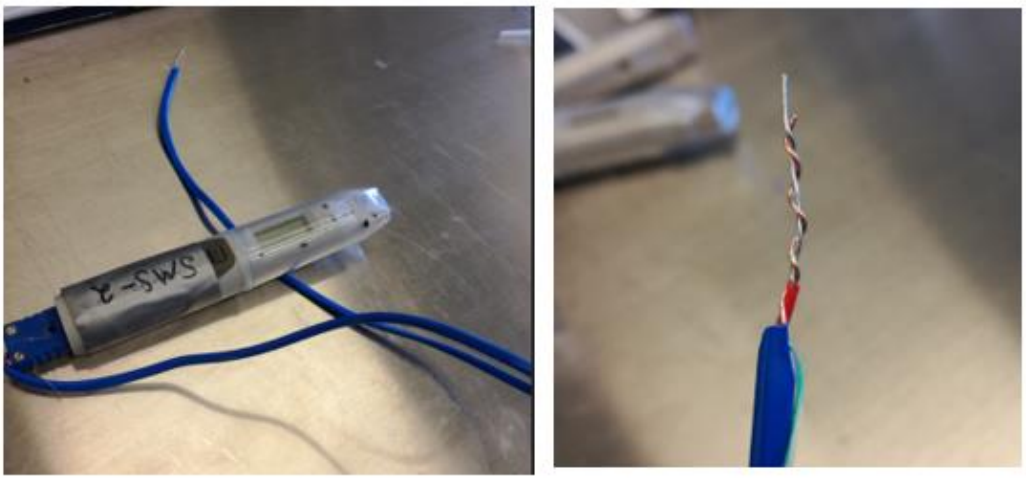

Figure 3-14: One of the four ESK·EL devices (Aarnes 2018)

3.4.1.6.2 Procedure

Two insulated polystyrene boxes with two compartments each, was used to store the cement plug specimens. The dimensions for each of the four compartments are 10cm ·10cm ·10cm. The cement plugs were formulated per usual method, and put in plastic cups, isolated with polystyrene and stored in a dry closet. All four temperature sensors measured the liberated heat every 30 minutes (5 minutes for the second test) for 3-5 consecutive days.

Figure 3-15: a) 4x 1.0-liter empty polystyrene compartments, b) cut polystyrene pieces to help isolate, c) temperature sensors installed in cement, d) packed and sealed boxes, stored in a cupboard (Aarnes 2018)

3.4.1.7 Leakage Test

3.4.1.7.1 Theory

The theory has been discussed in **section 3.4.1.6.1** above.

Device: *Blue M Constant Temperature Cabinet* was used to expose the cased cement to very high temperatures over longer periods of time.

Figure 3-16: Blue M Heat Cabinet in which the cased cement pipes were stored and exposed to temperatures of approximately 110 °C (Aarnes 2018)

3.4.1.8 Procedure

A worst-case scenario condition was imposed upon the cased cement by placing the casings in an oven for longer periods of time at high temperatures after which they would be rapidly cooled. This is discussed on **page 55** and **page 26** in this thesis. Four heat cycles were completed, and each cycle followed these steps: (1) 24 hours in an oven for 110 °C; (2) cool them under running water of approx. 9 °C; (3) fill casings with water to induce a hydrostatic pressure; (4) leave casings filled with water at room temperature of approx. 23 °C for 24 hours; (5) measure which additive in cement allowed for the largest migration and absorption of fluids; (6) repeat steps 1 through 6. **Figure 3-16** illustrates step 1 and **figure 3-17** illustrates step 4.

Figure 3-17: Cased cement, placed on top of plastic cups to measure leakage, if any, through or around the cement after heat treatment (Aarnes 2018)

3.4.1.9 Rheology

3.4.1.9.1 Theory

Rheology describes the flow of matter and generally accounts for fluids, but also soft solids, gels, pastes, etc. It is an important factor in the petroleum industry when it comes to producing and transporting fluids (e. g., crude oil, concrete, mud, etc.). A fluid may exhibit some desirable properties (e. g., strength development of cement), but at the same time display undesirable properties (e. g., too high viscosity, making it impossible to pump) and therefore doing these experiments with cement slurry mixed with MWCNTs is of great importance. Several models exist, but this thesis will use the same model outlined in the work of the former Ph.D. student **Marilyn Ochoa** [54, pp. 45-48], called; the Casson Model:

$$\tau^{0.5} = \tau_c^{0.5} + \mu_c^{0.5}\gamma^{0.5} \quad \text{For } \tau < \tau_c \tag{3-7}$$

$$\gamma = 0 \quad \text{For } \tau \geq \tau_c \tag{3-8}$$

Where

τ is the shear stress ($lb_f/100ft^2$)

τ_c is the Casson yield stress ($lb_f/100ft^2$)

μ_c is the Casson plastic viscosity ($lb_f\ s/100ft^2$)

γ is the shear rate (sec^{-1})

Device: Fann 35 Viscometer

Figure 3-18: Fann 35 viscometer (Aarnes 2018)

3.4.2 Destructive Testing

As the name heavily implies, destructive tests are a collective term for testing a material's strength up to its point of failure (**figure 3-11**) by imposing heavy loads upon the test specimen by mechanical force. Compared to non-destructive tests, the destructive tests are easier to perform, yield more information and are simpler to interpret.

3.4.2.1 Compressive strength testing

3.4.2.1.1 Theory

Most of the theory behind the uniaxial compressive strength of a material has been outlined in section 3.4.1.3.1.

The formula for compressive strength calculation, according to NS-EN 196-1:2016 [55], is presented below:

$$F_c = \frac{P_c}{A} = \frac{P_c}{\pi \cdot D^2} \tag{3-9}$$

Where

F_c- is the compressive strength, in megaPascals [MPa]

P_c-is the maximum load at fracture point, in Newtons [N]

D-is diameter of the specimen, in square millimeters [mm^2]

3.4.2.1.2 Procedure

Device: *The Zwick Z020* compressive apparatus can deliver a force of up to a maximum of 20 000 Newton. It applied force equal to 40 N/s. **Figure 3-19** shows the apparatus with a cement plug specimen firmly placed between the upper and lower loading plates.

Unit: Newtons

Figure 3-19: Zwick Z020 apparatus for destructive testing (Aarnes 2018)

3.4.2.2 Tensile Splitting Strength Test (Brazilian Test)

3.4.2.2.1 Theory

In comparison to the compressive strength of a material, which is its ability to resist compressive loads, the tensile strength is a measurement of how well a material can resist loads that induces physical deformation along the axis of a material. As stated previously the most common stress in any structural appliance for concrete is the compressive load, however, the tensile strength is also of significance as it indicates a resistance to cracking. Usually, the splitting tensile strength and compressive strength are closely related in the way that splitting tensile strength is somewhere between 8-14 % of the compressional strength of the specimen, but despite this one cannot assume direct proportionality [56]. Applying uniaxial tension to a concrete specimen is challenging and is determined by an indirect test, called split cylinder test. It is the common way to test tensile strength in an indirect manner [57]. **Figure 3-20** below illustrates how the tensile load is applied.

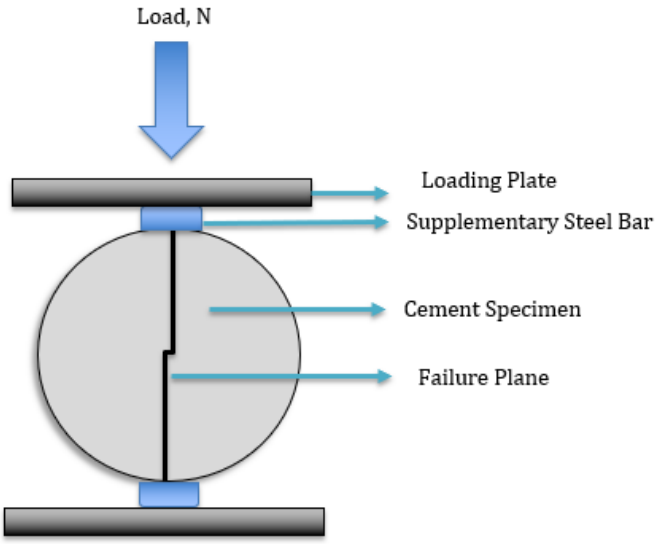

Figure 3-20: Illustration of the tensile load crack propagation (Aarnes 2018)

The following equation, according to NS-EN 12390-6 [58] is used to calculate the tensile splitting strength:

$$F_t = \frac{2 \cdot P_c}{\pi \cdot D \cdot L} \tag{3-10}$$

Where:

F_t- is the splitting tension strength, in megaPascals [MPa]

P_c-is the maximum load at fracture point, in Newtons [N]

D-is diameter of the specimen, in square millimeters [mm^2]

L-is the length of the specimen, in millimeters [mm]

3.4.2.2.2 Procedure

Device: *The Zwick Z020* apparatus was used for both compressive and tensile strength testing. With some adjustments to the software and the physical setup it was able to perform a tensile splitting test.

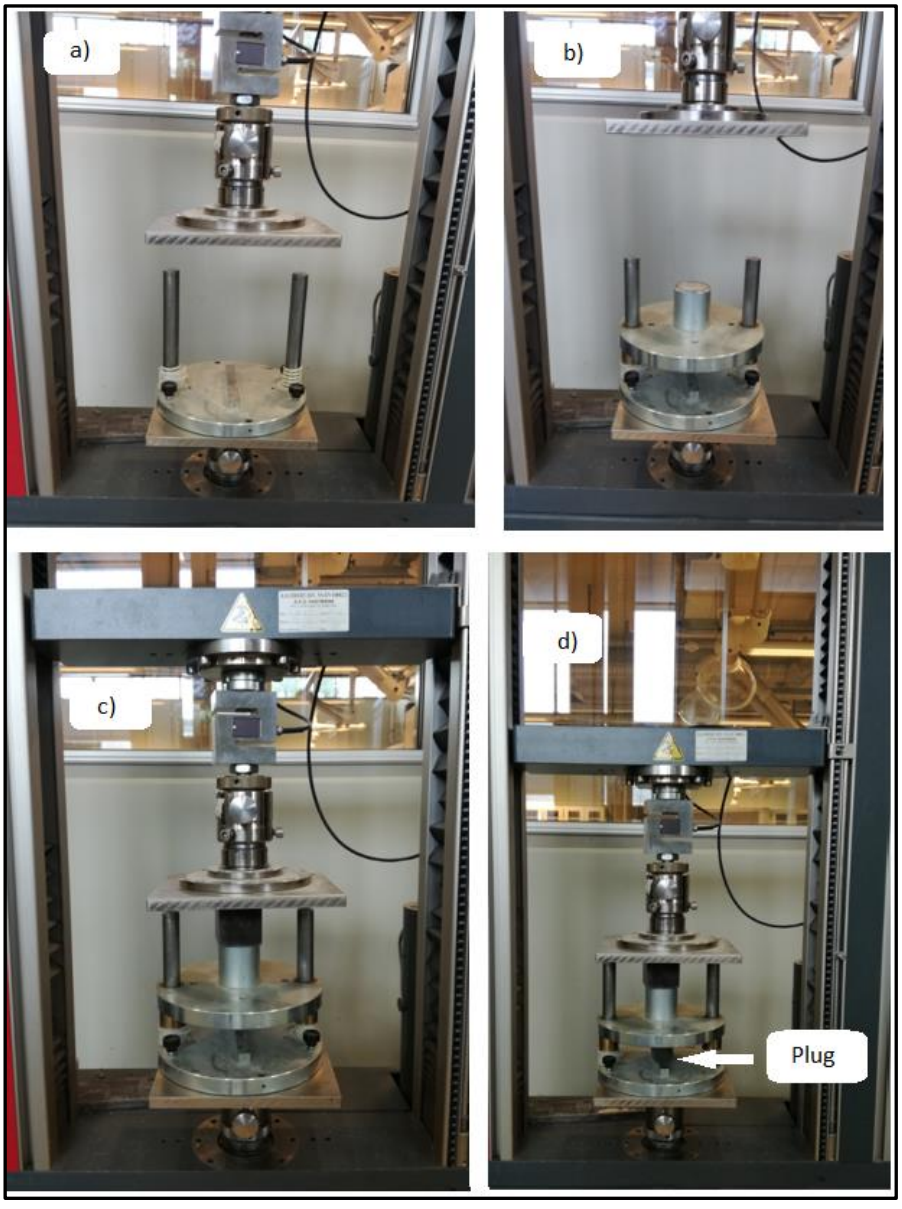

Figure 3-21: Modifications to repurpose the compressive apparatus, step by step. d) Shows the assembled test setup (Aarnes 2018)

4 Results and Discussions

This chapter presents the all the results, relevant discussions and comparisons with field cases or other data, if available. Both destructive (UCS, Tensile strength) and non-destructive (Modulus of elasticity) test results will be discussed. The discussion that is presented is based on test data obtained from 7 and 28 days of curing and will also involve heat development and effect of rubbers in the cement with respect to bonding/leakage.

Please note that the modulus of elasticity (M-modulus) presented in this chapter is computed from non-destructive test by using density and compressional wave velocity

4.1 28-day Non-destructive Test Results

Figure 4-1 presents the modulus of elasticity of TM#1, TM#2 and TM#3. TM#1 (**Figure 4-1a**) was formulated with a mix of synthetic brine (SYW) and freshwater (FW), TM#2 (**figure 4-1b**) was formulated using individual single salt brines (SSW) and lastly, TM#3 (**figure 4-1c**) was formulated using seawater (SW). They all contained a fixed amount of MWCNTs (arbitrarily chosen – 0.5g (0.26wt %)) which is simply referred to as "Nano" in figure a) and b). Please note that unless otherwise specified, Nano is henceforth referred to as MWCNTs. The aim with the different designs were the following: (TM#1) screen out an optimal mix between freshwater (FW) and synthetic brine (SYW) for cement slurry formulation with which further work in this thesis would be based upon later; (TM#2) investigate if MWCNTs' effects on cement was more apparent in one salt system than the other; (TM#3) investigate the effect of MWCNTs on cement treated with seawater.

From **figure 4-1a** it is observed that MWCNTs has a low effect on the elasticity modulus of cement treated with a SYW/FW mix, by comparing *plug 1* (SYW control) and *plug 2* (control + nano) with merely 4.4% variance after seven days and 1.5 % after 28 days. The same can be said about *plug 13* (FW control) and *plug 12* (control + nano) with 2 % variance after seven days and 3.2 % after 28 days. Salt content on the other hand seems to affect the system great deal based on the continuous decrease in M-modulus proportional to salt content with plug 1 being the highest and *plug 13*. *Plug 10* (20% SYW + 0.26wt% nano) is the exception to all the above, clearly showing higher elasticity values in all stages of the development, showing

an increase of 27% compared to FW control. This leads to the conclusion that cement treated with 80% FW and 20% SYW + nano is the optimal water system.

By comparing the individual salts from **figure 4-1b** with their respective references, it is observed that there is close to no effect of MWCNTs on the elasticity of cement treated with SSW. Like TM#1 it appears as if the results are more dependent on the salt utilized in the slurry formulation and not the addition of nano. Cement treated with $MgSO_4$-brine shows a 35% increase in M-modulus after 28 days of curing compared to the highest value from TM#1 and 72% increase compared to the freshwater control sample, also from TM#1**.**

Studying picture **figure 4-1c** it is apparent that MWCNT has a low effect on the M-modulus of cement treated with SW, with the highest plug; *plug 3* (0.2g/0.1wt% MWCNTs) showing merely a 5 % increase in comparison to the control sample. An interesting observation is that the M-modulus is almost identical between seven-day and 28-day curing. No doubt another effect of salt. Based on **figure 4-1** it is logical to assume that 0.26 wt% MWCNTs has very little effect on the development of elasticity of cement after 28 days of curing. Seawater on the other hand shows a significant improvement on the development of M-modulus, showing at higher values after seven days than most other matrices did after 28 days.

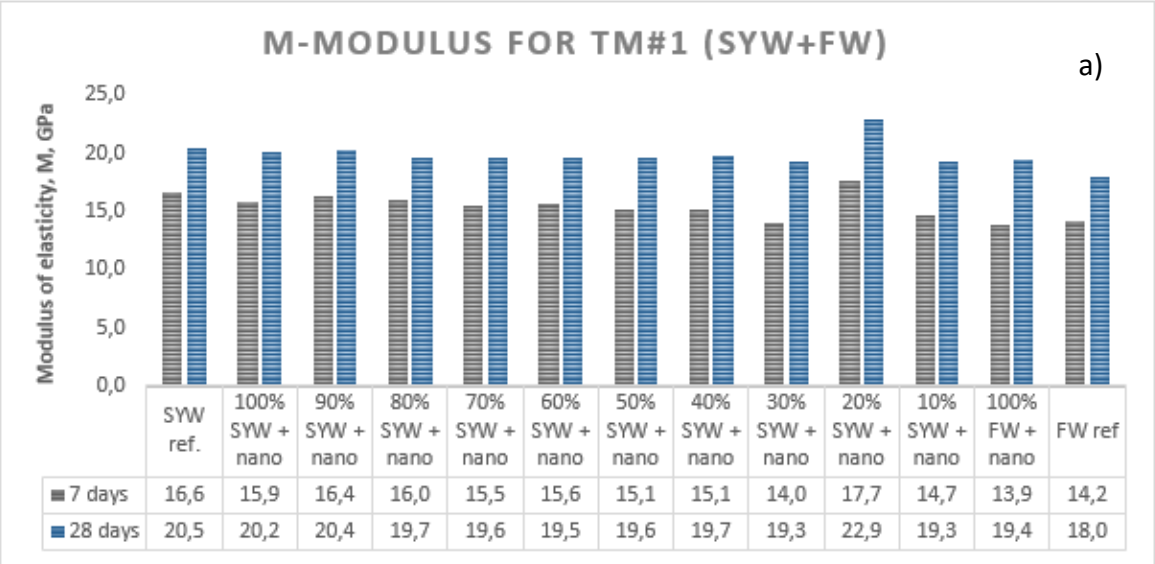

	SYW ref.	100% SYW + nano	90% SYW + nano	80% SYW + nano	70% SYW + nano	60% SYW + nano	50% SYW + nano	40% SYW + nano	30% SYW + nano	20% SYW + nano	10% SYW + nano	100% FW + nano	FW ref
7 days	16,6	15,9	16,4	16,0	15,5	15,6	15,1	15,1	14,0	17,7	14,7	13,9	14,2
28 days	20,5	20,2	20,4	19,7	19,6	19,5	19,6	19,7	19,3	22,9	19,3	19,4	18,0

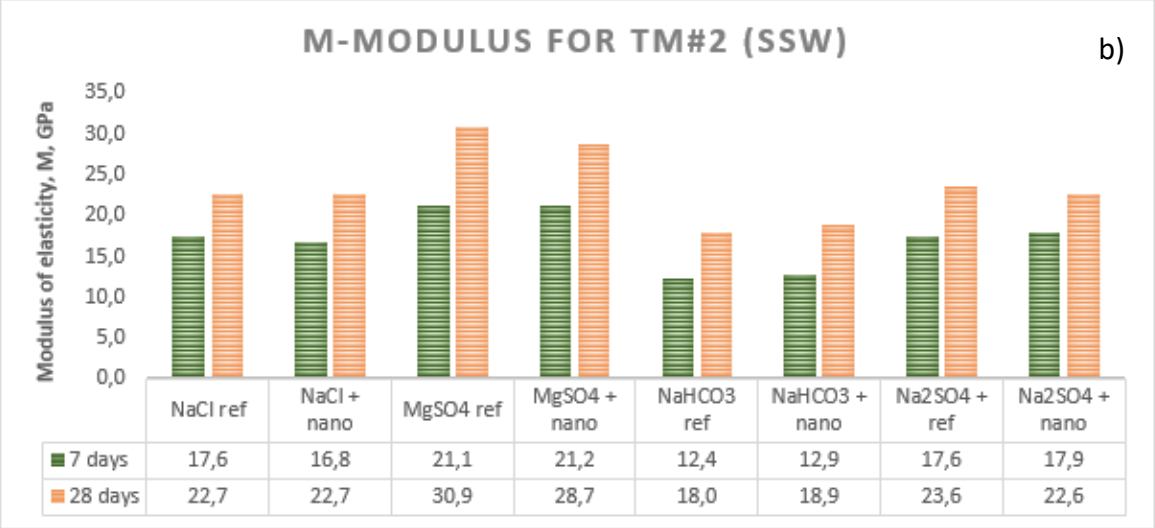

	NaCl ref	NaCl + nano	MgSO4 ref	MgSO4 + nano	NaHCO3 ref	NaHCO3 + nano	Na2SO4 + ref	Na2SO4 + nano
7 days	17,6	16,8	21,1	21,2	12,4	12,9	17,6	17,9
28 days	22,7	22,7	30,9	28,7	18,0	18,9	23,6	22,6

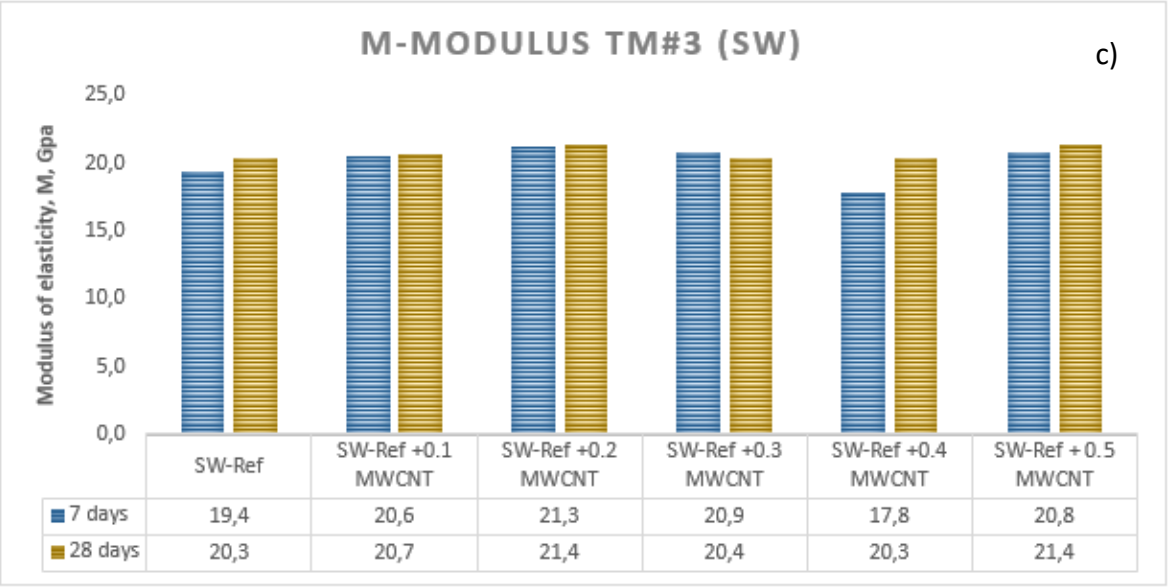

	SW-Ref	SW-Ref +0.1 MWCNT	SW-Ref +0.2 MWCNT	SW-Ref +0.3 MWCNT	SW-Ref +0.4 MWCNT	SW-Ref +0.5 MWCNT
7 days	19,4	20,6	21,3	20,9	17,8	20,8
28 days	20,3	20,7	21,4	20,4	20,3	21,4

Figure 4-1: M-modulus for TM#1, 2&3 after seven and 28 days of curing

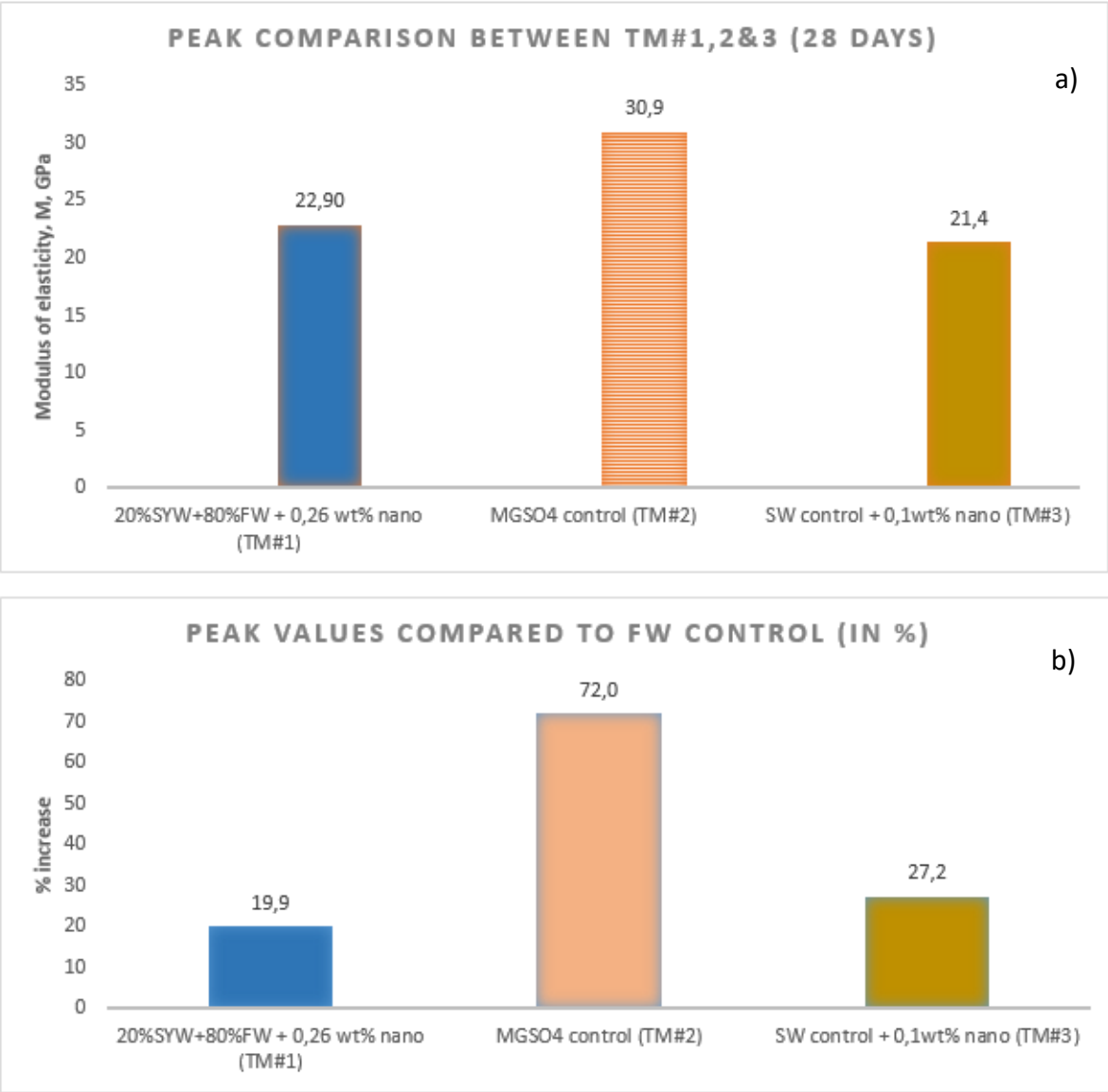

Figure 4-2: a) peak comparison between the matrices, b) top specimens compared to FW control

4.2 28-day Destructive Test Results

The destructive compressive test procedure is explained in in chapter 3. **Figure 4-3** presents the data results obtained from the destructive UCS test on TM#1, 2&3. The first observation from **figure 4-3a** is a similar trend as with the M-modulus chart; with *plug 1* (highest salt content) being the stronger plug, except for plug 10. Similarities between **figure 4-1** and **figure 4-3** was expected since the M-modulus is based on the sonic travel time through the cement plug specimen which in turn depends of the microstructure of the material. Low sonic values (corresponds to high M-values) are associated with a dense material with few cracks and small

pores, and thus one could *assume* that it would result in higher compressive strengths, which appears to be the case. It is interesting to observe that (apart from plug 10) the system seems to experience some disadvantages with the addition of MWCNTs: *Plug 1* (SYW control) experienced a 17 % decrease in UCS with the addition of 0.26wt% MWCNTs and *plug 13* (FW control) experienced a decrease of 33 % with the addition of 0.26wt% MWCNT, after 28 days of curing. This could possibly be due to the high concentration of MWCNTs used in the mix which could result in poor dispersion of nanoparticles (agglomeration) explained by **Hunashyal et al. (2014)** [59].

Plug 10 (containing 20%SYW and 0.26%MWCNT) experienced an increase in UCS of at least 3.0% and 19.4% compared to its SYW, - and FW-reference counterparts respectively, and sets itself apart from the rest as the strongest plug, but due to a physical limitation of 20kN of applied force from the compressive machine, the exact final compressive strength of *plug 10* is not known. In appendix B in the plugs from TM#1 can be observed with an equal amount of visual structural integrity compared to *plug 10*, which might indicate that no structural faults were to blame for their low strength, but rather their chemical composition. Based on the results from TM#1 one could conclude that the water system containing 20%SYW and 80% FW was indeed the optimal one for cement slurry formulation and was used on more occasions throughout this thesis.

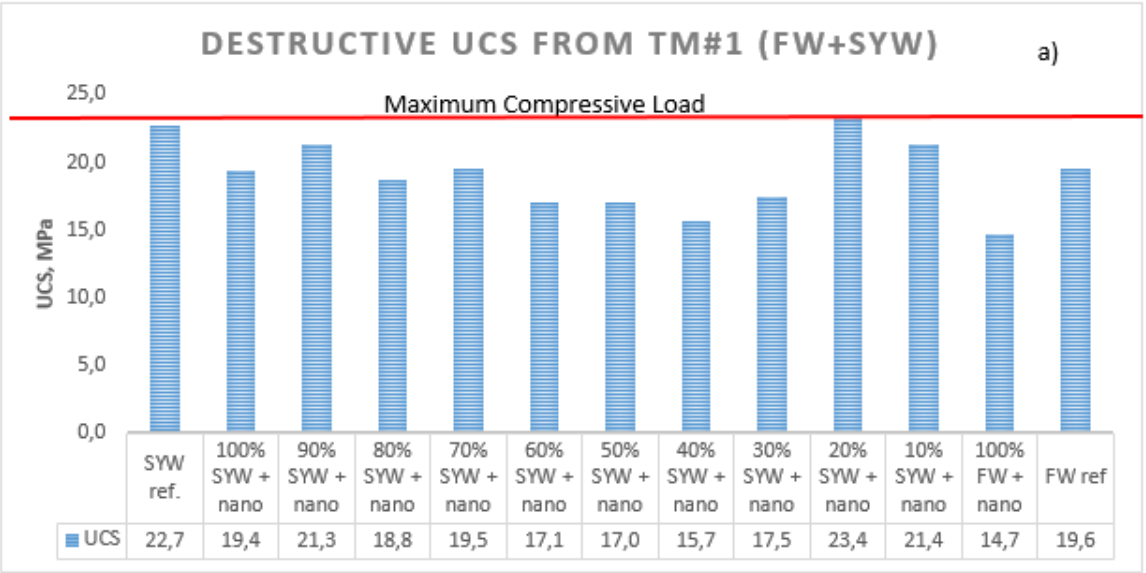

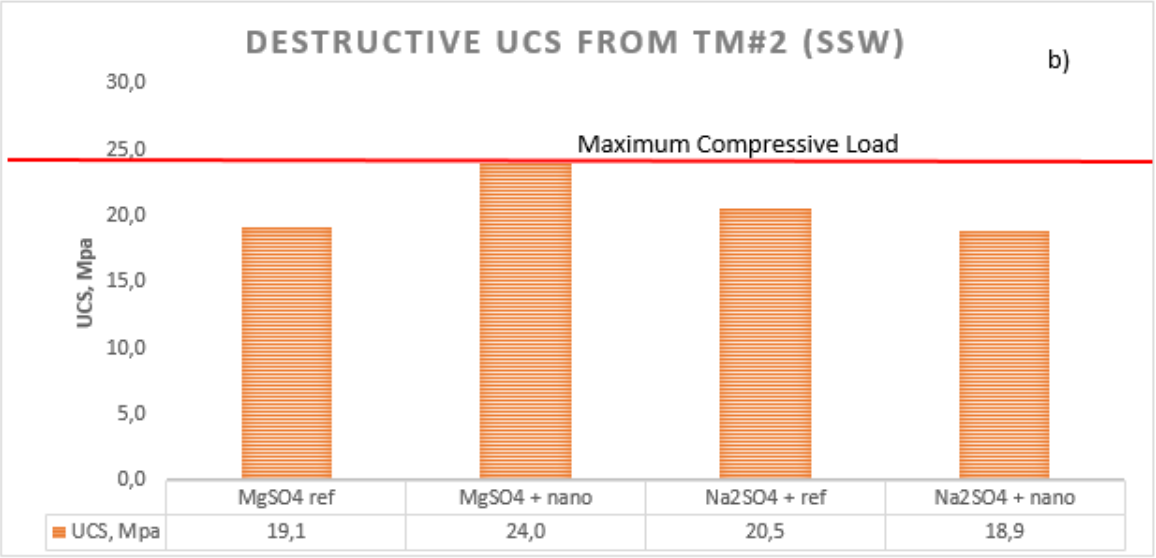

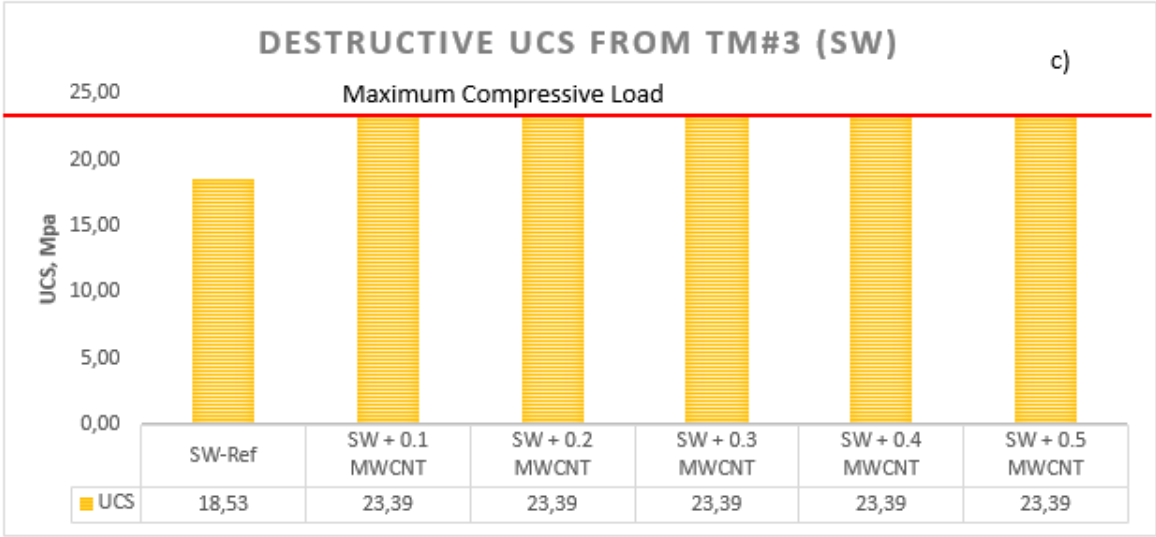

Figure 4-3: Destructive tests after 28 days on: a) FW+SYW plugs, b) SSW plugs and c) SW plugs

Figure 4-3b presents the data obtained from the destructive testing on TM#2**.** A choice was made, based on the non-destructive tests outlined in the previous section, to perform destructive tests only on the cement plugs treated with the following salts: $MgSO_4$ and Na_2SO_3. The highest UCS is observed in the cement plugs manufactured with $MgSO_4$ with the addition of 0.26wt% MWCNTs causing an increase in UCS of (at least) 26% compared to the control sample and 22.5% increase compared to the freshwater control (FW control). Like with plug 10 from TM#1, the compressive machine was unable to crush this plug and thus the exact compressive strength after 28 days is unknown. Despite showing very positive strength results, the student would *not* recommend its use in cement formulation since this salt especially, is associated with causing sulphate attacks on concrete structures over time, reducing its durability and longevity, as documented by **Wegian (2010)** [60].

Figure 4-3c presents the data obtained from the destructive strength tests performed on the seawater plugs (TM#3). All the plugs containing MWCNT proved to be able to carry the load of 20kN which makes it impossible in this thesis to determine the exact strength, like *plug 10* from TM#1, but at least one can conclude with a UCS increase of 26% compared to the control sample, as a minimum. Cement slurry treated with 0.26wt% MWCNTs and seawater is thus far the most successful batch of cement plug specimens. The results from the destructive tests leaves the student to conclude that salt, despite its negative factors regarding corrosion attacks and deterioration of a material, improves the strength of concrete significantly. This is also in accordance with the results presented by **Wegian (2010)** [60] despite using a different class of cement and some other dissimilarities.

Due to the physical limitation of the compressive strength testing machine it was decided to test the remainder of the cement plugs from the succeeding matrices after seven days of curing instead of 28. Also, the following matrices tested the effect of varying concentrations of MWCNTs additives and not a fixed amount.

4.3 Seven-day Non-destructive Test Results

Figure 4-4 presents the modulus of elasticity for TM#4, TM#5 and TM#6 and these matrix designs aimed to study the effect of different nano-concentrations on mechanical properties of cement. TM#4 (**Figure 4-4a**) was formulated using synthetic brine (SYW) while TM#5 (**figure 4-4b**) and TM#6 (**figure 4-4c**) was formulated using 80/20FW/SYW (established from TM#1). They all contained a varying amount of MWCNTs. The goal with the different designs were the following: (TM#4) investigate the effects of varying concentrations of nano on mechanical properties of cement made purely with SYW; (TM#5) study the effects of varying concentrations of nano on cement strength (UCS and tensile) formulated with the optimal water system from TM#1; (TM#6) investigate the effect of MWCNT-SiO_2 nanocomposite on mechanical properties of cement.

Figure 4-4a illustrates that adding just small amounts of MWCNTs yields the highest elasticity values for cement, with *plug 3* (0.15g (0.08wt%) MWCNTs) experiencing an increase of 20% compared to the control sample. When the concentration increases above 0.08wt% it appears as if the M-modulus drops drastically, falling below even that of the control sample. This corresponds to the preliminary matrices where it was apparent that the addition of a relatively high amount of nano (0.26wt% MWCNTs) decreased the M-value of the system.

Figure 4-4 b shows the similar trend as observed in test matrix 4, above, namely an inverse-proportional relationship between elasticity and nano wt% concentration, except for a peak with lower concentrations of added nano. *Plug 2* (0.05g/0.03 wt% MWCNTs) from TM#5 experience an increase of 7% compared to the control sample after seven days of water curing.

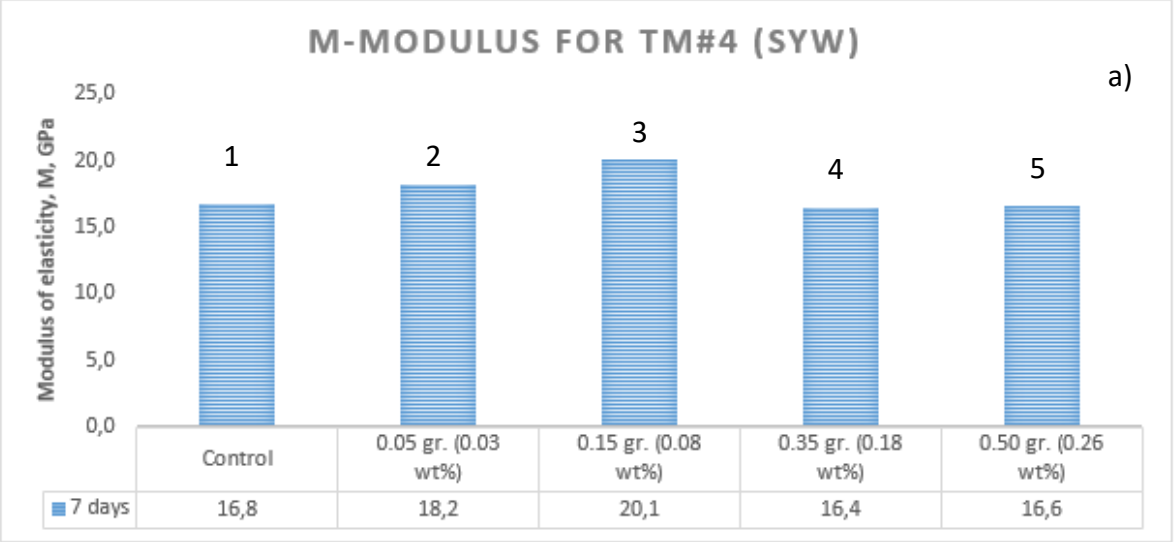

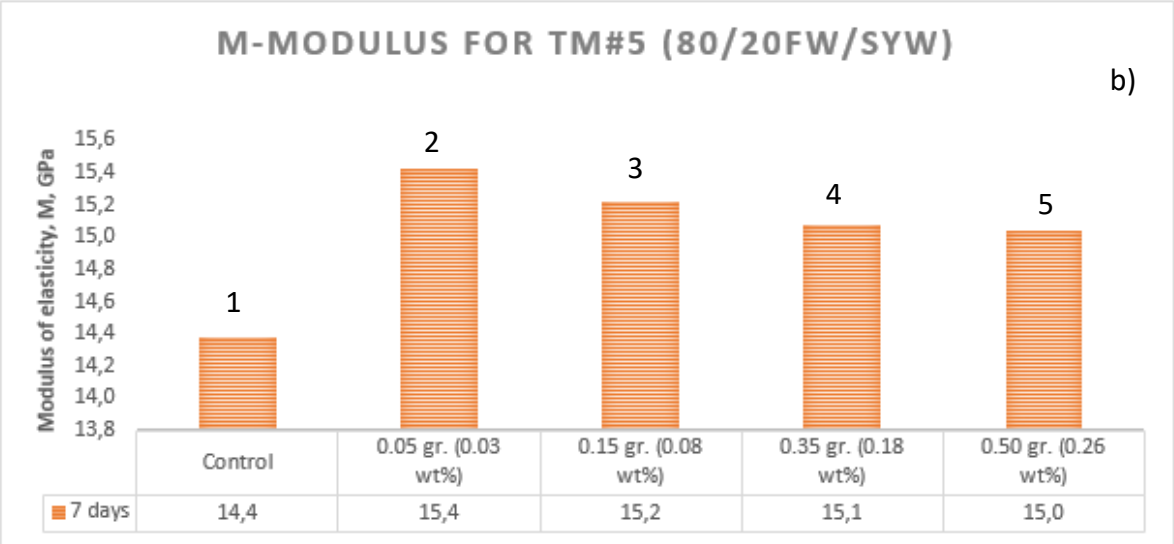

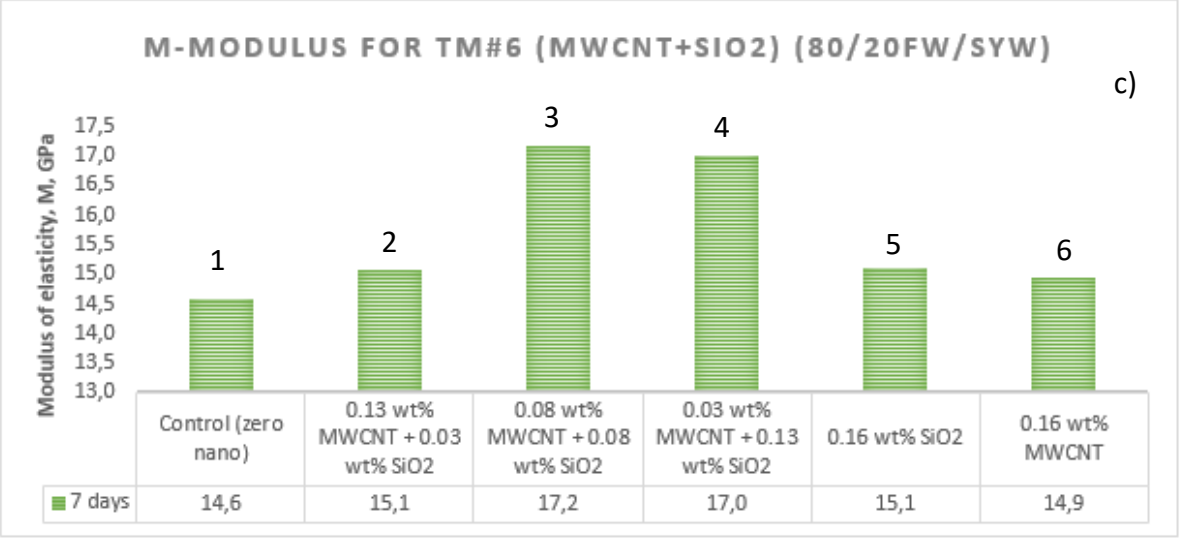

Figure 4-4: M-modulus for TM#4, 5&6 after seven days of curing

Figure 4-4 c presents the elasticity modulus of TM#6 which used a nano-composite consisting of MWNCT and SiO_2 with different wt% concentration from each, but the total sum amounted to 0.3g/0.16 wt %. *Plug 3* (0.15g/0.08wt% of each nano) seems to be doing best compared to the control sample with an 18% increase in the M-modulus. Studying the single effect of the nanomaterials tells us that there are barely any changes to the M-modulus with the addition 0.16wt% MWCNT or SiO_2. A conclusion can be drawn from these results stating that lower concentrations of MWCNT (<0.08wt %) treated slurry yields the highest M-modulus values after seven days of curing in freshwater and if it is a linear relationship; after 28 days as well, but see a decline in M-modulus with increasing nano-concentrations.

Figure 4-5: a) peak comparison between the matrices, b) top specimens compared to their respective controls

4.4 Seven-day Destructive Test Results

All plugs were crushed after curing for seven days in freshwater. **Figure 4-6** presents the data results obtained from the destructive UCS test on TM#4 and TM#5 and **figure 4-7** present the results from TM#6. **Table 4-1** shows the sample composition for TM#4.

Table 4-1: Sample composition for TM#4

Name	Content/purpose
TM4:0	Control
TM4:1	0.05 gr. (0.03 wt %)
TM4:2	0.15 gr. (0.08 wt %)
TM4:3	0.35 gr. (0.18 wt %)
TM4:4	0.50 gr. (0.26 wt %)

Studying **figure 4-6a** (TM#4) it looks as if adding MWCNTs in cement (despite it being small dosages) does very little for the compressive strength of cement after seven days. This is strange because all supporting literature ([32] [59]) would state otherwise. It is likely that a crack or some other faults within the microstructure of the cement, has somehow formed during its creation and propagated significantly during the physical deformation imposed by the compressive apparatus. The only plug stronger than the control is TM4_3 (0.18wt% MWCNT) and then only by 2%. TM4_4 (0.26wt%MWCNT) is 32% weaker than the control sample Since the chemistry of the MWCNT in the brine system was not studied, up to this point it is difficult to judge why the MWCNT seemed to weaken the control slurry. However, one can assume that the weaker system could be due to the incompatibility of the MWCNT with the degree of salinity in the considered brine systems. Had repeated tests been performed, one could probably have been to draw a conclusion about the performance of MWCNT in the synthetic brine fluid.

Table 4-2: Sample composition for TM#5

UCS	Content/purpose	Tensile
TM5:0	Control	TM5_0.0
TM5_1	0.05 gr. (0.03 wt %)	TM5_1.1
TM5_2	0.15 gr. (0.08 wt %)	TM5_1.2
TM5_3	0.35 gr. (0.18 wt %)	TM5_1.3
TM5_4	0.50 gr. (0.26 wt %)	TM5_1.4

Figure 4-6b and **figure 4-6c** present the results from compressive and tensile tests from TM#5, respectively. **Table 4-2** provides an explanation for the denotations and their respective nano-concentrations, used in the graphs.

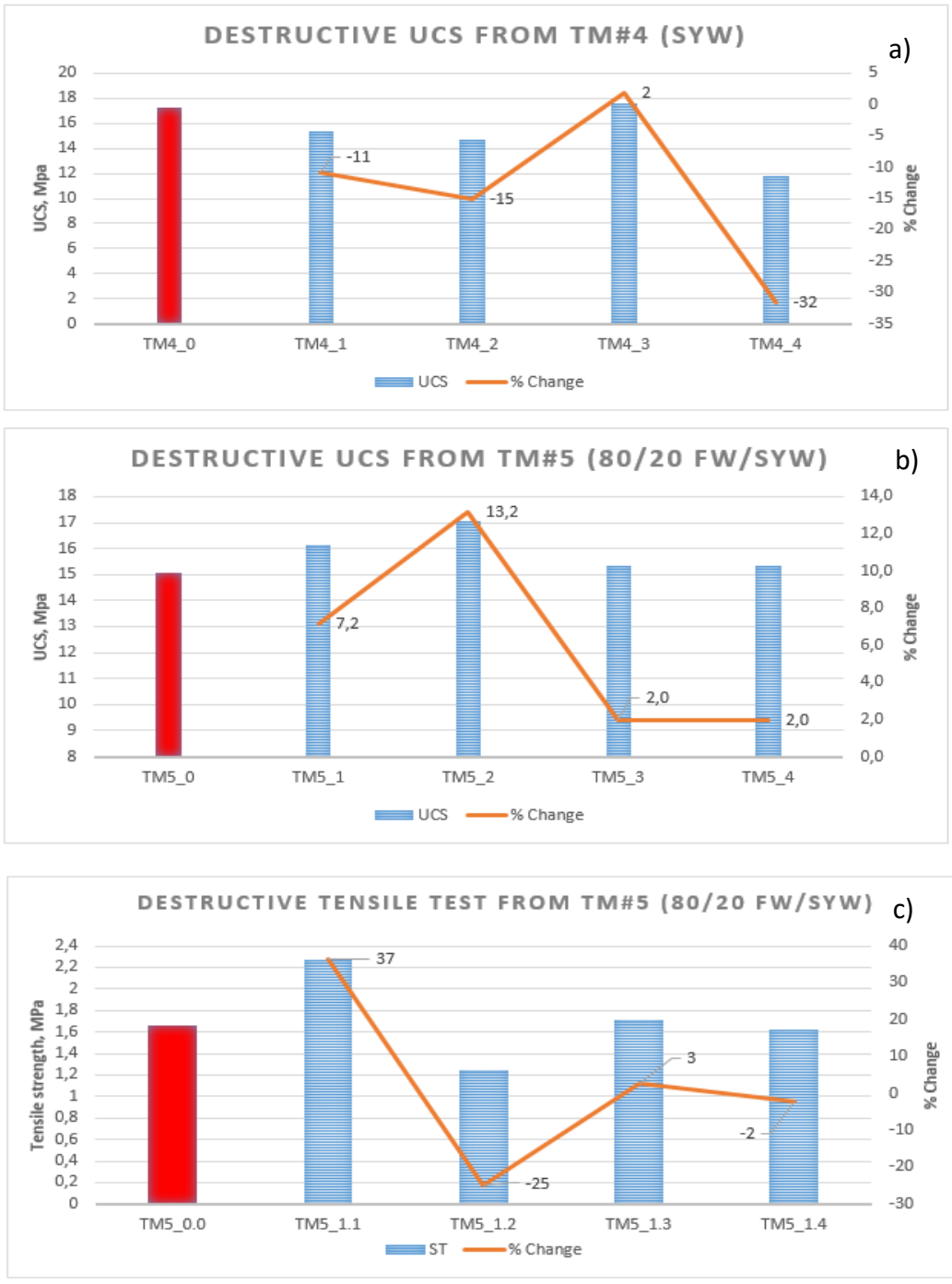

Figure 4-6: Destructive test results from TM#4 and TM#5 after seven days of curing

It is also observed from **figure 4-6b** that cement treated with 80/20 FW/SYW resulted in a much higher increase in UCS after the addition of MWCNT compared to cement treated purely with SYW, indicating a good effect of MWCNT additive. The reason could be due to the reduction of salinity by about 80%. As shown, TM5_1 (0.03wt % MWCNT) and TM5_2 (0.08wt% MWCNT) enhanced the UCS by 7.2 % and 13.3%, respectively. Higher concentrations of MWCNTs (>0.08wt %) in lower saline systems recorded lower UCS values. This shows that MWCNTs depends on salinity of the fluid. TM5_1.1 (0.03wt% MWCNT) shows an astounding increase of tensile splitting strength of 37% compared to the control sample, but a discrepancy, no doubt, is the case for TM5_1.2 (0.08wt%MWCNT) which experienced a severe decrease in tensile splitting strength of 25% in comparison to the control sample, seeing as the corresponding plug from the UCS test (TM5_2) was the strongest plug. Also, according to **Haranki (2009)** [56] the splitting tensile strength of the cement specimen should be roughly 8-14% of the compressive strength (although it is noted that one cannot assume a linear relationship) which is the case for all of them except plug TM5_1.2 further supporting the theory that this plug had a faulty structure.

Table 4-3: Sample composition for TM#6

NAME	MWCNT (gr) (wt%)	SIO2 (gr) (wt%)
TM6:0	0.0 (0.0)	0.0 (0.0)
TM6:1	0.25 (0.13)	0.05 (0.03)
TM6:2	0.15 (0.08)	0.15 (0.08)
TM6:3	0.05 (0.03)	0.25 (0.13)
TM6:SiO2	0.0 (0.0)	0.30 (0.16)
TM6: MWCNT	0.30 (0.16)	0.0 (0.0)

Figure 4-7a and **figure 4-7b** present the results from destructive tests on TM#6 showing the nanocomposites relative to the control sample and the single effect of SiO_2 and MWCNTs relative to the control sample, respectively. As can be seen from the figures, it is evident that an equal amount of both nano-additives – 0.08wt% each – yields the highest UCS strength (and M-modulus) with an increase of 14% compared to the control. Comparing the singe effect of nano-additives it is clear that nano SiO_2 is stronger with higher concentrations (18% increase in USC vs. control) than that of MWCNTs (0% increase in UCS vs. control).

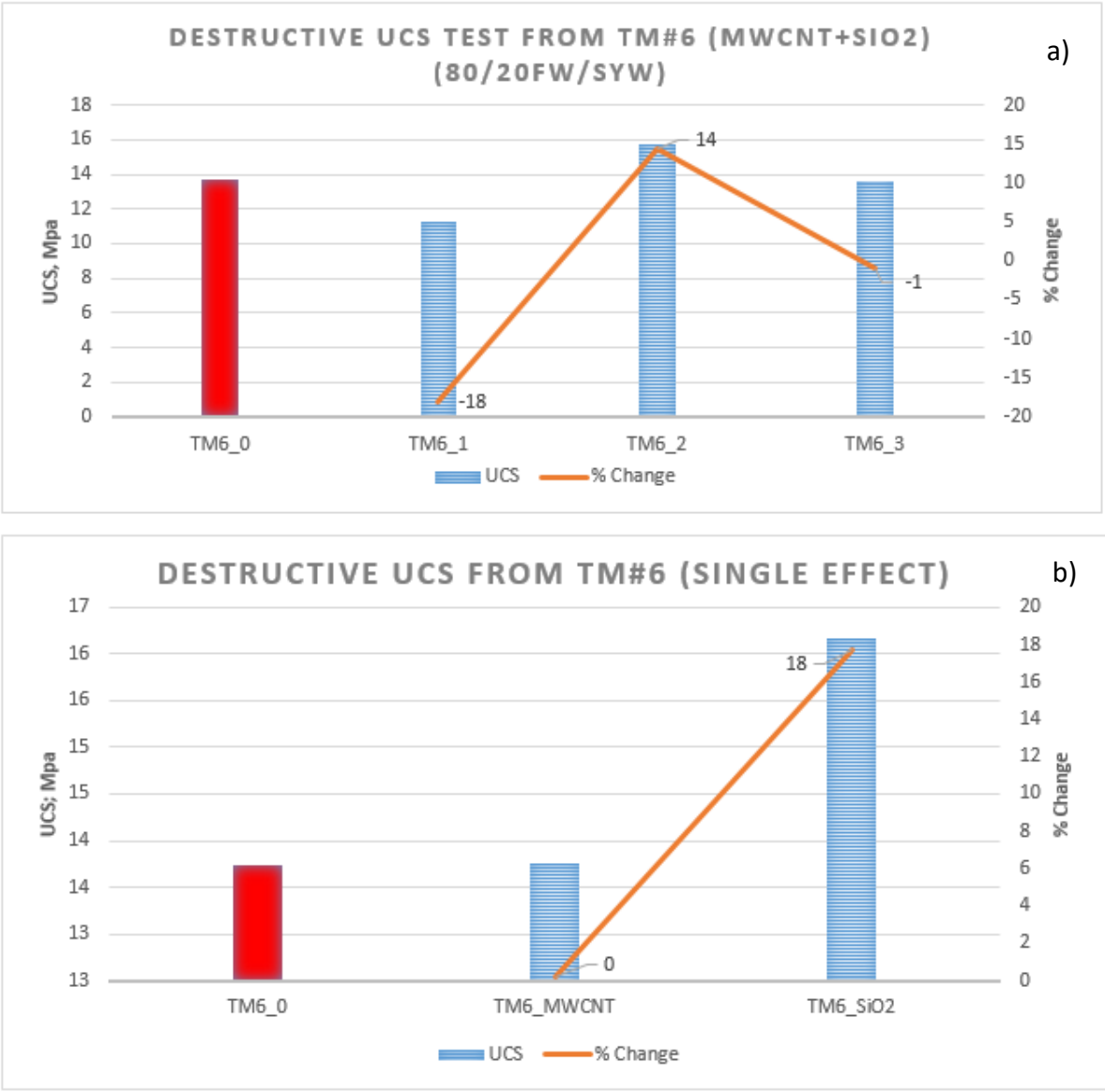

Figure 4-7: Destructive UCS from TM#6 after seven days of curing, using; a) nanocomposites, b) single nanos

These results lead the author to further support the conclusion that smaller concentrations of MWCNTs (<0.08wt %) yields more desirable properties in terms of elasticity and compressive strength of hardened cement paste. Additionally, when using MWCNT-SiO_2 nanocomposites, they complement each other better with an equally large concentration (as long as MWCNT stays below 0.08wt %). Why use a composite when the single-effect of SiO_2 yields the highest UCS? First of all, the composite is marginally weaker and in addition has a much higher elasticity (**figure 4-4c**). Both nanoparticles can boast desirable strengths which is highly beneficial to utilize, like that silica enhances production of C-S-H gel and MWCNTs' needle-like structure is good for reinforcing cement.

4.5 Heat of Hydration of cement with MWCNT-additive (TM#7)

The design background for this matrix is presented here. It is reiterated that a weaker cement (WCR: 100/166 ≈ 0.602) was utilized in this slurry formulation compared to most other matrices (WCR ≈ 0.523). The water system utilized is the one that was discovered from TM#1 as the optimal water solution; 20/80 SYW/FW mix. The procedure for the heat development is outlined in section 3.4.1.6. The temperature development was logged for five days, but it only required three days for the cement to reach room temperature.

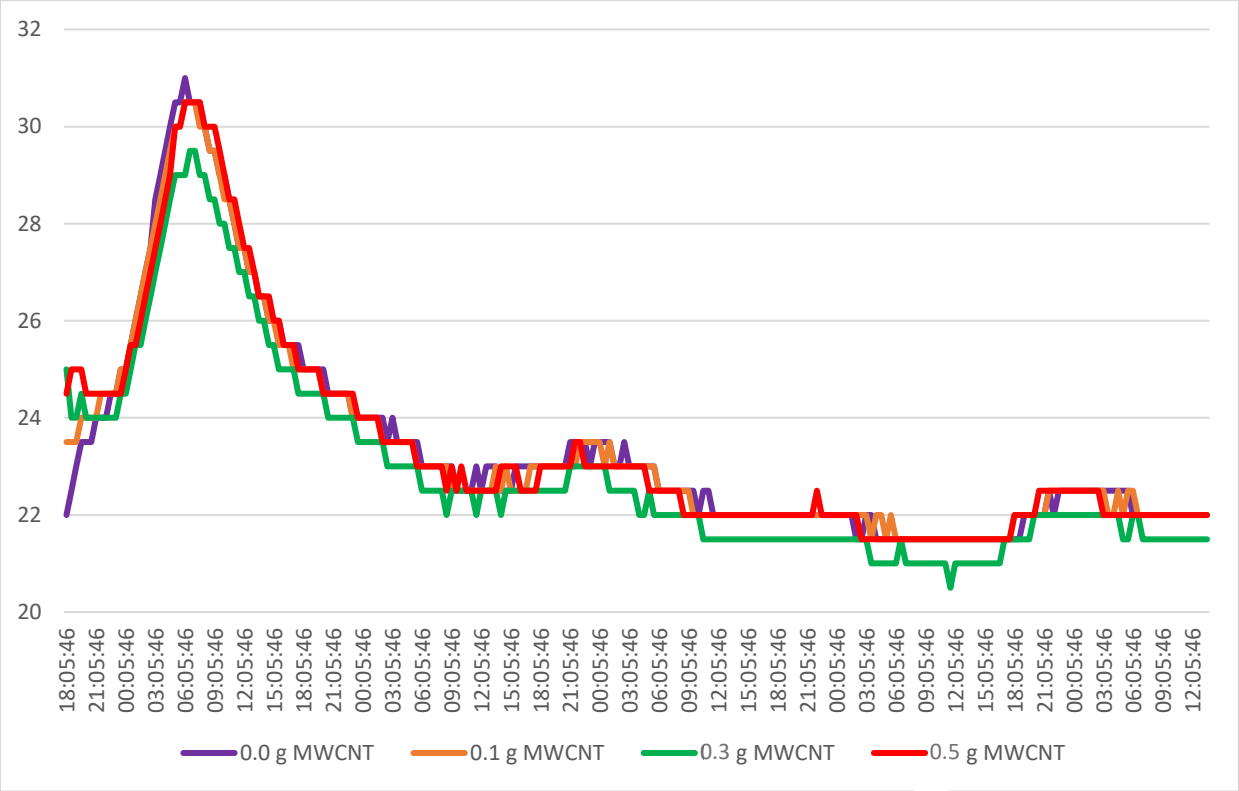

Figure 4-8: Exothermic reaction because of hydration of cement

Figure 4-8 presents the development of heat during the cement hydration process. The first observation we can make out is that this figure is comparable to the general heat of hydration curve from **figure 2-13** in subchapter 2.2.4, which indicates that the experiment was a success. The heat sensors were programmed to log the temperature every 30 minutes (instead of shorter intervals) which is the reason for the uneven curve. However, there is no problem observing a small trend. Some faults may exist in the setup in the way that the cement volume was so low that it is likely that the heat sensors were relatively close to the surface of the cup and thus closer to the outer environment, affecting the results.

The initial heat development (stage one-mixing) (ref) is not registered in this experiment as it begins the moment when cement makes contact with water and lasts only about 15 minutes, and therefore, the initial peak observed from **figure 2-13** is not observed in **figure 4-8**. Additionally, the heat sensors were not lowered into the respective cement slurry specimens before each of the four specimens had been created and the temperature sensors had been calibrated, which means that the initial stage was most likely already complete by the start of this experiment. A small "peak" can be observed right at the start of the experiment, from the green curve (0.3gr/0.18wt % MWCNT) and the red curve (0.5g/0.3wt %) MWCNT. It is likely that this early "peak" is the aftereffects of the initial exothermic reaction, which makes sense since said plugs were prepared last and thus had the sensors lowered into the cement relative to its formulation earlier compared to the first two, which shows no initial peaking. The dormancy period (stage two - induction) (ref) lasts approximately 2.5 hours before the hardening process begins (stage three – acceleration) (ref), which can be observed as the steep hill before the peak. In all cases it seems that MWCNT affects the temperature development in a positive way compared to the control sample which has the highest peak. It is noted, however, that the y-axis has very short intervals (to be able to make out the differences in the curves) but in reality the differences are quite low, as illustrated in **figure 4-9**.

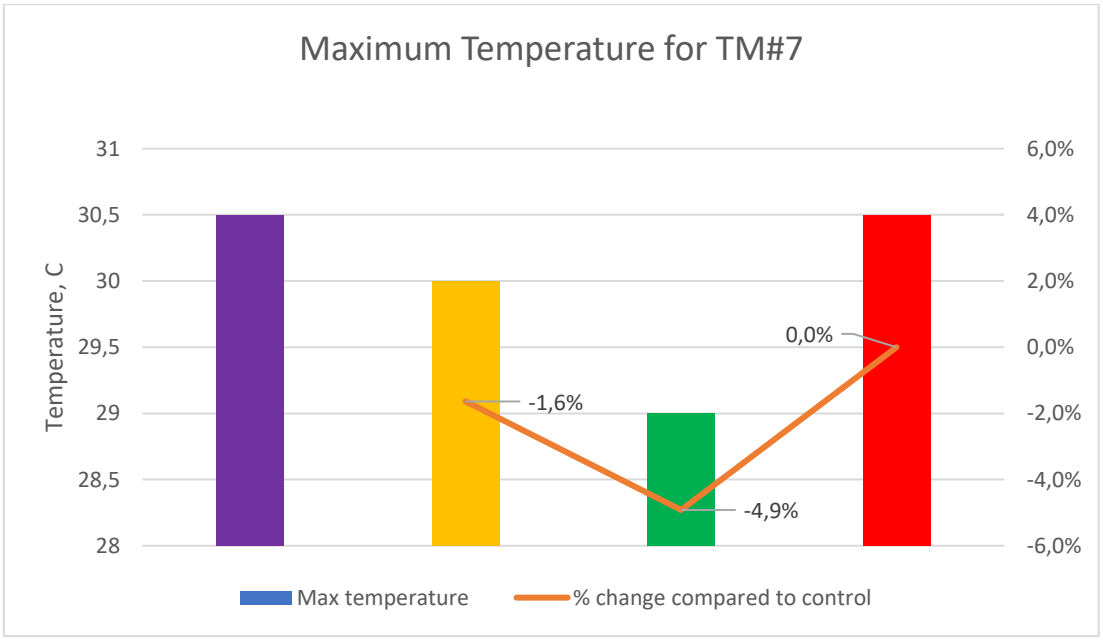

Figure 4-9: The peak differentials between the different slurries from TM#7

4.6 Heat of Hydration of cement with MWCNT-additive (TM#8)

The aim of the TM#8 design is of the same nature as for TM#7. However, in TM#8 the water system and cement strength differ, using freshwater (FW) and WCR≈0.523, respectively. A larger volume of cement slurry was utilized in this experiment with the intent on filling the entire compartment illustrated in **figure 3-15a**, in section 3.4.1.6.2, compared to the setup in TM#7, illustrated in the same figure with in **figure 3-15c**. The remainder of the slurry was poured into plastic cement molds to perform destructive tests on later (TM#9).

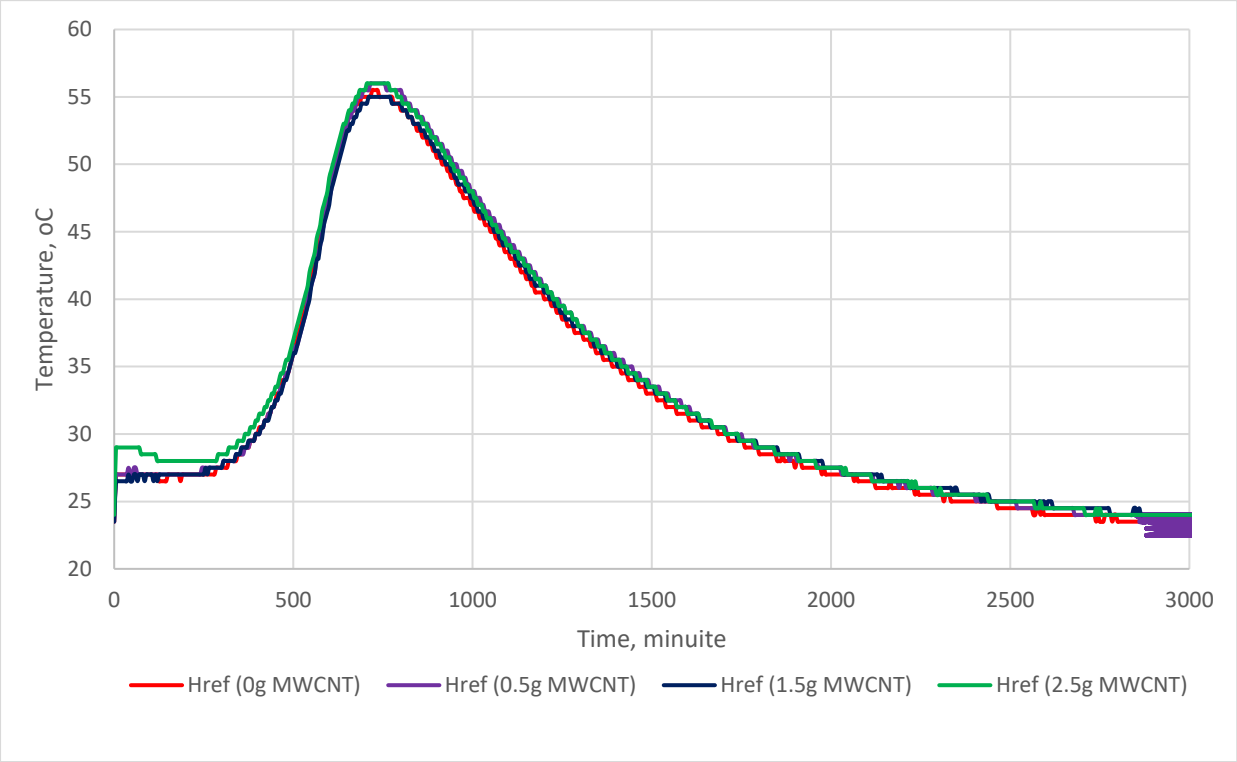

Figure 4-10: Heat of hydration for TM#8

Figure 4-10 display the data from the logged temperature experiments from TM#8. Like **figure 4-8** a similar trend can be seen relative to the expected hydration curves illustrated in **figure 2-13**. Immediately one can observe smoother curves from TM#8 compared to TM#7. This was due to programming the temperature sensors to log the temperature every five minutes, compared to every thirty minutes as in TM#7. As explained in the previous section, it is likely that the aftereffects of the initial exothermic reaction during the first stage is seen in the earliest phase of the cement specimen that was formulated last, namely the green curve containing 0.26 wt% MWCNTs. **Rahimirad et al. (2012)** [3] reported a 12-20% lower heat conductivity by adding 0.05wt% MWCNT into the slurry mix but is not seen in this study.

There is a large difference between the results from TM#7 and TM#8 with as much as 25.5 °C variation between the peaks. Since both experiments contains the same relative amount of MWCNT it is safe to assume that MWCNT is not the reason behind it, but rather the amount of cement, as TM#8 used five times the cement volume compared to TM#7 and according to **(PCA 1997)** [53] that is one of the major influencers on cement hydration.

Furthermore, no observation is made regarding any particular benefits to adding such a small amount of MWCNT in cement slurry treated with freshwater.

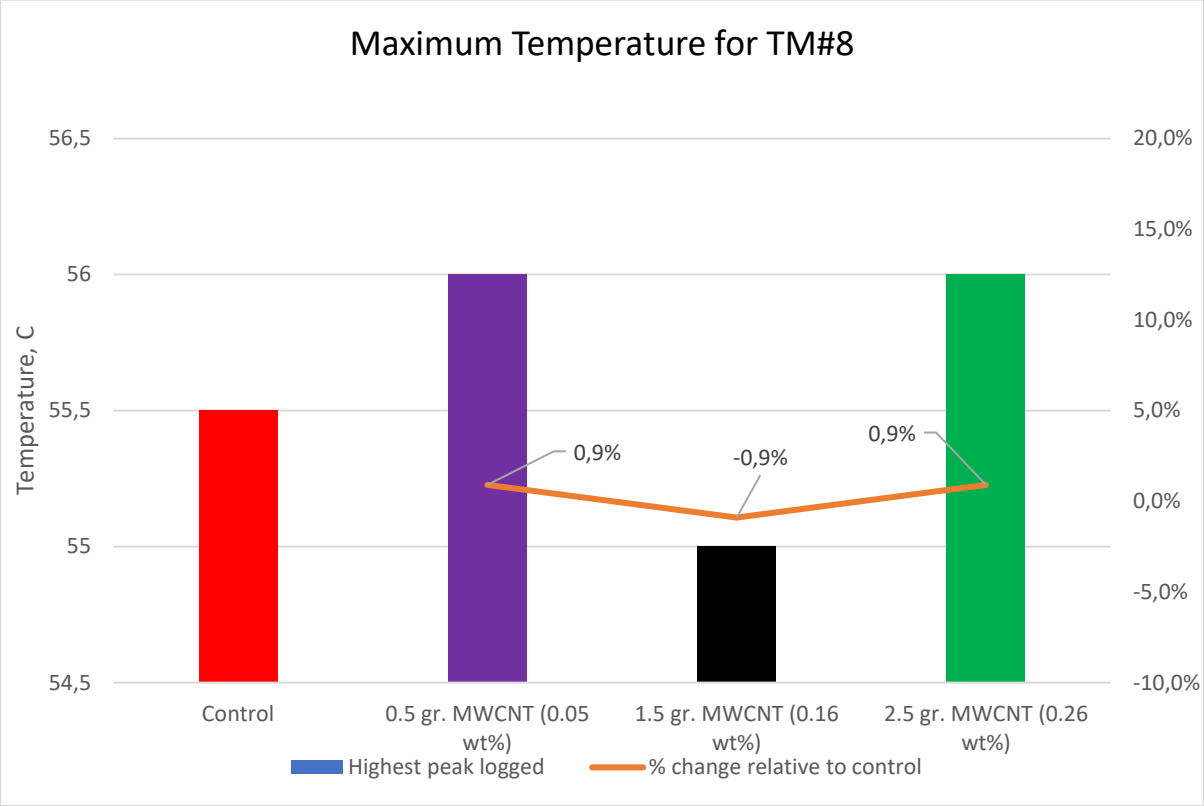

Figure 4-11: The peak differentials between the different cement slurries (TM#8)

4.7 Effect of Rubber Silicones on FW cement (TM#8 & TM#9)

One slurry mix for each specimen was created and poured into a steel cylinder (**figure 3-17,** section 3.4.1.7) with which leaking tests would be performed. The leftover slurry was poured into the cylindrical plastic molds, same as used for all other cement plug creations, and cured for one day, air dried for one additional day until being immersed in water until their destruction after seven days. A special emphasis was kept on keeping a high mechanical dispersion of the slurry between the two pouring sessions to avoid the particles conglomerating into solely the steel cylinder or plastic mold. Below is an explanation of the denotations used in the graphs below.

H1: 0.05wt%MWCNT, H2: 0.16wt%MWCNT, H3: 0.26wt%MWCNT

T: acid-treated, U: untreated, H: high concentration (4.0wt%), L: low concentration (1.5wt%)

4.7.1 Non-destructive Test Results From TM#8 & TM#9

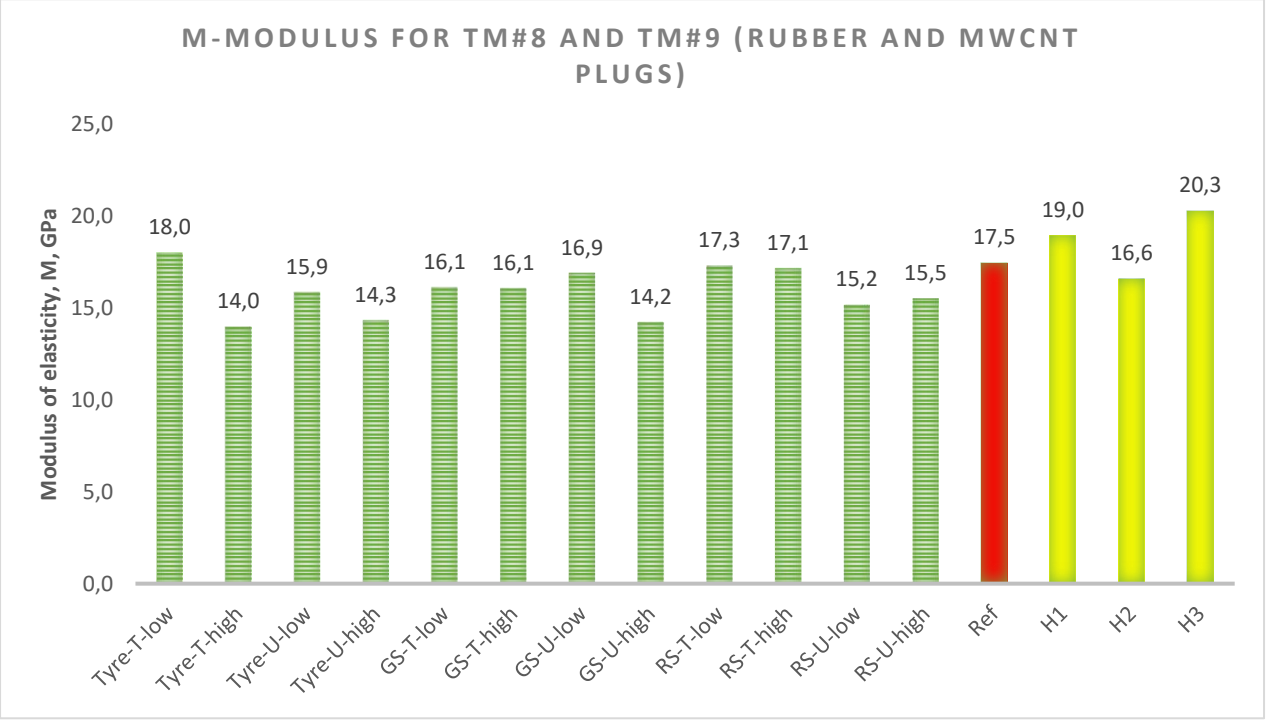

Figure 4-12: M-modulus for TM#8 and TM#9 after seven days of curing.

From **Figure 4-12** one can determine that are no clear trend on the development of M-modulus of cement comparing acid-treated rubber and untreated rubber, but when comparing concentrations of rubber replacement in cement, the lower dosage clearly outperforms the higher.

Compared to the reference (red) the addition of rubber elements into the cement, treated and untreated resulted in a decrease in M-modulus (except for Tyre-T-L). Most plugs containing MWCNTs are clearly outperforming those containing rubber. This can be due to many factors, one of them being that the particles are quite large (compared to nano-sized materials) and thus would do a poor job filling the pores of a cement structure where a nano-sized material would easily penetrate the pores making the material denser and stronger.

4.7.2 Destructive Test Results From TM#8 & TM#9

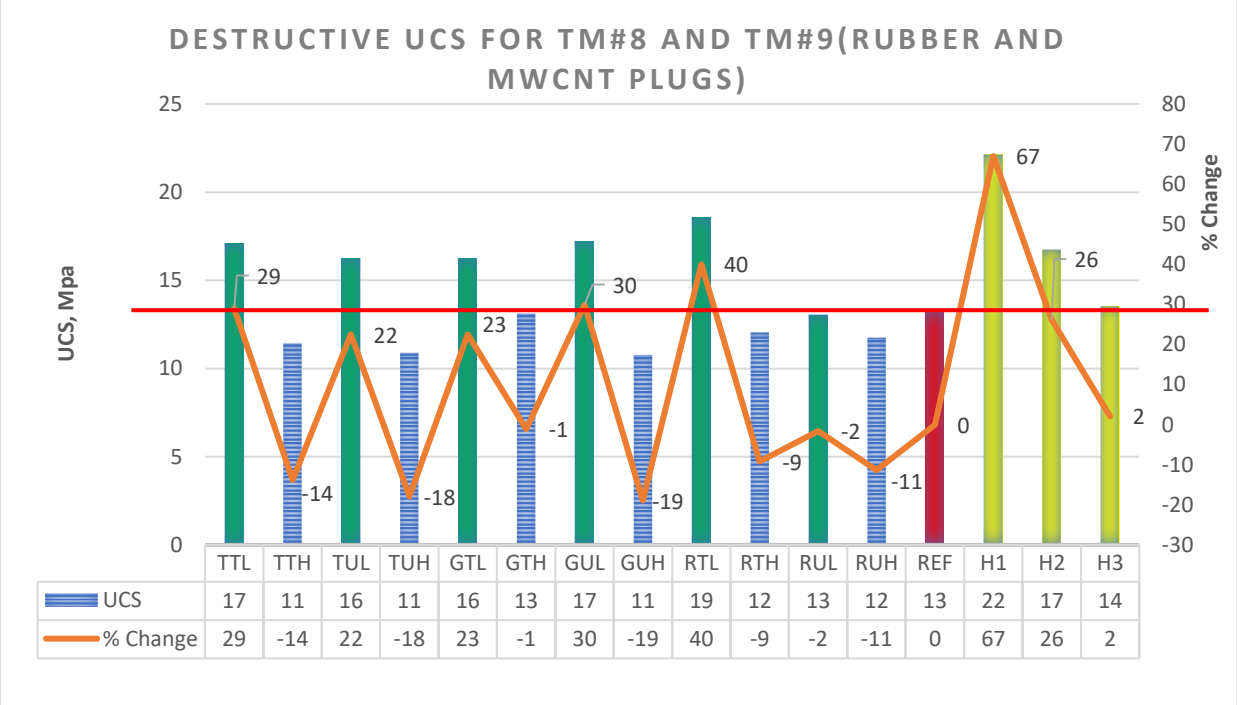

	TTL	TTH	TUL	TUH	GTL	GTH	GUL	GUH	RTL	RTH	RUL	RUH	REF	H1	H2	H3
UCS	17	11	16	11	16	13	17	11	19	12	13	12	13	22	17	14
% Change	29	-14	22	-18	23	-1	30	-19	40	-9	-2	-11	0	67	26	2

Figure 4-13: UCS results from TM#9 and TM#8 after seven days of curing

Figure 4-13 presents the results from the destructive test on the cement plugs from both TM#8 and TM#9. A reiteration to avoid confusion; except for TM#8 also being poured into polystyrene boxes to measure the temperature development, TM#8 and TM#9 was made at the same time and in the same way, both slurry mixes being poured into both steel cylinders and plastic molds, to measure leakage and strength respectively, and thus the results are comparable. The first observation from the destructive test result is the clear trend stating that a lower concentration of additive (both silicone and MWCNT) is considerably more desirable compared to higher concentrations. All lower-concentrations rubber plugs (except for untreated red silicone (RUL) and plug H3 shows a significant improvement in strength

compared to the control sample (red column). The ones containing higher concentrations of rubber is weaker than the control, which means that there is clearly an optimum concentration of rubber for cement replacement. The results of TM#9 with respect to the rubber from scrap tyres contrast with what was discovered by **Abdullah et al. (2016)** [61] whom in their experiments claimed that a higher concentration of rubber replacement for cement yielded better results in terms of the compressive strength (up to a certain point) and also stated that generally cement would be 6-21% weaker with rubber replacements than normal cement, while in this thesis was discovered that rubber additives (in low concentrations did in fact increase strength of cement by 22-40% compared to control.

H1 – 0.05 wt% MWCNT – is clearly the strongest plug and towers above the rest. This can be due to its much smaller size (prepared before purchased) in contrast to the silicones (manually cut and prepared after purchase) and thus is more efficient at penetrating the pores and help make the cement denser. It is also known to affect the formation of C-H-S gel, which in turn is a major factor in strength development [62]. Comparing the rubbers individually, small deviations in strength is observed between the acid-treated and untreated rubber samples except for (GTH and GUH) and (RTL & RUL). SEM analysis performed on one rubber sample (red silicone) before and after acid treatment (from section 3.2.4) showed a severely changed surface area (as intended) and one would expect the samples with the rougher surface fusing better with the cement's intergranular structure, as documented by **Colom et al. (2007)** [47].

4.8 Effect of MWCNT and Rubber Additives on Leakage

Cement was mixed and poured into ad-hoc casing cylinders. They cured for one day and was put into an oven at 110 ^{o}C for 24 hours, then rapidly cooled under running water to create a worst-case scenario (rapid cooling) discussed on **page 26** and **page 57** of this thesis. In lack of a proper pressure testing machine to detect leaks and bonding, water was poured on top of the cased cement to induce a hydrostatic pressure and the casings were left in room temperature for 24 hours and leaks were registered the next day. This process was repeated in four thermal loading cycles. After the rapid cooling of the casings, some of the cement specimens inside the casing would move when inverted, which would indicate a broken cement-casing-bond compared to the samples that were still locked tight within the casing after being exposed to the same conditions. Cycle 1 through 4 for all the cased cement

subjects had a dissimilar volume of water on top due to the varying volume of cement within the casing, but the results have been normalized in **figure 4-15** and **figure 4-16.**

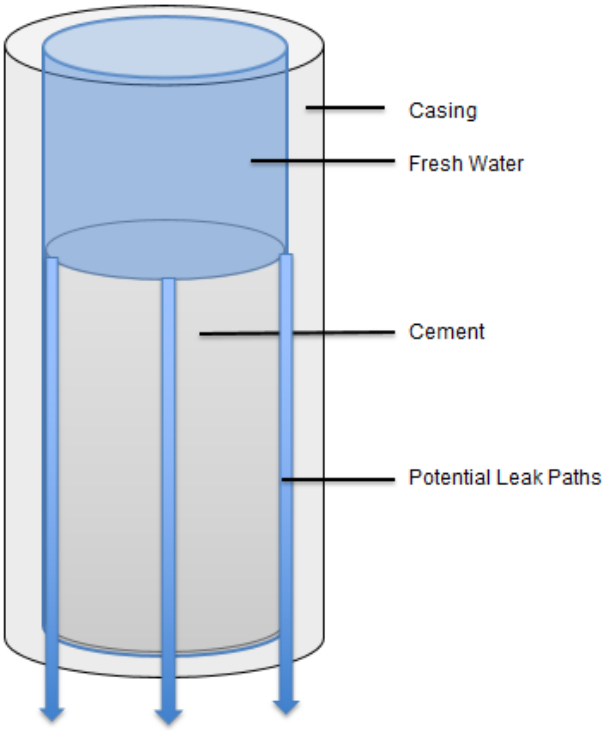

Figure 4-14: Expected leaks around cement when the casing-cement-bond has failed (Aarnes 2018)

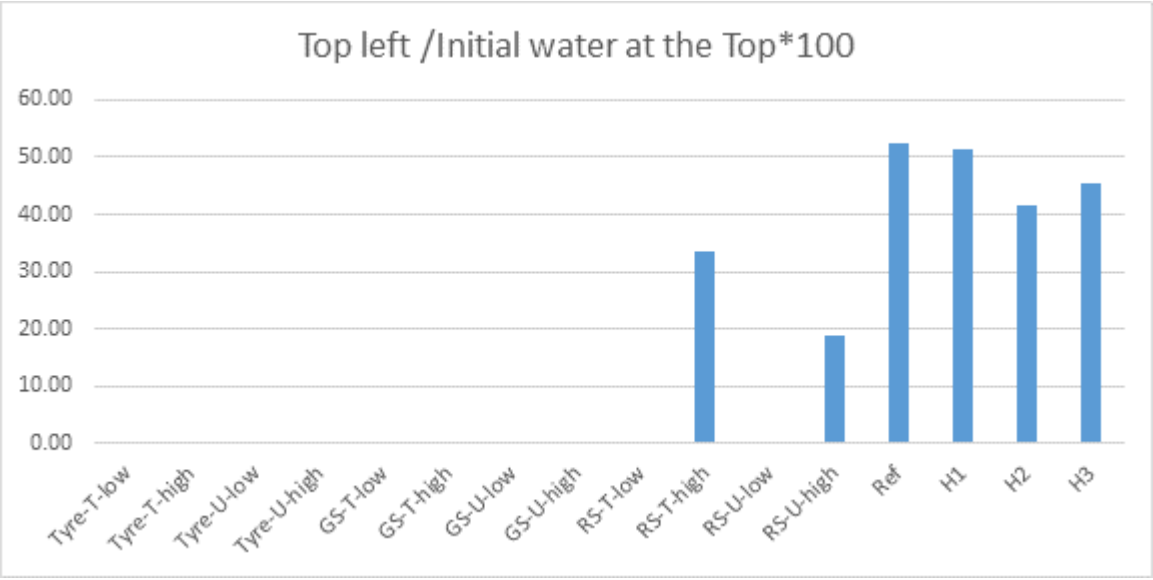

Figure 4-15: Original water content on top relative to what remains after 24 hours (in %)

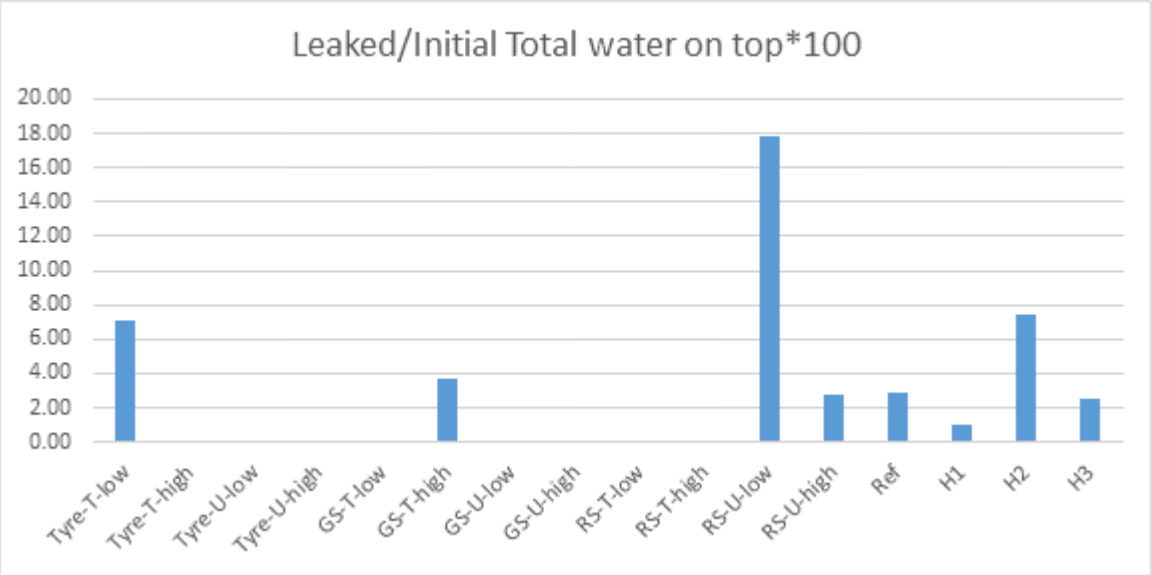

Figure 4-16: Leaked volume with respect to original water content (in %)

4.8.1 Observations and Results from Leakage Tests

The first comment of figure **4-15** and **figure 4-16** is that plug TTH, TUL, TUH, GTL, GUL, GUH, RTL and RTH have all retained the entire volume of water that was added on top, as there was no water in either the cup or the top of cement at the end of a cycle. Likely there has been some water evaporation, but with normal room temperatures and 24-hour timeframe it is expected to be insignificant.

Though no leakage could be measured from the abovementioned plugs it does not disclose them as impermeable, however, as a leak would most likely occur given more time and more water. The rubber plugs with a registered leak (TTL, GTH. RUL and RUH) all had 15±5ml more water content than the first-mentioned specimens, which would make this theory correct. The case for all rubber plugs is that the water content is much lower (in terms of volume) than that of cement which makes it a possibility that the cement has absorbed every drop of water (excluding evaporation). In contrast, all the plugs containing MWCNTs (in addition to "Ref") had more than 30ml of water added on top compared to the rubber plugs and despite this, 40-50% of the water had not penetrated the cased cement. Although the rubber plugs with a low concentration was proven to be significantly stronger than the control, they are however, exposed to extensive leaking, which according to NORSOK would be an unacceptable design.

Cement containing 0.05wt% MWCNT comes out on top (again) as the one with the lowest leak %, taking into consideration leakage through the cement core and water retention.

4.9 MWCNTs' Effect on Rheology

Rheology describes the flow of matter and is an important factor in the petroleum industry when it comes to producing and transporting fluids. A fluid may exhibit some desirable properties (e. g., strength development of cement), but at the same time display undesirable properties (e. g., too high viscosity, making it impossible to pump) and therefore doing these experiments with cement slurry mixed with MWCNTs is of great importance. Four different slurries were mixed, adjusting only the concentration of nanoparticles. In a similar fashion to most experiments in this thesis; low concentrations of MWCNTs were used.

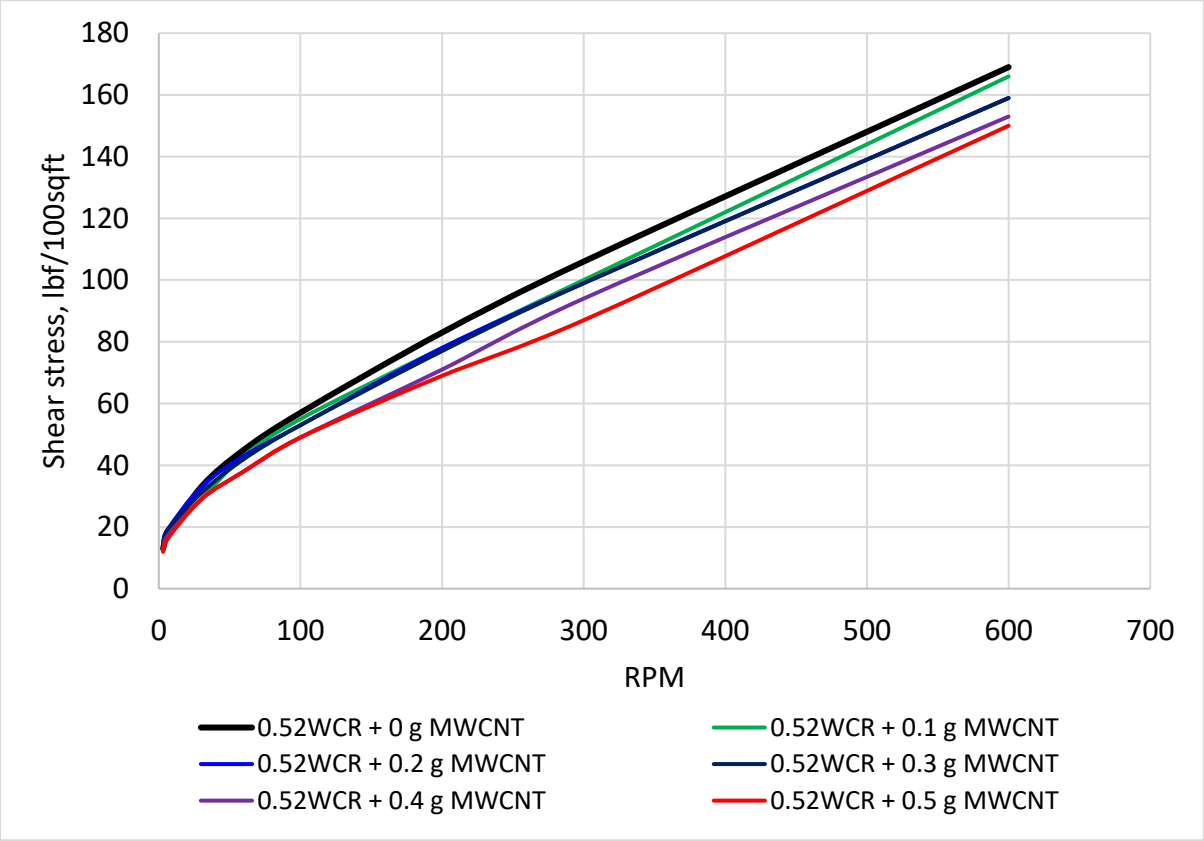

Figure 4-17: Shear Stress of cement slurry with MWCNT (lbf/100sqft)

Figure 4-17 shows that by increasing the amount of MWCNT additives in cement, the shear stress (lbf/100sqft) exhibits substantially lower shear rheology properties compared to the control sample in the interval 50-600 RPM. In fact, a reverse proportional trend is observed

between shear stress and concentration of MWCNTs added to the slurry mix in the interval 50-600RPM with the control sample – zero nano – facing the highest shear stress at 600 RMP and sample 6 – highest nano – facing the lowest shear stress at 600RPM.

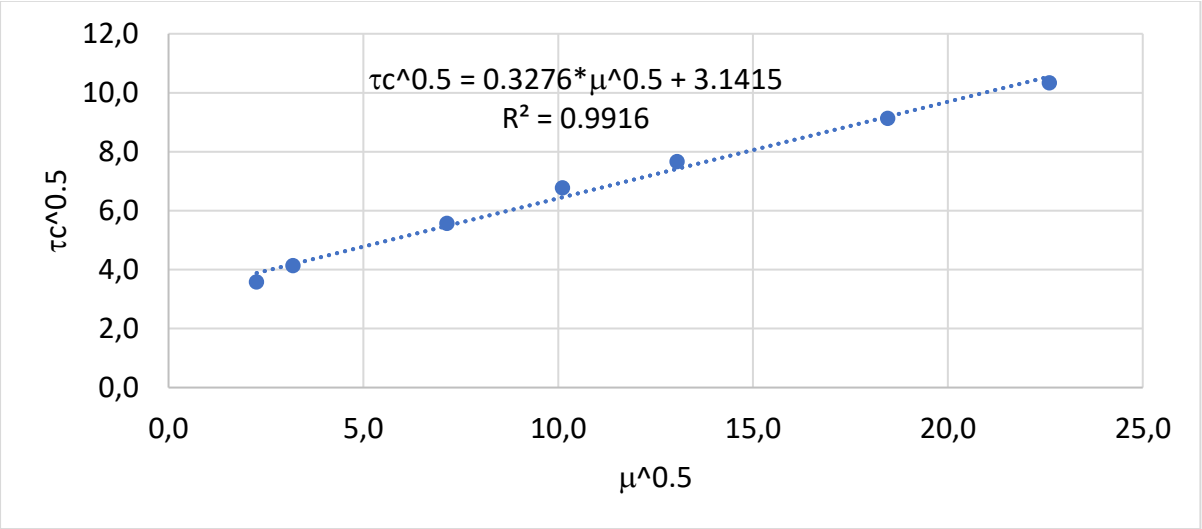

Figure 4-18: Rheology modelling example

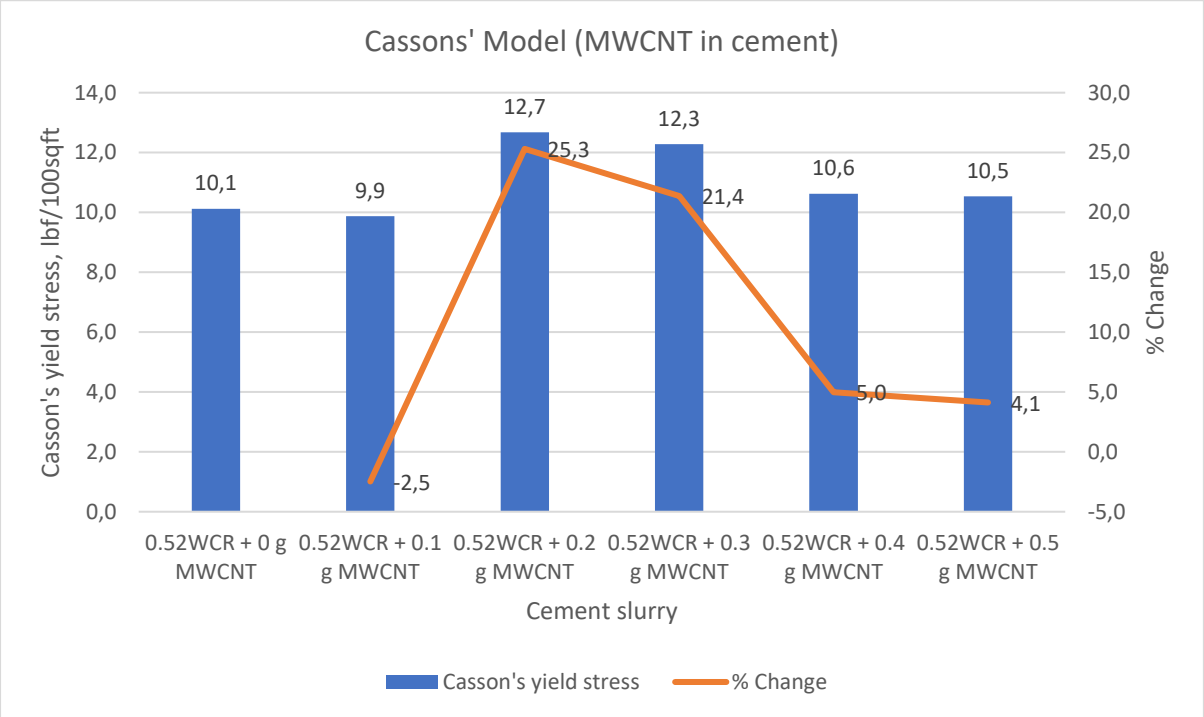

Figure 4-19: Casson's yield stress (lbf/100sqft)

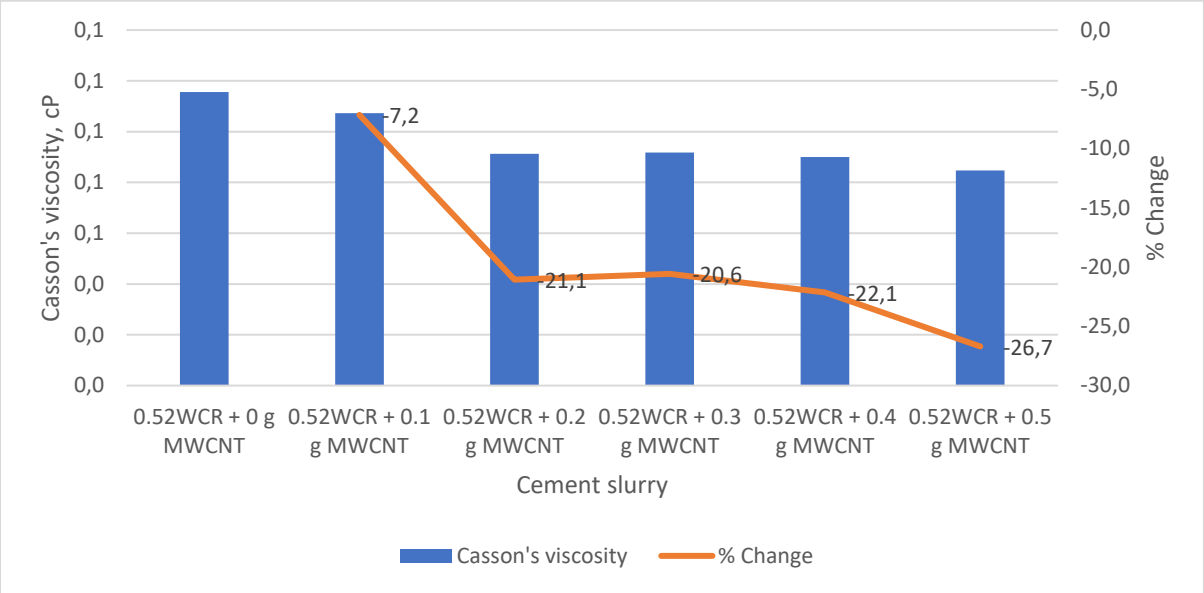

Figure 4-20: Casson's viscosity, cP

As discussed, rheology is an important factor in the petroleum industry as it describes the motion of fluids. Many fluids exhibit higher viscosities (e. g., oil, shampoo, sour cream) and thus would need external forces (input of stress) to behave like we want. How said fluids behave when this stress is imposed upon them is the very heart of rheology. Yield stress of a fluid for instance, determines how much energy is needed to cause it to flow (e. g., cement slurry pumps or oil pumps through pipelines) [63]. **Figure 4-19** present the results from Casson's model of yield stress and display no clear trend of fluid yield stress and MWCNTs added. **Figure 4-20** on the other hand, display a trend of decreasing viscosity in a reverse proportional relationship with concentration of MWCNTs added in the slurry, with 0.5g (0.26wt%) MWCNT addition reducing the Casson's viscosity by 26.7 % compared to the control sample. No plateau was reached during this experiment, so the optimum concentration of MWCNT for the lowest possible viscosity is not known. It is hard to conclude if the results are good or bad as sometimes it is preferable with higher viscosities (e. g., cutting transport and hole cleaning) and other times it would be beneficial with lower viscosities (e. g., fluid transport). However, for a better evaluation with regards to the rheology of the slurries, it is important to design a simulation-well and simulate the measured viscometer data influence the well pressure during a cementing job. This can be done with commercially available softwares, but due to time constraints, this was not investigated in this thesis' work.

4.10 SEM, - and EDS-Analysis

Scanning Electron Microscopy (SEM) and Energy Dispersive X-ray spectroscopy (EDS) has been discussed in section 3.4.1.5 and in this segment only a short introduction will be made. The SEM-analysis provides very high-resolution images of the surface of a material (better than 1mm) [52] whilst the EDS-analysis provides an element content analysis for a specific point. The aim with these analyses was to analyze the internal structure of the cement slurry and how MWCNT deposited in the pore structure and how they are distributed in cement. Preparing the samples and locating MWCNTs dispersed in the cement slurry mix, manually, is time-consuming and generally has a low impact on the results. That is why only one set of samples were chosen to be studied. **Figure 4-21** presents a SEM-image of plug TM#4_4 – containing 0.5g (0.26wt %) MWCNT –. By comparing this image with other sources (**Geng et al. (2015)** [64]) one could conclude that these indeed are MWCNTs. This is further evidenced by **figure 4-22** from the EDS-analysis showing a very high presence of carbon.

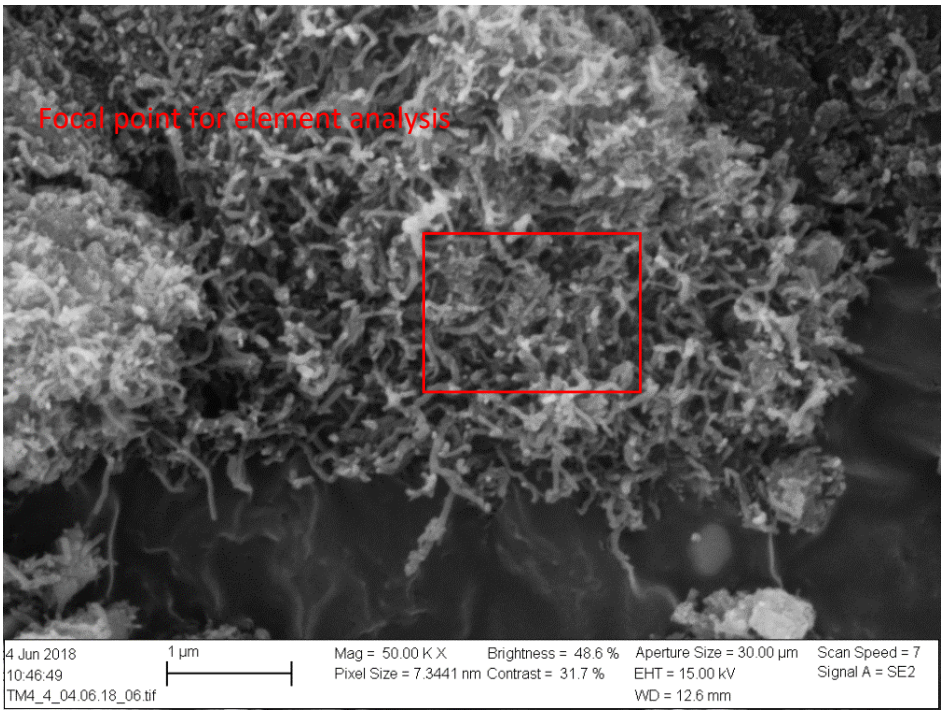

Figure 4-21: MWCNT after crushing samples to powder from TM#4_4

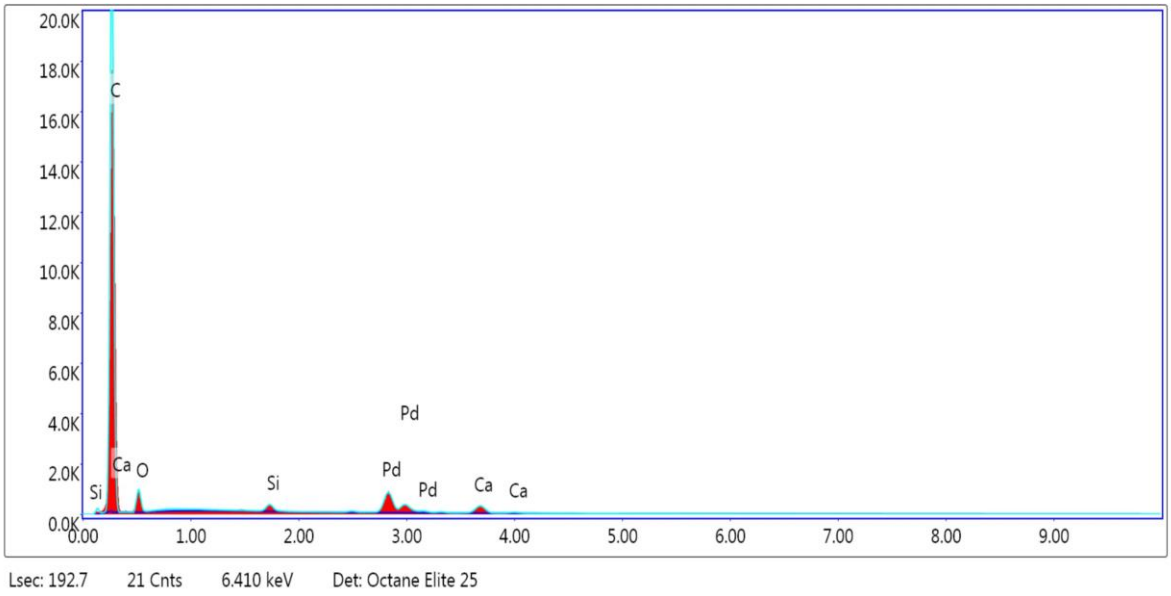

Figure 4-22: Element analysis of figure 4-34 proving a presence of MWCNT

Figure 4-23 is another image of the same specimen at a different location finding carbon nanotubes embedded in the cement structure. By visual comparison with **figure 4-23** these MWCNTs are clustered within the cement structure and a bond can be seen between them.

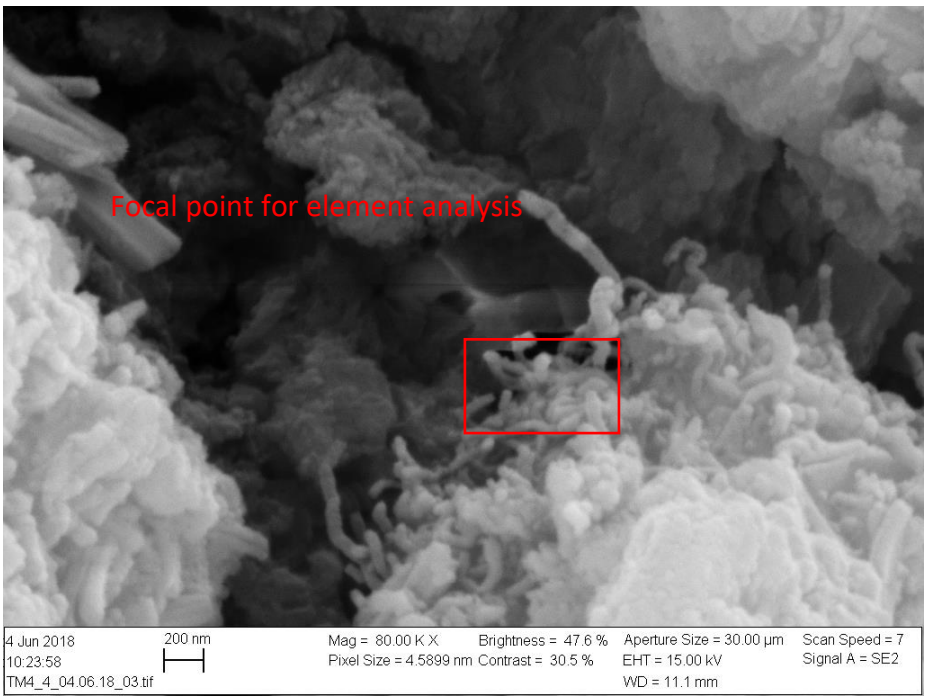

Figure 4-23: Another sample from TM#4_4 showing MWCNT embedded in cement

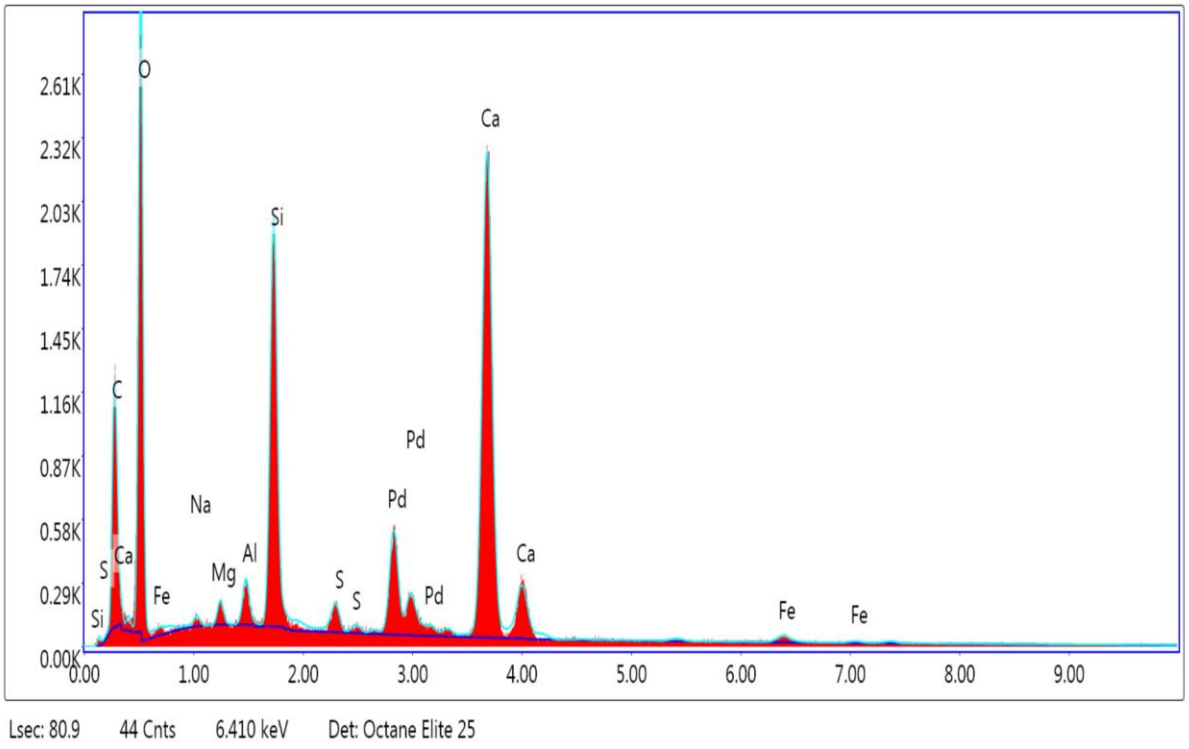

Figure 4-24: Element analysis of figure 4-36, hinting to presence of MWCNT

The element analysis from the second image shows a lesser degree of carbon than in **figure 4-22** which was expected since the first image (**figure 4-21**) the MWCNTs observed was from a powdered sample which makes each element much easier to spot with SEM-imaging, but **figure 4-23** was a solid sample directly plucked from central parts of the remains after destructive tests where the nanoparticles would be more embedded in the cement structure and thus the element analysis would not depict equally high presence of carbon and much higher oxygen and calcium content.

These analyses would be crucial if the goal were to study micro cracks or pores of materials, but in this thesis, however, they serve a purpose of providing supportive data. Besides, it is very difficult to observe the SEM images and conclude if the dispersion of MWCNTs in cement is uniform or not.

4.11 Potential Failure Modes and Uncertainties

This section provides some factors that would likely have affected some experimental results.

Equipment: Most papers and field cases used as sources for this thesis have significant financial support to perform their experiments, ranging from oil companies to research institutes, ensuring high-quality laboratory equipment. As a student with no external funding and access to only basic and heavily used laboratory equipment, there were cases where creativity took precedence over quality (e. g., table legs from *Biltema* as ad-hoc casings).

Preparation of samples: Due to safety hazard and property rules set by the University of Stavanger, cementitious residue was not allowed to be rinsed with water as it might cure and clog the pipes and as such, manual paper towel hand-cleaning of the had to be performed between each plug, but cement residue was still present after each batch. Eradicating all traces of the previous mix would then be impossible unless a new cup was used between every mix, which is unrealistic.

Dispersion of nanoparticles: Ultrasonic dispersion methods are usually what researchers adopt when the dispersion of a nanomaterial in a fluid is the goal. **Gillani et al. (2017)** stated that "*The effect and behavior of MWCNT are entirely dependent upon the dispersion of MWCNT in the mix*". The mixes in this thesis were hand-mixed (due to the absence of a sonication device) and no surfactants were used. From each batch, some nanomaterial residue was observed on the inner surface of the cups. work The result of non-uniform dispersion (or an excessive amount of nanoparticles added) might be that the nanomaterials self-aggregate and as such will increase the particle size which might result in generating weak zones and void spaces, making the material's strength and overall durability less than ideal.

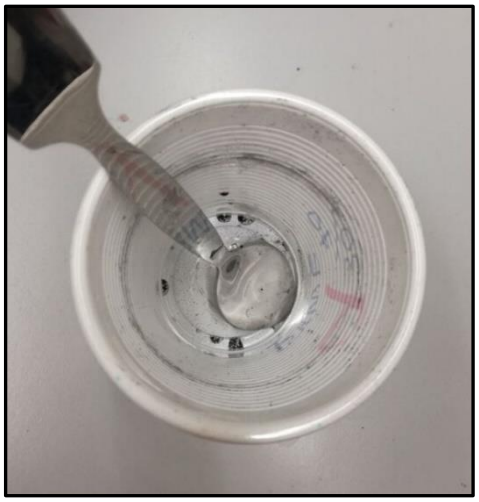

Repetitiveness of the experiments: To achieve the highest possible accuracy on experimental results, it is commonly advised to repeat an experiment several times over to continuously test and challenge that which is established after one trial run. However, in this thesis most experiments were performed over a single interval.

5 Modelling

In this chapter, a new empirical UCS-V_P based model will be derived. In literature, there are several empirical models available for use, among others Horsrud's model, presented in section 3.4.1.3.1. The model has been derived based on shale, which was extracted from the North Sea. First, the predictive power of the model will be tested using experimental data obtained in this thesis work.

5.1 Background for the Modelling

To evaluate the Horsrud model's predictive power, actual destructive UCS results were used from TM#1 and TM#2. As shown in **figure 5-1** and **figure 5-2** one can clearly observe a very significant difference between the measured UCS and the Horsrud model prediction (**equation 3-2**) with up to 54% deviation. Based on these results, it was clear that a new model for predicting the correct UCS value based on the P-wave velocity (sonic velocity) was needed.

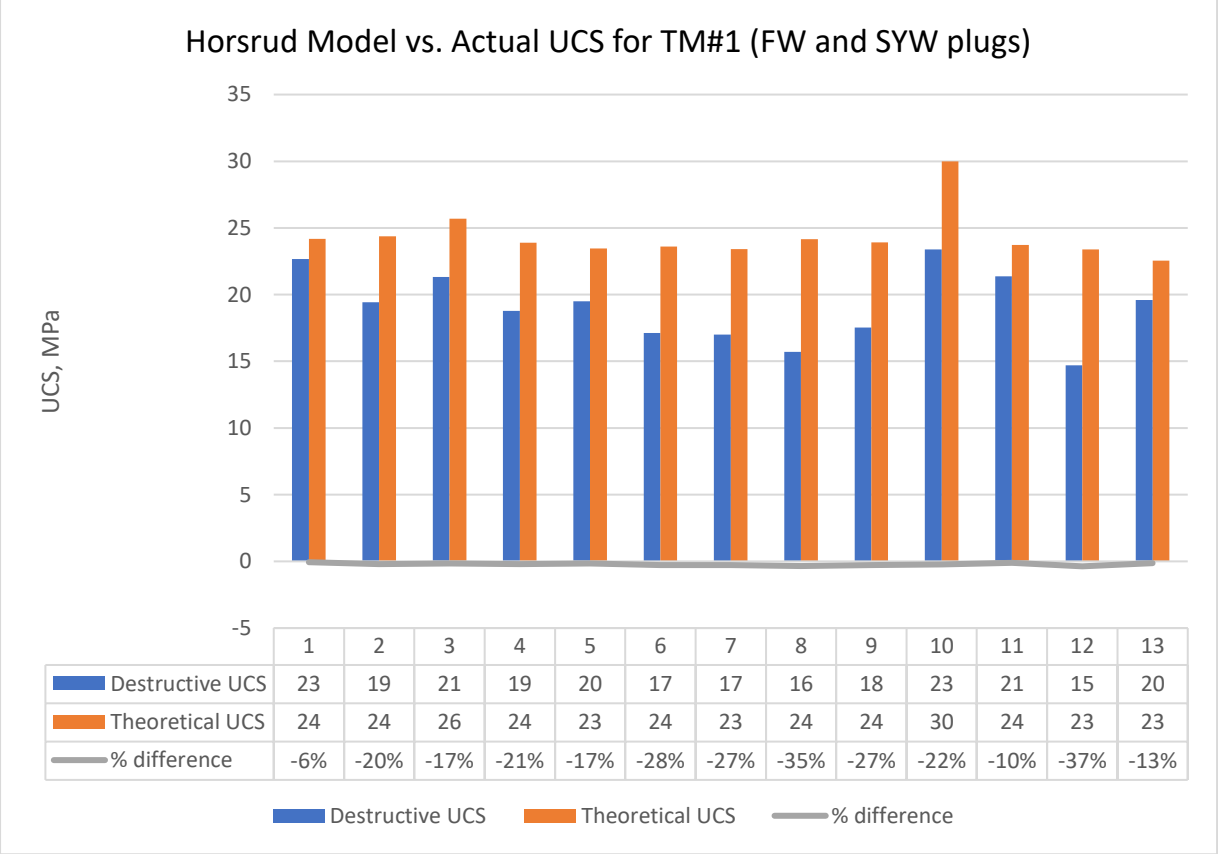

	1	2	3	4	5	6	7	8	9	10	11	12	13
Destructive UCS	23	19	21	19	20	17	17	16	18	23	21	15	20
Theoretical UCS	24	24	26	24	23	24	23	24	24	30	24	23	23
% difference	-6%	-20%	-17%	-21%	-17%	-28%	-27%	-35%	-27%	-22%	-10%	-37%	-13%

Figure 5-1: Horsrud's prediction of UCS based on sonic velocity vs. Aarnes' actual UCS test results (TM#1)

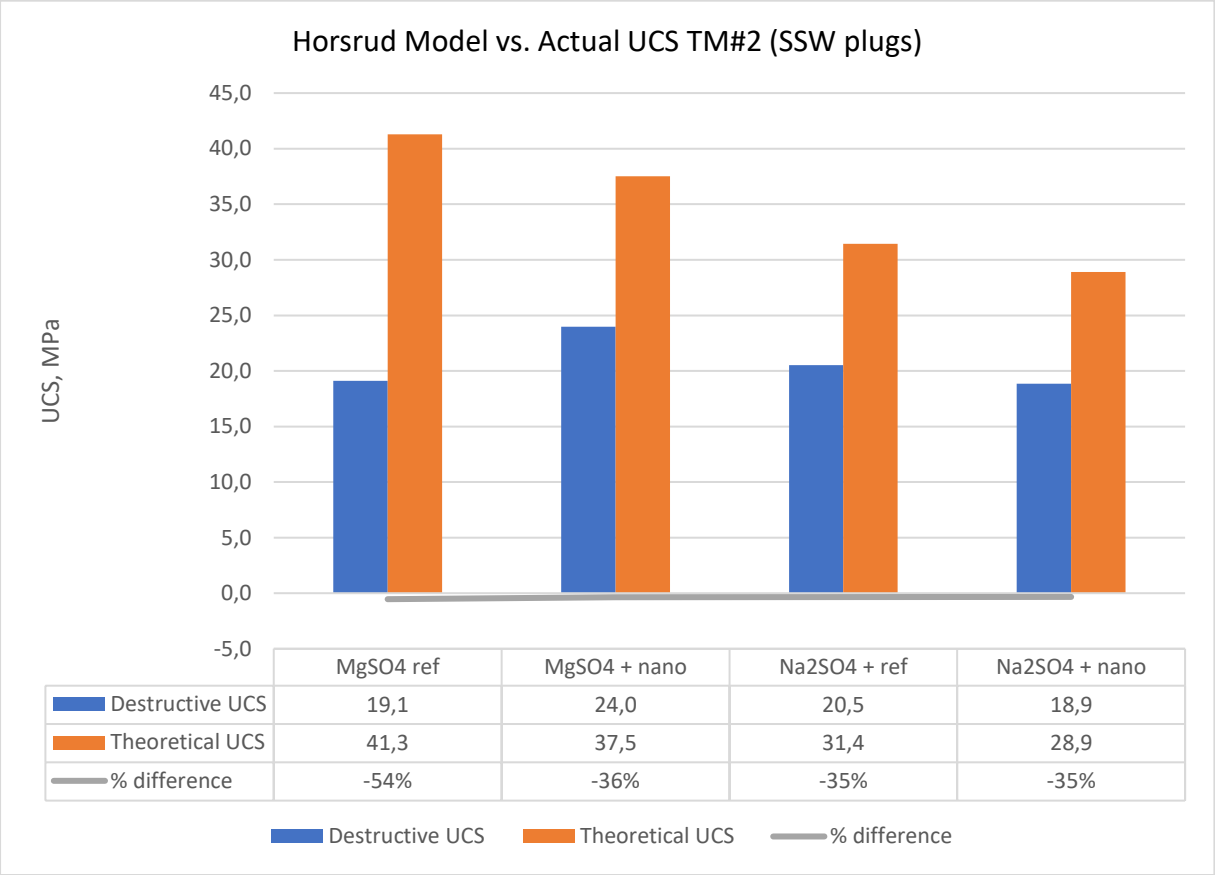

Figure 5-2: Horsrud's prediction of UCS based on sonic velocity vs. Aarnes' actual UCS test results (TM#2)

5.2 New Model Development and Testing

This section will present the new model based on the measured dataset. For the modelling, data from different test matrices of other students were used. Some of the UCS and V_p data were used for modelling and some of them were used for model testing. Moreover, cement-related data obtained from **Senoor & Zakaria (2018), Fridriksson (2017)** [65] and **Esquivel (2015)** [66] were used for model evaluation. The new model developed in this thesis work is given as **equation 5-1** and the modelling result is shown in **figure 5-3.** This modelling has used some of the UCS and V_p values from the experiments to predict the correct UCS based on P-wave velocity. **Figure 5-4, 5-5** & **5-6** presents some comparisons made with other experimental data to test the model.

$$UCS = 2.0 \cdot e^{0.65\,Vp} \quad (5\text{-}1)$$

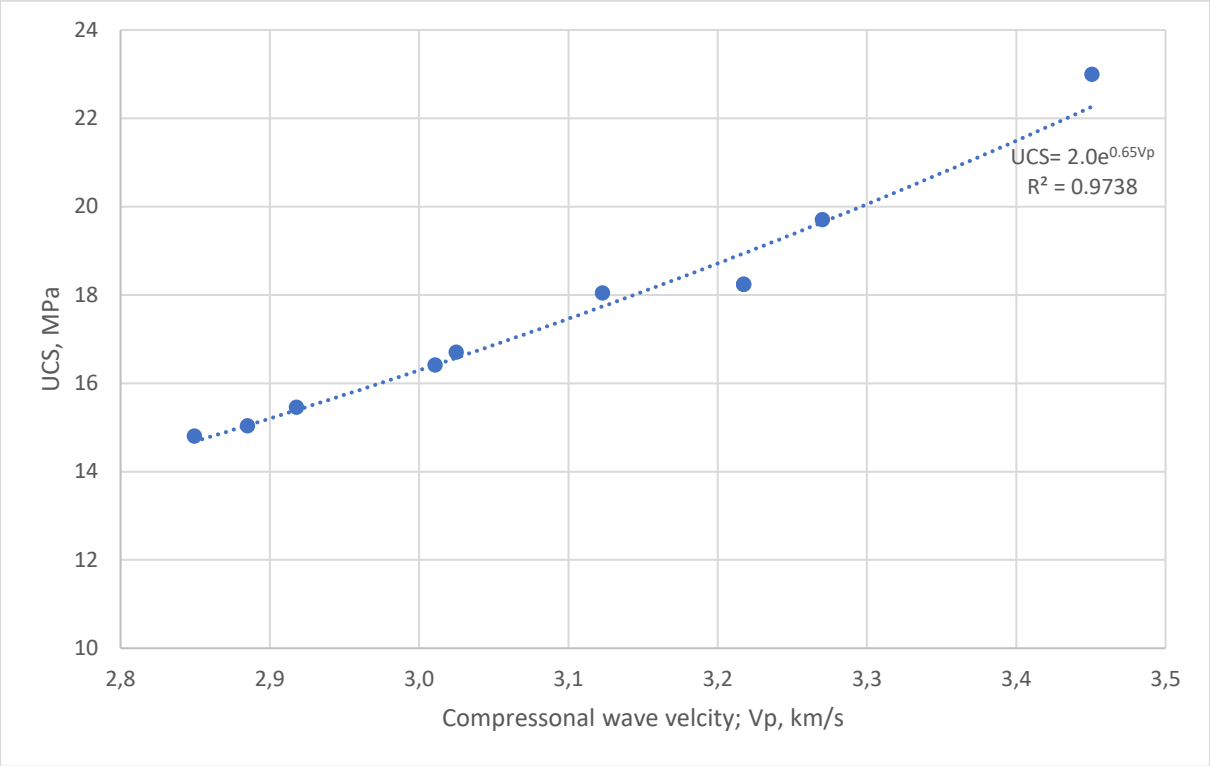

Figure 5-3: Modelling chart to increase the accuracy of UCS prediction

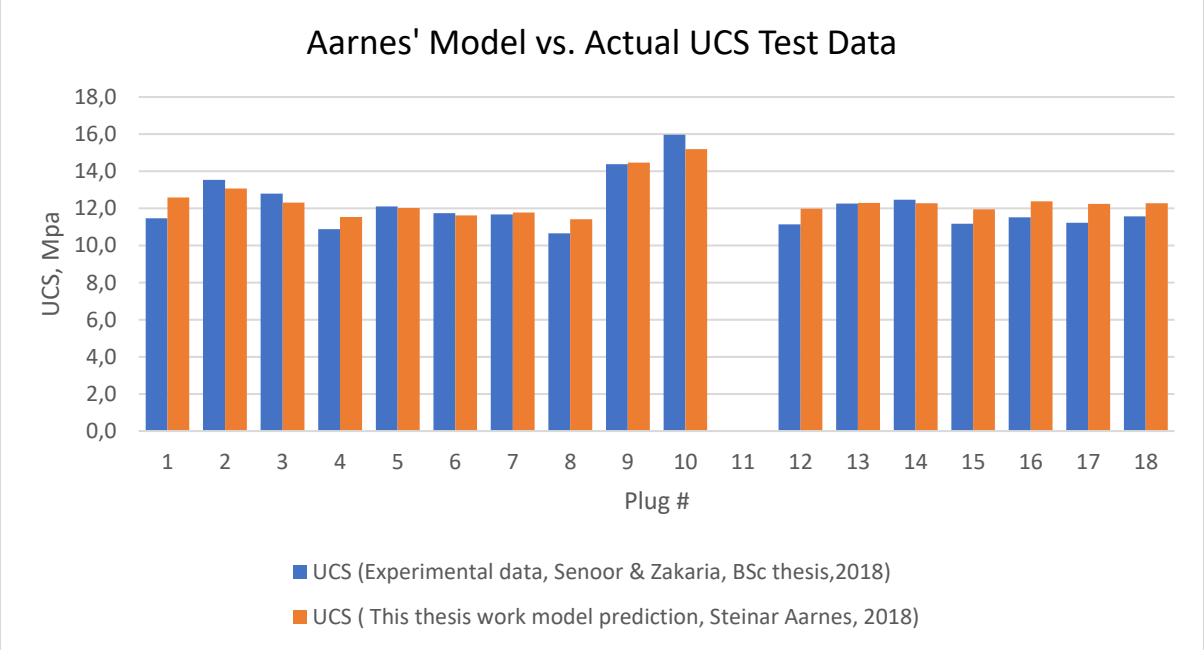

Figure 5-4: Aarnes' model vs. actual UCS results

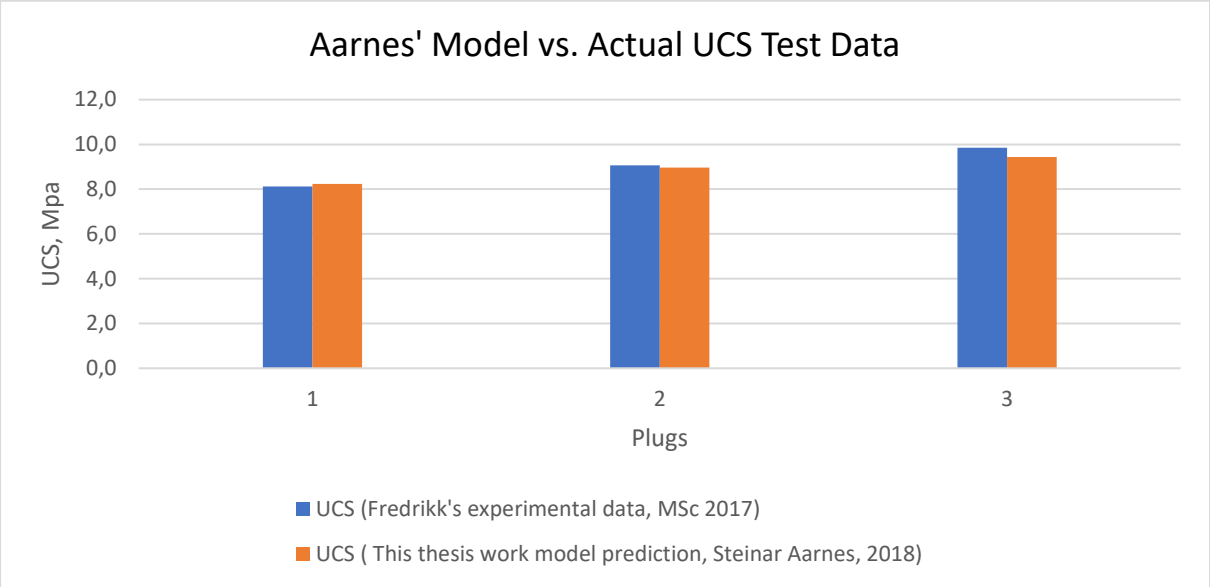

Figure 5-5: Aarnes' model vs. actual UCS results

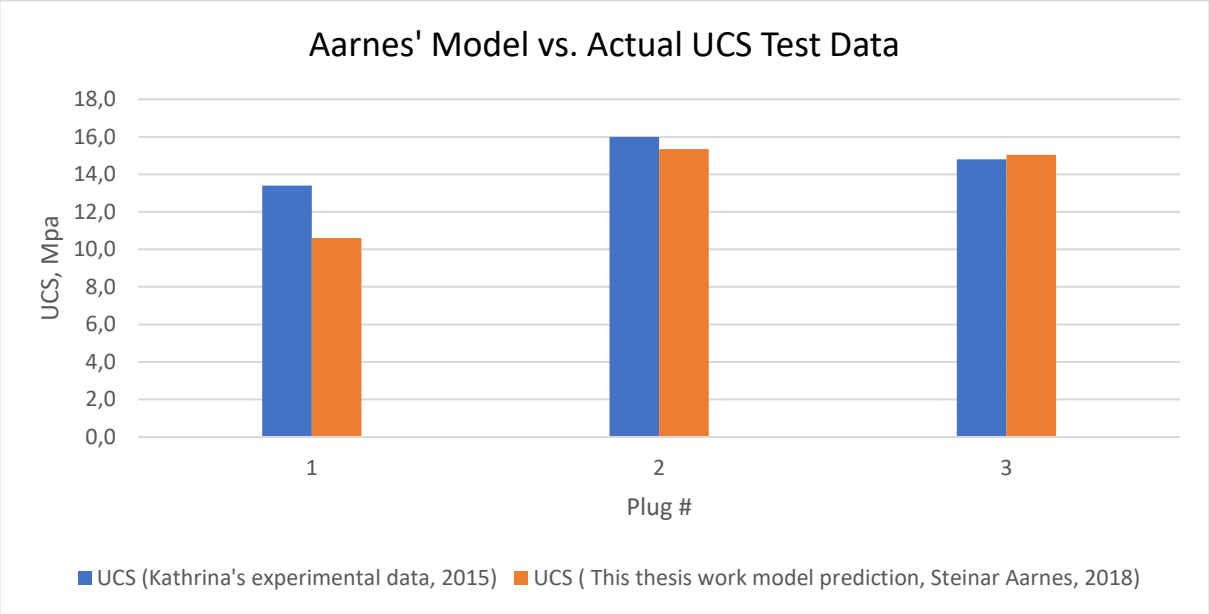

Figure 5-6: Aarnes' model vs. actual UCS results

A comment made in **subchapter 3.4.1.3.1** regarding the Horsrud model; was that most likely it would predict faulty estimations since it is based on different premises (shale prediction). This model, however, may be able to more adequately provide a prediction for UCS in sedimentary rock. Not a lot of time was dedicated to exploring this further, but it would be an interesting idea for further work.

6 Conclusions

6.1 Conclusions from the Experimental Study

The results from the experimental program of this thesis with respect to its objectives are compiled below. The general conclusions will be presented in accordance with how the problem statements are listed and the specific conclusion will be based on the optimized best results from each test matrix.

General observations

- Salt, alone and together with MWCNTs, shows extraordinarily good results with regards to the compressive strength of cement after 28 days of curing. Usually, the strength of cement decreases as the content of salt decreases, indicating a proportional relationship. Some salts do better than others
- The concentration of MWCNTs plays a significant role in the development of compressive strength of cement whereas high concentrations (>0.08wt%) usually display a reduction of compressive strength of cement while lower concentrations (<0.08wt%) usually display an increase
- Nano-silica is known for their part in concrete strength through the development additional C-H-S gel and MWCNTs are known as a solid reinforcement material due to their needle-like structure, but it was found in this experiment that a MWCNT-SiO_2 nanocomposite and SiO_2's single effect yielded a higher UCS of cement than that of MWCNTs alone
- The addition of MWCNTs has a very low impact on the development of heat during cement hydration
- Compared to other concentrations, a low amount of MWCNT showed very good capabilities of reducing leaks through the cement core, but compared to the control sample, only a marginal difference was observed
- In terms of UCS of cement, no rubber element performed as well as MWCNTs but still displayed some promising effects after adding tyre rubber, grey silicone and red silicone in low concentrations

- Rubber cement replacements are unfortunately more prone to leaking and fluid migration than with MWCNTs, which is likely due to their much larger dimensions (and thus pores) compared to nano-sized materials. Acid-treated red silicone rubber (high concentration) displayed great resistance to leaking but exhibits poor compressive strength
- Only acid-treated red silicone (RTL) and acid-treated grey silicone (GTH) shows a significant improvement in UCS from the acid treatment compared to their untreated counterparts
- The addition of MWCNTs change the rheological properties of cement slurry in the way that an increase in MWCNTs reduces the Casson's viscosity and reduces the shear stress of the slurry. A reduction in said properties is considered good in the way that the slurry requires less energy to be pumped

Specific conclusions based on optimized best results:

Table 6-1: Best results from heat development test

TM	Test Cup	Water system	Slurry	WCR	Concentration (wt%)	Logging (days)	Peak T (°C)	Change in T (°C)
TM#7	Cup OD:33mm L:67mm	80/20 FW/SYW	control	≈ 0.602	-	5	30.5	-4.90%
			nanobased		0.18		29	
TM#8	Standard Cube	FW	control	≈0.523	-		55.5	-0.90%
			nanobased		0.16		55	

Table 6-2: Best results from leakage test

TM	Name	Water system	Slurry	Concentration (wt%)	Percentage left on top	percent leaked through	Water retained
TM#8	H1	FW	nanobased	0.05	52.00%	1.00%	47.00%
	Ref		Control	-	53.00%	2.30%	44.70%
TM#9	RS-T-high		rubber-based	0.16	34.00%	0.00%	66.00%

Table 6-3: Best results from UCS and tensile tests

TM	Plug	Water system	Slurry	Concentration (wt%)	Curing Time (days)	UCS (Mpa)	M (Gpa)	Tensile (Mpa)	UCS (or tensile) increase (%)
TM#1	13	SYW+FW	control	-	28	19.6	18.0	-	19.4
	10		nanobased	0.26		23.4	22.9	-	
TM#2	MgSO4-ref	SSW	control	-		19.1	30.9	-	25.7
	MGSO4 nano		nanobased	0.26		24.0	28.7	-	
TM#3	SW-ref	SW	control	-		18.5	20.3	-	26.5
	SW-ref + 0.5 MWCNT		nanobased	0.26		23.4	21.4	-	
TM#4	TM4_0	SYW	control	-	7	17.6	16.8	-	2
	TM4_3		nanobased	0.18		17.9	16.4	-	
TM#5 UCS	TM5_0	80/20 FW/SYW	control	-		15.0	14.4	-	13.2
	TM5_2		nanobased	0.08		17.0	15.2	-	
TM#5 Tensile	TM5_0.0		control	-		-	-	1.61	37
	TM5_1.1		nanobased	0.03		-	-	2.21	
TM#6	TM6_0		control	-		14.0	14.6	-	14
	TM6_2		nanobased	0.08+0.08		16.0	17.2	-	
TM#8	REF	FW	control	-		13.0	17.5	-	67
	H1		nanobased	0.05		22.0	19.0	-	
TM#9	REF		control	-		13.0	17.5	-	40
	RTL		nanobased	1,5		19.0	17.3	-	

7 Future Work

Since this thesis investigated so many effects of MWCNTs on oil-well cementing, no ideas for further work with this particular nanoparticle comes to mind, however, other ideas blossomed over the course of this thesis:

Impermeable cement: Of all the requirements to the cement placed by the NORSOK standard, cement strength and ductility are just some of them. Given more time and more advanced equipment it would have been very interesting to advance the work of this thesis further, delving deeper into the effect of nano-additives with the goal to achieve total impermeability of cement. In this thesis work we only looked at how much mass was absorbed and how severe the leakage was after heat treatment as a way of determining permeability.

Heat of hydration: As oil companies are slowly but steadily migrating further north in hopes of discovering the next big oil reservoir so too are the temperatures they face more challenging. The effect of MWCNT on heat of hydration was studied in this thesis but no effort was put into actually decreasing the heat of hydration. Formulating cement slurries that actually decrease the liberation of heat would be highly beneficial.

UCS prediction (Aarnes' Model): As stated here, it would be very interesting and highly beneficial to further enhance this model to such a degree that actual strength tests of cement core specimens would be rendered obsolete, saving the industry fortunes in time consumption and equipment.

Seven-day strength vs. 28-day strength: Some theories states that the strength development after seven, or so days, is in a linear proportion to the final strength developed after 28 days and thus testing after 28 days is not necessary [48] [49]. This was not assumed in the work of this thesis, but it would have been an interesting experiment to perform granted more time.

References

[1] D. G. Erik Nelson, Well Cementing, Second Edition, Texas: Schlumberger, 2006.

[2] B. A. Birgit Vignes, "Well Integrity Issues Offshore Norway," Society of Petroleum Engineers, Orlando, Florida, 2010.

[3] B. Rahimirad, "Properties of Coil Well Cement Reinforced by Carbon Nanotubes," Society of Petroleum Engineers (SPE), Omidiyeh, Iran, 2012.

[4] Petro Wiki, "Cementing Operations," [Online]. Available: http://petrowiki.org/Cementing_operations.

[5] D. Stokes, "Integrated milling, underreaming approach streamlines P&A operations in the North Sea," 5 August 2017. [Online]. Available: https://www.offshore-mag.com/articles/print/volume-77/issue-5/engineering-construction-installation/integrated-milling-underreaming-approach-streamlines-p-a-operations-in-the-north-sea.html. [Accessed April 2018].

[6] Oil Industry Association, Norwegian Manufacturing Industries, "NORSOK," Standards Norway, Lysaker, 2013.

[7] H. M. K. Rocha-Valadez, "Assessing Wellbore Integrity in Sustained-Casing-Pressure Annulus," Society of Petroleum Engineers (SPE), 2014.

[8] A. W. J. A. W. H. G. W. Davies, "Oil and gas wells and their integrity: Implications for shale and unconventional resource exploitation," *Marine and Petroleum Geology,* vol. 56, pp. 239-254, March 2014.

[9] Nanowerk, "Nanoparticle production – How nanoparticles are made," Nanowerk, [Online]. Available: https://www.nanowerk.com/how_nanoparticles_are_made.php. [Accessed March 2018].

[10] D. Patil, "Use of Nanomaterials in Cementing Applications," Society of Petroleum Engineers, Noordwjik, Netherlands, 2012.

[11] S. R. El-Diasty, "Applications of Nanotechnology in the Oil & Gas industry: Latest Trends Worldwide & Future Challenges," Society of Petroleum Engineers (SPE), Egypt, 2013.

[12] S. Fakoya, "Science Direct," in *Petroleum, Volume 3, Issue 4*, Oklahoma, USA, KeAi Communications Co., Ltd., 2017, pp. 391-405.

[13] D. Vollath, Nanomaterials: An Introduction to Synthesis, Properties and Applications, 2nd Edition, Weinheim: Wiley-VCH, 2013.

[14] J. T. B. Khalil, "Advanced nanomaterials in oil and gas industry: Design, application and challenges," in *Applied Energy, Volume 191*, Elsevier Ltd., 2017, pp. 287-310.

[15] E. B. Richard Booker, Nanotechnology For Dummies, Indianapolis, Indiana: Wiley Publishing, 2011.

[16] C. Steinbach, "Silicon Dioxide-Material Information," Federal Ministry of Education and Research, [Online]. Available: https://www.nanopartikel.info/en/nanoinfo/materials/silicon-dioxide/material-information#literatur. [Accessed 16 April 2018].

[17] S. A. Aggarwal, "Use of Nano-silica in cement based materials- A review," Cogent Engineering, Kurukshetra, India, Published: 24 August 2015.

[18] Y. C. S. Ahmed, "Numerical and experimental investigations on the heat transfer enhancement in corrugated channels using SiO2–water nanofluid," in *Case Studies in Thermal Engineering*, Elsevier Publishing, September 2015, pp. 77-92.

[19] R. Krishnamoorti, "Extracting benfits of Nanotechnology for the Oil Industry," SPE, Houston, 2006.

[20] E. Y. R. Y. C. R. R. J. M. B. H. Zhang, "Engineered Nanoparticles as Harsh-Condition Emulsion and Foam Stabilizers and as Novel Sensors," SPE, Houston, 2011.

[21] C. V. F. Matteo, "Current and Future Nanotech Applications in the Oil Industry," Science Publications, Italy, 2012.

[22] K. B. Zargartalebi, "Enhancement of surfactant flooding performance by the use of silica nanoparticles," in *Fuel*, Elsevier, 01. March 2015, pp. 21-27, volume 143.

[23] P. F. M. E. Moradi, "Application of SiO2 Nano Particles to Improve the Peformance of Water Alternating Gas EOR Process," SPE, 2015.

[24] O. M. O. O. N. A. Ogolo, "Enchanced Oil Recovery Using Nanoparticles," Society of Petroleum Engineers (SPE), Rivers State, Nigeria, 2012.

[25] E.-B. Tarek, "Comprehensive Investigation of Effects of Nano-Fluid Mixtures to Enhance Oil Recovery," Society of Petroleum Engineers (SPE), 2015.

[26] L. Taha, "Nano Graphene Application Improving Drilling Fluids Performance," Society of Petroleum Engineers (SPE), Quatar, 2015.

[27] C. R. P. Kumar, "Scale Inhibition using Nano-silica Particles," Society of Petroleum Engineers (SPE), 2012.

[28] P. U. Jauhari, "Corrosion Inhibition Of Mild Steel In Acidic Media Using A Nanomagnetic Fluid As A Novel Corrosion Inhibitor," NACE International, Houston, Texas, 2011.

[29] B. J. Pang, "Nanosilicas as Accelerators in Oilwell Cementing at Low Temperatures," Society of Petroleum Engineers (SPE), 2014.

[30] B. G. B. L. L. Maserati, "Nano-Emulsions as Cement Spacer Imrpove the Cleaning of Casing Bore during Cementing Operations," Society of Petroleum Engineers (SPE), Florence, Italy, 2010.

[31] L. S. M. Z. Lv, "Effect of GO nanosheets on shapes of cement hydration crystals and their formation process," in *Construction and Building Materials*, Xi'an, China, Elsevier Publishing, 14. August 2014, pp. 231-239.

[32] K. A. K. F. K. Q. R. Gillani, "Improving the mehcanical performance of cement composites by carbon nanotubes addition," in *Procedia Structural Integrity*, Elsevier Publishing, 2017, pp. 11-17, volume 3.

[33] P. S. W. D. Chuah, "Nano reinforced cement and concrete composites and new perspective from graphene oxide," in *Construction and Building MATERIALS*, Elsevier Ltd., 2014, pp. 113-124.

[34] M. Vipulandan, "Smart cement modified with iron oxide nanoparticles to enhance the piezoresistive behavior and compressive strength for oil well applications," IOP Publishing, Houston, Texas, 2015.

[35] C. C. B. Roddy, "Cement Compositions and Methods utilizing Nano-clay," United States Patent, 2013.

[36] J. Thomas, "Types of Portland Cement," Northwestern University, Evanston, IL, [Online]. Available: http://iti.northwestern.edu/cement/monograph/Monograph3_8.html. [Accessed 14 May 2018].

[37] A. S. o. t. I. A. f. T. Materials, "Standard Specification for Concrete Aggregates," ASTM , [Online]. Available: https://www.astm.org/Standards/C33. [Accessed 14 May 2018].

[38] Website, "Cementing," [Online]. Available: http://www.eng.cu.edu.eg/users/aelsayed/Cementing.pdf. [Accessed 2018].

[39] S. M. Riaz, "Hydration of Cement," [Online]. Available: https://www.slideshare.net/rizwansamor/hydration-of-cement. [Accessed 16 April 2018].

[40] K. y. Salaam, "NEO GRIOT, Kalamu ya Salaam's information blog," June 22 2010. [Online]. Available: http://kalamu.posthaven.com/gulf-oil-disaster-what-do-we-know-about-the-d. [Accessed 12 April 2018].

[41] Petro Wiki, "PEH: Cementing," [Online]. Available: http://petrowiki.org/PEH:Cementing#Remedial_Cementing. [Accessed 12 April 2018].

[42] Pars Petro Kupal Kish, "Pars Petro Kupal Kish, Oil & Gas Engineering Service Company," [Online]. Available: http://parspk.co/services/. [Accessed 12 April 2018].

[43] A. A. H. Q. P. R. R. v. H. v. H. v. O. Paramor, "North Sea Atlas," MEFEPO , Liverpool, August 2009.

[44] M. T. Tare, "Mitigating Wellbore Stability Problems while Drilling with Water-Based Muds in Deepwater Environments," Offshore Technology Conference, 2002.

[45] EPRUI Nanoparticles & Microspheres Co. Ltd., "Carbon Nanoparticles," EPRUI Nanoparticles & Microspheres Co. Ltd., [Online]. Available: https://www.nanoparticles-microspheres.com/Products/carbon-nanoparticles.html. [Accessed 09 05 2018].

[46] EPRUI Nanoparticles & Microsphere Co. Ltd, "Nano Silica Particles," [Online]. Available: https://www.nanoparticles-microspheres.com/Products/Nano-SiO2.html. [Accessed 09 05 2018].

[47] C. C. Colom, "Composites reinforced with reused tyres: Surface oxidant treatment to improve the interfacial compatibility," in *Composites Part A: Applied Science and Manufacturing. Volume 38, Issue 1.*, Elsevier, 2007, pp. 44-50.

[48] E. Barger, "28-day myth," Npca, [Online]. Available: https://precast.org/2013/10/28-day-myth/.

[49] C. C. Staff, "Relationship between seven and 28 day strengths," Concrete Construction, 1994. [Online]. Available: http://www.concreteconstruction.net/how-to/relationship-between-seven-and-28-day-strengths_o. [Accessed 2018].

[50] P. Horsrud, "Estimating Mechanical Properties in Shale From Empirical Correlations," SPE Drilling & Completion, 2001.

[51] American Section of the International Association for Testing Materials, "ASTM International," Last Revised 2016.. [Online]. Available: https://www.astm.org/Standards/C597.htm. [Accessed 5 April 2018].

[52] M. Q. G. H. X. Z. Shouceng, "Experiment and SEM Analysis on Rock Breaking Mechanism by Swirling-Round SC-CO2 Jet," ARMA, American Rock Mechanics Association, Bejing, 2017.

[53] Portland Cement Association, "Concrete Technology Today: Portland Cement, Concrete and Heat of Hydration," Portland Cement Association, Skokie, Illinois, 1997.

[54] M. V. Ochoa, "Analysis of Drilling Fluid Rheology and Tool Joint Effect to Reduce Errors in Hydraulics Calculations," August 2006. [Online]. Available: http://oaktrust.library.tamu.edu/bitstream/handle/1969.1/4334/etd-tamu-2006B-PETE-viloria.pdf?sequence=1. [Accessed 23 May 2018].

[55] European Commitee for Standardization, "EN 196-1. Method of testing cement - Part 1: Determination of strength," CEN-CENELEC Management Centre, Brussel, 2016.

[56] B. Haranki, "Strength, modulus of elasticity, creep and shrinkage of concrete used in Florida," University of Florida, Florida, 2009.

[57] Building Research Institute, [Online]. Available: http://www.buildingresearch.com.np/services/mt/mt2.php.

[58] S. Norsk, "Testing hardened concrete - Part 6: Tensile splitting strength of test specimens," Last revised 2010.

[59] B. J. Q. S. Hunashyal, "Experimental investigation of multiwalled carbon nanotubes and nano-SiO2 addition on mechanical properties of hardened cement paste," in *Advances in Materials*, Science Publishing Group, 2014, pp. 45-51.

[60] F. Wegian, "Effect of seawater for mixing and curing on structural concrete," *The IES Journal Part A: Civil & Structural Engineering,* pp. Volume 3, Issue 4, 2010.

[61] A. S. Abdullah, "Strength of Concrete Containing Rubber Particle as Partial Cement Replacement," EDP Sciences, 2016.

[62] H. R. G. Fakhim, "Predicting the Impact of Multiwalled Carbon Nanotubes on the Cement Hydration Products and Durability of Cementitious Matrix Using Artificial Neural Network Modeling Technique," 2013. [Online]. Available: https://www.ncbi.nlm.nih.gov/pmc/articles/PMC3892931/. [Accessed 2 June 2018].

[63] "Understanding Rheology of Structured Fluids," [Online]. Available: http://www.tainstruments.com/pdf/literature/AAN016_V1_U_StructFluids.pdf.

[64] J. C. L. Geng, "In Situ Synthesis and Characterization of Polyethyleneimine-Modified Carbon Nanotubes Supported PtRu Electrocatalyst for Methanol Oxidation," Hindawi Publishing Corporation, 2015.

[65] F. Z. Fridriksson, "An improved cement slurry formulation for oil and geothermal wells," University of Stavanger, Stavanger, 2017.

[66] K. Esquivel, "Nanotechnology applications and experimental investigation of nano-graphene on cement slurry treated with synthetic brine," University of Stavanger, Stavanger, 2016.

[67] M. J. Karim, "Experimental data based empirical UCS-velocity model development and comparision with literature models," University of Stavanger, Stavanger, 2017.

[68] H. S. Saleh, "Proper Cementing to Reduce Time and Cost," University of Stavanger, Stavanger, 2016.

[69] B. Vignes, "Contribution to well integrity and increased focus on well barriers from a life cycle aspect," University of Stavanger, Stavanger, 2011.

[70] M. R. G. Y. G. P. S. Z. Z. J. H. Narjes Jafariesfrad, "Cement Sheath Modification Using Nanomaterials for Long-term Zonal Isolation of Oil Wells: Review," Norwegian University of Science and Technology (NTNU), Trondheim.

[71] A. Nikiforuk, "Shale Gas: How Often Do Cracked Wells Leak," 9 January 2013. [Online]. Available: https://thetyee.ca/News/2013/01/09/Leaky-Fracked-Wells/.

[72] J. B. Mohammad Rahimirad, "Properties of Oil Well Cement Reinforced by Carbon Nanotubes," SPE, Iran, 2012.

[73] A. E.-B. Mohamed Tarek, "Comprehensive Investigation of Effects of Nano-Fluid Mixtures to Enhance Oil Recovery," SPE, 2015.

[74] J. Bensted, "Class G and H Basic Oilwell Cements," World Cement, 1992.

[75] J. M. Crow, "The Concrete Conundrum," March 2008. [Online]. Available: http://www.rsc.org/images/Construction_tcm18-114530.pdf. [Accessed 05 April 2018].

[76] B. P. Santra, "Influence of Nanomaterials in Oilwell Cement Hydration and Mechanical Properties," Society of Petroleum Engineers (SPE), 2012.

[77] E. C. o. Standardization, "Testing hardened concrete - Part 1: Shape, dimensions and other requirements for specimens and moulds," Standard Norge, Last revised: (2012-12-01).

Appendix A: All directly read and calculated values from all matrices

Test Matrix 1 (TM#1)

ELASTIC MODULUS

PLUG #	Start	24hr	48hr	72hr	96hr	7days	28days
SYW REF.	10,1	12,5	14,0	14,8	15,7	16,6	20,5
100% SYW + NANO	9,9	12,8	12,9	14,3	14,8	15,9	20,2
90% SYW + NANO	9,9	12,6	13,0	14,8	15,3	16,4	20,4
80% SYW + NANO	9,4	12,5	12,3	14,2	15,0	16,0	19,7
70% SYW + NANO	9,3	12,0	12,7	13,9	14,3	15,5	19,6
60% SYW + NANO	9,0	12,2	13,2	13,7	14,7	15,6	19,5
50% SYW + NANO	9,4	11,9	12,1	13,5	14,0	15,1	19,6
40% SYW + NANO	9,6	12,1	12,6	14,1	14,2	15,1	19,7
30% SYW + NANO	8,4	11,0	11,2	12,5	13,2	14,0	19,3
20% SYW + NANO	11,2	14,3	14,3	16,1	16,6	17,7	22,9
10% SYW + NANO	9,1	11,7	11,7	13,1	13,9	14,7	19,3
100% FW + NANO	8,5	10,8	11,2	12,5	12,9	13,9	19,4
FW REF	8,2	10,7	11,3	12,1	13,3	14,2	18,0

SONIC

PLUG #	Start	24hr	48hr	72hr	96hr	7days	28days
SYW REF.	27,1	25,9	24,5	23,9	23,3	22,7	20,5
100% SYW + NANO	27,1	25,4	25,3	24,1	23,6	21,3	20,4
90% SYW + NANO	27,6	26,0	25,7	24,1	23,6	22,0	20,7
80% SYW + NANO	27,5	25,4	25,7	23,9	23,3	22,5	20,5
70% SYW + NANO	28,0	26,3	25,6	24,5	24,0	23,0	20,8

60% SYW + NANO	28,2	25,8	24,9	24,4	23,7	22,1	20,6
50% SYW + NANO	27,7	26,3	26,1	24,8	24,2	23,1	20,7
40% SYW + NANO	27,5	26,0	25,5	24,1	24,1	22,0	20,6
30% SYW + NANO	29,1	27,3	27,1	25,7	25,2	21,3	20,8
20% SYW + NANO	25,3	23,2	23,2	21,9	21,5	20,4	18,5
10% SYW + NANO	28,3	26,7	26,7	25,3	24,7	23,1	21,0
100% FW + NANO	28,8	27,4	27,0	25,6	25,2	23,6	20,7
FW REF	28,6	27,1	26,4	25,5	24,4	23,4	20,6

EMPIRICAL UCS

PLUG #	**Start**	**24hr**	**48hr**	**72hr**	**96hr**	**7days**	**30days**
SYW REF.	11	12	14	15	17	18	24
100% SYW + NANO	11	13	13	15	16	17	24
90% SYW + NANO	11	13	14	16	18	19	26
80% SYW + NANO	10	13	12	15	16	17	24
70% SYW + NANO	10	12	13	15	15	16	23
60% SYW + NANO	9	12	14	14	16	17	24
50% SYW + NANO	10	12	12	14	15	16	23
40% SYW + NANO	10	12	13	15	15	16	24
30% SYW + NANO	9	11	11	13	14	15	24
20% SYW + NANO	12	15	15	18	19	21	30
10% SYW + NANO	10	12	12	14	15	16	24
100% FW + NANO	9	10	11	13	13	15	23
FW REF	9	10	11	12	14	15	23

	MASS ABSORPTION						
PLUG #	**Mass Start**	**24hr**	**48hr**	**72hr**	**96hr**	**7days**	**30days**
SYW REF.	92,65	104,79	105,24	105,54	105,39	105,53	107,40
100% SYW + NANO	92,39	104,30	104,68	104,85	104,82	104,72	106,30
90% SYW + NANO	92,31	104,41	104,82	105,10	105,00	105,03	106,60
80% SYW + NANO	90,22	102,51	103,27	103,46	103,39	103,44	105,05
70% SYW + NANO	91,20	103,92	104,51	104,72	104,74	104,79	106,30
60% SYW + NANO	91,81	104,73	105,19	105,42	105,36	105,39	106,90
50% SYW + NANO	92,72	105,36	105,99	106,26	106,26	106,32	107,90
40% SYW + NANO	92,51	104,16	104,62	104,78	104,85	104,64	107,00
30% SYW + NANO	91,01	104,46	104,81	105,07	105,05	105,09	106,70
20% SYW + NANO	93,98	100,94	101,32	101,50	101,50	101,63	102,96
10% SYW + NANO	91,73	105,03	105,42	105,69	105,65	105,64	107,29
100% FW + NANO	89,72	103,59	104,06	104,29	104,23	104,27	105,92
FW REF	88,19	102,31	102,70	102,84	102,87	103,09	104,50

	WT % ABSORPTION						
PLUG #	**0hr**	**24hr**	**48hr**	**72hr**	**96hr**	**7days**	**30days**
SYW REF.	0	13,10	13,59	13,91	13,75	13,90	15,92
100% SYW + NANO	0	12,89	13,30	13,49	13,45	13,34	15,05
90% SYW + NANO	0	13,11	13,55	13,86	13,75	13,78	15,49
80% SYW + NANO	0	13,62	14,47	14,67	14,59	14,64	16,44
70% SYW + NANO	0	13,95	14,59	14,82	14,85	14,90	16,56
60% SYW + NANO	0	14,07	14,57	14,82	14,75	14,79	16,43
50% SYW + NANO	0	13,63	14,31	14,60	14,60	14,67	16,37
40% SYW + NANO	0	12,59	13,09	13,26	13,34	13,11	15,66
30% SYW + NANO	0	14,79	15,17	15,45	15,43	15,47	17,24
20% SYW + NANO	0	7,40	7,80	8,00	7,99	8,14	9,55

10% SYW + NANO	0	14,50	14,92	15,21	15,16	15,16	16,96
100% FW + NANO	0	15,46	15,99	16,24	16,17	16,22	18,06
FW REF	0	16,01	16,44	16,61	16,64	16,89	18,49

Test Matrix 2 (TM#2)

ELASTIC MODULUS

PLUG	Start	24hr	48hr	72hr	96hr	7days	28days
NACL REF	12,5	16,0	17,2	16,5	16,9	17,6	22,7
NACL + NANO	12,3	15,6	17,1	16,1	16,5	16,8	22,7
MGSO4 REF	14,9	19,7	21,9	21,6	22,2	21,1	30,9
MGSO4 + NANO	14,3	18,8	21,0	20,4	20,6	21,2	28,7
NAHCO3 REF	9,0	11,3	12,1	11,7	12,2	12,4	18,0
NAHCO3 + NANO	9,0	11,4	12,4	12,0	12,7	12,9	18,9
NA2SO4 + REF	14,0	17,2	18,4	17,1	17,1	17,6	23,6
NA2SO4 + NANO	14,4	16,8	17,7	17,1	16,8	17,9	22,6

SONIC

PLUG	Start	24hr	48hr	72hr	96hr	7days	28days
NACL REF	24,5	22,5	21,7	22,2	21,9	21,5	19,1
NACL + NANO	24,9	23,0	22,0	22,7	22,4	22,2	19,2
MGSO4 REF	23,2	21,0	19,9	20,1	19,8	20,3	16,9
MGSO4 + NANO	22,7	20,5	19,4	19,7	19,6	19,3	16,7
NAHCO3 REF	28,0	26,7	25,8	26,2	25,7	25,5	21,2
NAHCO3 + NANO	28,8	27,3	26,1	26,6	25,9	25,7	21,3
NA2SO4 + REF	23,4	21,9	21,2	22,0	22,0	21,7	18,8
NA2SO4 + NANO	23,4	22,5	21,9	22,3	22,5	21,8	19,5

EMPRICAL UCS

PLUG	Start	24hr	48hr	72hr	96hr	7days	28days
NACL REF	14	18	20	19	19	20	29
NACL + NANO	14	17	20	18	19	19	29
MGSO4 REF	16	22	26	25	26	24	41
MGSO4 + NANO	15	21	24	23	24	25	38
NAHCO3 REF	9	11	12	11	12	12	21
NAHCO3 + NANO	9	11	12	12	13	13	23
NA2SO4 + REF	17	20	22	20	20	21	31
NA2SO4 + NANO	17	19	21	20	19	21	29

MASS ABSORPTION

PLUG	Mass Start	24hr	48hr	72hr	96hr	7days	28days
NACL REF	96,72	104,91	104,88	105,08	104,99	105,03	106,90
NACL + NANO	96,93	105,46	105,41	105,61	105,44	105,51	106,80
MGSO4 REF	96,10	103,94	104,05	104,33	104,26	104,41	105,62
MGSO4 + NANO	96,73	103,83	103,92	104,11	104,09	104,16	105,24
NAHCO3 REF	92,73	105,28	105,32	105,41	105,40	105,44	106,37
NAHCO3 + NANO	94,84	107,83	107,88	108,05	108,03	108,10	109,01
NA2SO4 + REF	99,00	107,09	107,14	107,22	107,11	107,25	108,21
NA2SO4 + NANO	99,90	108,01	108,01	108,14	108,10	108,10	109,15

	WT % ABSORPTION						
PLUG	**0hrs**	**24hr**	**48hr**	**72hr**	**96hr**	**7days**	**28days**
NACL REF	0	8,46	8,44	8,65	8,55	8,59	10,52
NACL + NANO	0	8,80	8,75	8,95	8,77	8,85	10,18
MGSO4 REF	0	8,16	8,27	8,56	8,49	8,64	9,91
MGSO4 + NANO	0	7,34	7,44	7,63	7,61	7,68	8,80
NAHCO3 REF	0	13,53	13,58	13,67	13,66	13,71	14,71
NAHCO3 + NANO	0	13,70	13,75	13,93	13,90	13,98	14,94
NA2SO4 + REF	0	8,17	8,22	8,31	8,19	8,33	9,30
NA2SO4 + NANO	0	8,12	8,12	8,24	8,21	8,21	9,26

Test Matrix 3 (TM#3)

	ELASTIC MODLUS						
PLUG	**Start**	**24hr**	**48hr**	**72hr**	**96hr**	**7days**	**28days**
SW0	14,5	17,3	16,6	18,2	19,0	19,4	20,3
SW1	14,0	17,2	17,2	18,8	19,2	20,6	20,7
SW2	16,4	18,9	19,5	21,1	21,2	21,3	21,4
SW3	15,7	17,3	18,2	20,0	20,2	20,9	20,4
SW4	14,8	17,1	17,6	18,6	18,9	17,8	20,3
SW5	14,2	17,4	18,3	19,4	20,5	20,8	21,4

SONIC

PLUG	Start	24hr	48hr	72hr	96hr	7days	28days
SW0	23,7	22,3	22,8	21,8	21,5	21,1	20,7
SW1	23,2	21,6	21,6	20,7	20,2	19,8	19,8
SW2	22,1	21,1	20,8	20,0	19,9	19,7	19,2
SW3	22,3	21,8	21,3	20,3	20,1	19,9	19,3
SW4	23,2	22,2	21,9	21,3	21,0	21,8	20,5
SW5	23,7	22,0	21,5	20,9	20,4	20,2	20,0

EMPIRICAL UCS

PLUG	Start	24hr	48hr	72hr	96hr	7days	28days
SW0	17	20	19	22	23	24	25
SW1	16	20	20	23	24	26	26
SW2	20	23	24	27	28	28	30
SW3	19	20	21	25	26	26	29
SW4	18	20	21	23	22	21	25
SW5	16	20	22	24	25	26	27

MASS ABSORPTION

PLUG	Start	24hr	48hr	72hr	96hr	7days	28days
SW0	102,01	107,60	107,84	107,96	108,05	108,08	108,90
SW1	98,55	104,66	104,93	105,06	105,10	105,14	105,93
SW2	101,96	106,88	107,29	107,39	107,98	108,00	108,40
SW3	100,00	105,74	105,84	105,99	106,13	106,17	106,98
SW4	102,08	107,76	108,06	108,17	108,21	108,30	109,22
SW5	100,90	107,06	107,30	107,44	107,51	107,57	108,39

WT% ABSORPTION

PLUG	Start	24hr	48hr	72hr	96hr	7days	28days
SWO	0,0	5,5	5,7	5,8	5,9	6,0	6,8
SW1	0,0	6,2	6,5	6,6	6,6	6,7	7,5
SW2	0,0	4,8	5,2	5,3	5,9	5,9	6,3
SW3	0,0	5,7	5,8	6,0	6,1	6,2	7,0
SW4	0,0	5,6	5,9	6,0	6,0	6,1	7,0
SW5	0,0	6,1	6,3	6,5	6,6	6,6	7,4

Test Matrix 4, 5 & 6 (TM#4, TM#5, TM#6)

	ELASTIC MODULUS						
PLUG	**Start**	**24hr**	**48hr**	**72hr**	**96hr**	**120hrs**	**7days**
TM4:0	10,7	12,8	13,6	15,18	15,5	16,4	16,8
TM4:1	11,4	14,0	15,5	15,63	15,0	15,9	18,2
TM4:2	11,7	12,9	14,7	16,47	15,2	15,5	20,1
TM4:3	11,6	13,5	14,5	15,03	15,0	15,6	16,4
TM4:4	10,8	12,4	13,8	14,40	15,2	16,2	16,6
TM5:0	9,2	10,4	11,3	11,88	12,6	13,0	14,4
TM5:1	10,2	12,2	13,1	13,24	13,3	13,8	15,4
TM5:2	9,7	11,6	12,2	13,05	12,5	13,0	15,2
TM5:3	10,7	11,9	12,7	13,26	13,4	14,0	15,1
TM5:4	9,6	10,9	11,2	13,64	13,2	14,0	15,0
TM5:0.0	9,5	11,3	12,4	13,38	13,0	14,3	15,2
TM5:1.1	12,1	13,7	15,3	15,89	15,0	15,5	17,4
TM5:1.2	10,4	11,6	13,0	13,01	13,1	13,7	15,1
TM5:1.3	10,7	12,0	13,4	14,08	13,5	13,9	16,2
TM5:1.4	9,2	11,0	12,2	13,27	13,2	14,2	11,8
TM6:0	9,6	11,3	11,8	13,04	13,3	14,3	14,6
TM6:1	10,6	12,2	12,7	13,85	13,4	13,9	15,1
TM6:2	11,6	13,0	14,0	14,81	14,9	14,8	17,2
TM6:3	10,4	12,4	13,4	13,40	14,0	14,1	17,0
TM6:SIO2	9,3	11,0	12,0	13,26	13,5	14,4	15,1
TM6:CNT	9,7	11,2	11,8	13,13	13,5	14,4	14,9

SONIC

PLUG	Start	24hr	48hr	72hr	96hr	120hrs	7days
TM4:0	26,2	25,1	24,4	23,1	22,9	22,3	22,0
TM4:1	25,9	24,5	23,3	23,2	23,7	23,0	21,5
TM4:2	25,7	25,6	24,0	22,7	23,6	23,4	20,4
TM4:3	25,4	24,8	23,9	23,5	23,5	23,1	22,5
TM4:4	26,4	25,8	24,5	24,0	23,4	22,7	22,4
TM5:0	28,0	27,8	26,7	26,0	25,3	24,9	23,7
TM5:1	26,6	25,7	24,8	24,7	24,6	24,2	22,9
TM5:2	27,0	26,2	25,5	24,7	25,2	24,8	22,9
TM5:3	26,2	26,3	25,4	24,9	24,8	24,3	23,4
TM5:4	27,5	27,3	26,9	24,4	24,8	24,1	23,3
TM5:0.0	27,6	26,7	25,6	24,6	25,0	23,8	23,1
TM5:1.1	25,8	25,4	24,0	23,6	24,3	23,9	22,5
TM5:1.2	26,4	26,4	25,0	25,0	24,9	24,4	23,2
TM5:1.3	26,5	26,3	24,9	24,3	24,8	24,5	22,7
TM5:1.4	28,2	27,3	26,0	24,9	25,0	24,1	26,5
TM6:0	27,6	26,8	26,3	25,0	24,8	23,9	23,7
TM6:1	27,0	26,6	26,1	25,0	25,4	25,0	23,9
TM6:2	25,3	25,1	24,1	23,5	23,4	23,5	21,8
TM6:3	27,5	26,5	25,5	25,5	25,0	24,9	22,5
TM6:SIO2	27,9	27,1	26,0	24,7	24,5	23,7	23,2
TM6:CNT	27,4	26,9	26,3	24,9	24,6	23,8	23,4

	EMPIRICAL UCS						
PLUG	**Start**	**24hr**	**48hr**	**72hr**	**96hr**	**120hr**	**7days**
TM4:0	12	13	15	17	18	19	20
TM4:1	13	15	17	18	16	18	22
TM4:2	13	13	16	19	17	17	26
TM4:3	14	14	16	17	17	18	19
TM4:4	12	13	15	16	17	19	19
TM5:0	10	10	11	12	13	14	16
TM5:1	11	12	14	14	14	15	17
TM5:2	11	12	13	14	13	14	17
TM5:3	12	12	13	14	14	15	17
TM5:4	10	11	11	15	14	15	17
TM5:0.0	10	11	13	14	14	16	17
TM5:1.1	14	14	17	18	16	17	21
TM5:1.2	12	12	14	14	14	15	17
TM5:1.3	12	12	14	15	14	15	19
TM5:1.4	10	11	12	14	14	16	12
TM6:0	10	11	12	14	14	16	16
TM6:1	12	13	13	15	14	15	17
TM6:2	14	14	16	17	18	17	22
TM6:3	11	13	14	14	15	15	21
TM6:SIO2	10	11	12	14	15	16	17
TM6:CNT	11	11	12	14	15	16	17

	MASS ABSORPTION						
PLUG	**Mass Start**	**24hr**	**48hr**	**72hr**	**96hr**	**120hrs**	**7days**
TM4:0	94,90	104,25	104,43	104,49	104,74	104,91	104,96
TM4:1	95,20	104,96	104,92	105,06	105,00	105,15	104,95
TM4:2	95,30	104,90	104,92	105,02	105,00	105,05	103,57
TM4:3	96,00	106,17	106,17	106,22	106,24	106,40	106,41
TM4:4	95,67	105,65	105,84	105,92	106,16	106,36	106,47
TM5:0	92,90	103,59	103,78	103,86	104,07	104,22	104,38
TM5:1	93,40	104,30	104,32	104,45	104,40	104,51	104,60
TM5:2	92,54	103,57	103,55	103,68	103,62	103,73	103,93
TM5:3	94,33	105,37	105,39	105,52	105,47	105,70	105,88
TM5:4	93,67	104,33	104,59	104,69	104,86	105,03	105,25
TM5:0.0	93,31	103,81	104,08	104,11	104,27	104,45	104,58
TM5:1.1	97,00	106,50	106,64	106,78	106,70	106,83	106,46
TM5:1.2	93,63	104,50	104,50	104,68	104,45	104,70	104,85
TM5:1.3	95,34	105,78	105,80	105,93	105,81	105,94	106,15
TM5:1.4	93,94	105,13	105,37	105,44	105,65	105,78	106,00
TM6:0	93,60	104,19	104,46	104,53	104,59	104,83	105,06
TM6:1	95,40	106,90	106,95	107,16	107,10	107,25	106,50
TM6:2	96,50	105,70	105,65	105,89	105,81	105,90	105,60
TM6:3	95,70	106,35	106,40	106,46	106,60	106,64	105,15
TM6:SIO2	93,36	103,71	103,98	104,12	104,22	104,42	104,58
TM6:CNT	93,50	104,69	104,94	105,02	105,21	105,34	105,57

	WT % ABSORPTION						
PLUG	**Start**	**24hr**	**48hr**	**72hr**	**96hr**	**120hrs**	**7days**
TM4:0	0	9,85	10,04	10,11	10,37	10,55	10,60
TM4:1	0	10,25	10,21	10,36	10,29	10,45	10,24
TM4:2	0	10,07	10,09	10,20	10,18	10,23	8,68
TM4:3	0	10,59	10,59	10,64	10,67	10,83	10,84
TM4:4	0	10,44	10,63	10,71	10,96	11,17	11,28
TM5:0	0	11,50	11,71	11,80	12,03	12,18	12,36
TM5:1	0	11,67	11,69	11,83	11,78	11,90	11,99
TM5:2	0	11,92	11,90	12,04	11,97	12,09	12,31
TM5:3	0	11,70	11,72	11,86	11,81	12,05	12,24
TM5:4	0	11,39	11,66	11,77	11,95	12,13	12,37
TM5:0.0	0	11,25	11,54	11,58	11,74	11,94	12,08
TM5:1.1	0	9,79	9,94	10,08	10,00	10,14	9,75
TM5:1.2	0	11,61	11,61	11,80	11,56	11,83	11,98
TM5:1.3	0	10,95	10,97	11,11	10,98	11,12	11,34
TM5:1.4	0	11,91	12,16	12,24	12,46	12,60	12,84
TM6:0	0	11,31	11,60	11,68	11,74	12,00	12,24
TM6:1	0	12,05	12,11	12,32	12,26	12,42	11,64
TM6:2	0	9,53	9,48	9,73	9,65	9,74	9,43
TM6:3	0	11,13	11,18	11,25	11,39	11,43	9,87
TM6:SIO2	0	11,08	11,37	11,52	11,63	11,84	12,02
TM6:CNT	0	11,97	12,23	12,32	12,52	12,66	12,91

Test Matrix 8 (TM#8)

ELASTIC MODULUS

PLUG #	Start	24hr	48hr	72hr	96hr	7days
REF	13,6	14,3	15,6	16,8	16,7	17,5
H1	14,8	15,2	17,2	18,6	18,4	19,0
H2	12,4	12,6	14,8	15,7	15,6	16,6
H3	15,2	16,0	17,6	19,7	19,7	20,3

SONIC

PLUG #	Start	24hr	48hr	72hr	96hr	7days
REF	23,1	23,00	22,1	21,3	21,4	21,0
H1	22,3	22,50	21,2	20,4	20,5	20,3
H2	24,0	24,30	22,5	21,9	22,0	21,4
H3	21,5	21,50	20,5	19,4	19,4	19,2

EMPIRICAL UCS

PLUG #	Start	24hr	48hr	72hr	96hr	7days
REF	15,7	16	18	20	19,6	20,7
H1	17,4	17	20	23	22,3	22,9
H2	13,9	13	17	18	17,9	19,4
H3	18,1	18	21	24	24,4	25,2

MASS ABSORPTION

PLUG #	Start	24hr	48hr	72hr	96hr	7days
REF	96,21	100,76	101,50	101,54	101,70	102,39
H1	97,74	101,97	102,47	102,62	102,83	103,60
H2	95,55	99,18	99,96	100,23	100,53	101,42
H3	94,13	98,64	99,05	99,13	99,21	99,98

WT % ABSORPTION

PLUG #	Start	24hr	48hr	72hr	96hr	7days
REF	0,0	4,7	5,5	5,5	5,7	6,4
H1	0,0	4,3	4,8	5,0	5,2	6,0
H2	0,0	3,8	4,6	4,9	5,2	6,1
H3	0,0	4,8	5,2	5,3	5,4	6,2

Test Matrix 9 (TM#9)

ELASTICITY

PLUG	Start	24hr	48hr	72hr	96hr	7days
TYRE-T-LOW	13,8	14,5	16,3	17,57	17,9	18,0
TYRE-T-HIGH	10,5	11,1	12,3	12,23	12,7	14,0
TYRE-U-LOW	11,6	13,0	14,0	14,36	14,9	15,9
TYRE-U-HIGH	11,1	11,8	13,2	13,68	13,8	14,3

GS-T-LOW	12,2	13,0	14,4	14,96	15,4	16,1
GS-T-HIGH	11,9	12,6	14,1	14,88	15,4	16,1
GS-U-LOW	12,8	13,6	15,0	15,79	16,2	16,9
GS-U-HIGH	11,1	10,7	12,6	13,46	13,2	14,2
RS-T-LOW	13,9	13,9	16,1	17,25	17,1	17,3
RS-T-HIGH	13,7	14,6	15,3	17,08	16,4	17,1
RS-U-LOW	12,0	12,3	13,8	14,47	14,9	15,2
RS-U-HIGH	10,8	11,5	13,4	13,82	14,2	15,5

SONIC

PLUG	Start	24hr	48hr	72hr	96hr	7days
TYRE-T-LOW	22,4	22,5	21,3	20,5	20,3	20,3
TYRE-T-HIGH	26,0	26,2	24,9	25,0	24,5	23,4
TYRE-U-LOW	25,4	24,8	23,9	23,6	23,2	22,5
TYRE-U-HIGH	25,3	25,4	24,0	23,6	23,5	23,1
GS-T-LOW	24,3	24,3	23,1	22,7	22,4	21,9
GS-T-HIGH	24,6	24,6	23,3	22,7	22,3	21,9
GS-U-LOW	23,9	23,9	22,8	22,2	21,9	21,5
GS-U-HIGH	25,3	26,7	24,6	23,8	24,0	23,2
RS-T-LOW	22,6	23,2	21,6	20,9	21,0	20,9
RS-T-HIGH	22,9	22,8	22,3	21,1	21,5	21,1
RS-U-LOW	24,8	25,3	23,8	23,4	23,1	22,9
RS-U-HIGH	26,1	26,1	24,3	23,9	23,6	22,6

EMPIRICAL UCS

PLUG	Start	24hr	48hr	72hr	96hr	7days
TYRE-T-LOW	16,3	16	19	21	21,78	21,78
TYRE-T-HIGH	11,7	11	13	13	13,91	15,90
TYRE-U-LOW	13,1	14	16	16	17,04	18,63
TYRE-U-HIGH	12,5	12	15	15	15,55	16,35
GS-T-LOW	14,0	14	16	17	17,72	18,93
GS-T-HIGH	13,6	14	16	17	18,12	19,10
GS-U-LOW	14,5	15	17	18	18,78	19,82
GS-U-HIGH	12,4	11	13	15	14,45	15,95
RS-T-LOW	16,3	15	19	20	20,16	20,44
RS-T-HIGH	16,3	16	18	21	19,55	20,65
RS-U-LOW	13,9	13	16	16	17,11	17,55
RS-U-HIGH	12,0	12	15	15	16,05	18,22

MASS ABSORPTION

PLUG	Mass Start	24hr	48hr	72hr	96hr	7 days
TYRE-T-LOW	94,42	100,32	100,59	100,69	100,75	101,15
TYRE-T-HIGH	93,80	100,51	100,79	100,89	100,93	101,15
TYRE-U-LOW	96,32	102,54	102,90	102,96	103,03	103,44
TYRE-U-HIGH	91,78	98,07	98,33	98,35	98,35	98,71
GS-T-LOW	96,20	102,50	102,87	102,96	103,02	103,30
GS-T-HIGH	94,55	100,56	100,91	101,02	101,08	101,55
GS-U-LOW	96,10	102,32	102,58	102,66	102,70	103,07
GS-U-HIGH	93,10	99,89	100,22	100,29	100,32	100,67
RS-T-LOW	94,61	100,08	100,39	100,50	100,46	100,80

RS-T-HIGH	95,10	100,58	100,89	100,97	100,95	101,38
RS-U-LOW	96,70	102,98	101,89	103,43	103,50	103,83
RS-U-HIGH	95,05	101,15	101,50	101,54	101,54	101,89

WT % ABSORPTION

PLUG	Start	24hr	48hr	72hr	96hr	7days
TYRE-T-LOW	0,00	6,25	6,54	6,64	6,71	7,13
TYRE-T-HIGH	0,00	7,15	7,45	7,56	7,60	7,84
TYRE-U-LOW	0,00	6,46	6,83	6,89	6,97	7,40
TYRE-U-HIGH	0,00	6,86	7,13	7,16	7,16	7,55
GS-T-LOW	0,00	6,55	6,93	7,02	7,09	7,38
GS-T-HIGH	0,00	6,35	6,73	6,84	6,91	7,40
GS-U-LOW	0,00	6,48	6,75	6,82	6,87	7,25
GS-U-HIGH	0,00	7,29	7,65	7,72	7,76	8,13
RS-T-LOW	0,00	5,78	6,11	6,22	6,18	6,54
RS-T-HIGH	0,00	5,76	6,09	6,18	6,16	6,60
RS-U-LOW	0,00	6,49	5,37	6,96	7,03	7,37
RS-U-HIGH	0,00	6,41	6,78	6,83	6,82	7,20

Leakage-test data from TM#8 and TM#9

START OF 1ST CYCLE (24 HRS IN OVEN 110C)

NAME OF SPECIMEN	Casing Without Water	Casing With Water On Top	Empty Cup	Weight Of Water On Top
TYRE-T-LOW	232,80	265,20	2,841	32,400
TYRE-T-HIGH	233,14	260,83	2,699	27,690
TYRE-U-LOW	240,61	266,47	2,679	25,860
TYRE-U-HIGH	239,03	277,44	2,855	38,410
GS-T-LOW	238,74	265,26	2,930	26,520
GS-T-HIGH	248,44	276,82	2,867	28,380
GS-U-LOW	237,75	264,65	3,060	26,900
GS-U-HIGH	237,19	263,64	2,966	26,450
RS-T-LOW	240,93	265,40	2,994	24,470
RS-T-HIGH	231,89	259,66	2,894	27,770
RS-U-LOW	228,20	265,24	2,881	37,040
RS-U-HIGH	229,38	264,13	2,893	34,750
REF	203,98	256,88	2,721	52,900
H1	205,87	256,38	2,878	50,510
H2	208,72	259,70	2,814	50,980
H3	210,03	259,88	2,901	49,850

END OF 1ST CYCLE (24 HRS IN ROOM C TO MEASURE LEAK)

NAME OF SPECIMEN	Cup With Water(or empty)	Cup + Leftover Top	Saturated Casing	Weight of Leaked Water	Weight of Leftover Water Top
TYRE-T-LOW	3,805	3,805	263,640	0,964	0,000
TYRE-T-HIGH	2,699	2,699	260,310	0,000	0,000
TYRE-U-LOW	2,679	2,679	265,980	0,000	0,000
TYRE-U-HIGH	8,995	8,995	270,400	6,140	0,000
GS-T-LOW	2,930	4,610	263,200	0,000	1,680
GS-T-HIGH	2,867	9,989	269,310	0,000	7,122
GS-U-LOW	3,060	3,060	264,290	0,000	0,000
GS-U-HIGH	2,966	2,966	263,300	0,000	0,000
RS-T-LOW	2,994	12,320	255,440	0,000	9,326
RS-T-HIGH	2,894	20,135	241,760	0,000	17,241
RS-U-LOW	2,881	11,902	255,660	0,000	9,021
RS-U-HIGH	2,893	18,637	247,890	0,000	15,744
REF	2,721	33,001	225,950	0,000	30,280
H1	2,878	29,770	228,810	0,000	26,892
H2	2,814	29,040	232,850	0,000	26,226
H3	2,901	28,099	234,020	0,000	25,198

START OF 2ND CYCLE (24 HRS IN OVEN 110C)

NAME OF SPECIMEN	Casing Without Water	Casing With Water On Top	Empty Cup	Weight Of Water On Top
TYRE-T-LOW	233,302	266,502	2,841	33,200
TYRE-T-HIGH	232,211	260,474	2,699	28,263
TYRE-U-LOW	239,829	267,025	2,679	27,196
TYRE-U-HIGH	237,891	264,507	2,855	26,616
GS-T-LOW	237,507	263,280	2,930	25,773
GS-T-HIGH	247,031	276,901	2,867	29,870
GS-U-LOW	236,419	263,051	3,060	26,632
GS-U-HIGH	236,510	263,447	2,966	26,937
RS-T-LOW	238,193	264,036	2,994	25,843
RS-T-HIGH	229,800	259,310	2,894	29,510
RS-U-LOW	226,762	263,741	2,881	36,979
RS-U-HIGH	227,864	262,876	2,893	35,012
REF	203,635	258,863	2,721	55,228
H1	205,840	258,620	2,878	52,780
H2	208,526	260,651	2,814	52,125
H3	209,733	260,470	2,901	50,737

END OF 2ND CYCLE (24 HRS IN ROOM C TO MEASURE LEAK)

NAME OF SPECIMEN	Cup With Water(or empty)	Cup + Leftover Top	Saturated Casing	Weight of Leaked Water	Weight of Leftover Water Top
TYRE-T-LOW	4,547		263,362	1,706	0,000
TYRE-T-HIGH	2,699		259,381	0,000	0,000
TYRE-U-LOW	2,679		266,040	0,000	0,000
TYRE-U-HIGH					
GS-T-LOW	2,930		262,442	0,000	0,000
GS-T-HIGH	2,867		273,645	0,000	2,231
GS-U-LOW	3,060		262,256	0,000	0,000
GS-U-HIGH	2,966		262,497	0,000	0,000
RS-T-LOW	2,994		260,209	0,000	2,752
RS-T-HIGH	2,894		242,585	0,000	15,133
RS-U-LOW	5,943		255,679	3,062	3,527
RS-U-HIGH	2,893		254,766	0,000	6,974
REF	2,987		225,903	0,266	30,913
H1	3,327		228,742	0,449	27,608
H2	3,288		232,904	0,474	25,614
H3	3,484		233,930	0,583	24,127

Empty column because of calculations being performed in another spreadsheet

START OF 3RD CYCLE (24 HRS IN OVEN 110C)

NAME OF SPECIMEN	Casing Without Water	Casing With Water On Top	Empty Cup	Weight Of Water On Top
TYRE-T-LOW	234,171	268,453	2,841	34,282
TYRE-T-HIGH	233,010	262,868	2,699	29,858
TYRE-U-LOW	241,470	268,225	2,679	26,755
TYRE-U-HIGH	238,999	267,103	2,855	28,104
GS-T-LOW	237,588	265,820	2,930	28,232
GS-T-HIGH	247,775	277,994	2,867	30,219
GS-U-LOW	236,227	264,207	3,060	27,980
GS-U-HIGH	236,966	264,680	2,966	27,714
RS-T-LOW	238,336	264,106	2,994	25,770
RS-T-HIGH	229,673	260,715	2,894	31,042
RS-U-LOW	227,703	265,678	2,881	37,975
RS-U-HIGH	228,443	265,844	2,893	37,401
REF	204,115	260,181	2,721	56,066
H1	206,322	261,002	2,878	54,680
H2	209,415	261,150	2,814	51,735
H3	210,537	261,725	2,901	51,188

END OF 3RD CYCLE (24 HRS IN ROOM C TO MEASURE LEAK)

NAME OF SPECIMEN	Cup With Water(or empty)	Cup + Leftover Top	Saturated Casing	Weight of Leaked Water	Weight of Leftover Water Top
TYRE-T-LOW	4,856	6,255	263,120	2,015	1,399
TYRE-T-HIGH	2,699	2,699	261,761	0,000	0,000
TYRE-U-LOW	2,679	2,679	261,344	0,000	0,000
TYRE-U-HIGH	2,855	2,855	266,049	0,000	0,000
GS-T-LOW	2,930	2,930	265,087	0,000	0,000
GS-T-HIGH	2,867	6,601	273,305	0,000	3,734
GS-U-LOW	3,060	3,060	263,501	0,000	0,000
GS-U-HIGH	2,966	2,966	263,776	0,000	0,000
RS-T-LOW	2,994	9,343	261,665	0,000	6,349
RS-T-HIGH	2,894	18,298	243,709	0,000	15,404
RS-U-LOW	4,842	11,510	255,716	1,961	6,668
RS-U-HIGH	3,185	12,193	255,420	0,292	9,008
REF	3,236	35,022	226,135	0,515	31,786
H1	3,417	33,172	228,915	0,539	29,755
H2	3,255	29,122	233,250	0,441	25,867
H3	3,388	28,566	234,312	0,487	25,178

START OF 4TH CYCLE (24 HRS IN OVEN 110C)

NAME OF SPECIMEN	Casing Without Water	Casing With Water On Top	Empty Cup	Weight Of Water On Top
TYRE-T-LOW	232,892	266,264	2,841	33,372
TYRE-T-HIGH	231,944	262,151	2,699	30,207
TYRE-U-LOW	240,537	268,362	2,679	27,825
TYRE-U-HIGH	238,128	265,555	2,855	27,427
GS-T-LOW	236,341	264,444	2,930	28,103
GS-T-HIGH	246,104	276,712	2,867	30,608
GS-U-LOW	235,002	263,527	3,060	28,525
GS-U-HIGH	235,785	263,919	2,966	28,134
RS-T-LOW	237,146	263,493	2,994	26,347
RS-T-HIGH	228,765	260,510	2,894	31,745
RS-U-LOW	226,382	264,508	2,881	38,126
RS-U-HIGH	229,110	265,289	2,893	36,179
REF	203,592	259,424	2,721	55,832
H1	205,492	260,077	2,878	54,585
H2	208,766	260,969	2,814	52,203
H3	209,688	261,489	2,901	51,801

END OF 4TH CYCLE (24 HRS IN ROOM C TO MEASURE LEAK)

NAME OF SPECIMEN	Cup With Water(or empty)	Cup + Leftover Top	Saturated Casing	Weight of Leaked Water	Weight of Leftover Water Top
TYRE-T-LOW	5,200	5,200	261,913	2,359	0,000
TYRE-T-HIGH	2,699	2,699	260,696	0,000	0,000
TYRE-U-LOW	2,679	2,679	267,174	0,000	0,000
TYRE-U-HIGH	2,855	2,855	264,104	0,000	0,000
GS-T-LOW	2,930	2,930	263,716	0,000	0,000
GS-T-HIGH	3,996	3,996	273,980	1,129	0,000
GS-U-LOW	3,060	3,060	262,887	0,000	0,000
GS-U-HIGH	2,966	2,966	262,870	0,000	0,000
RS-T-LOW	2,994	2,994	262,534	0,000	0,000
RS-T-HIGH	2,894	13,488	247,821	0,000	10,594
RS-U-LOW	9,665	9,665	255,438	6,784	0,000
RS-U-HIGH	3,885	10,688	255,630	0,992	6,803
REF	4,351	33,685	226,013	1,630	29,334
H1	3,433	31,481	228,836	0,555	28,048
H2	6,680	28,339	233,057	3,866	21,659
H3	4,242	27,824	233,828	1,341	23,582

Appendix B: Photographs of all plugs from all test matrices

Plugs from TM#1

Plugs from TM#2

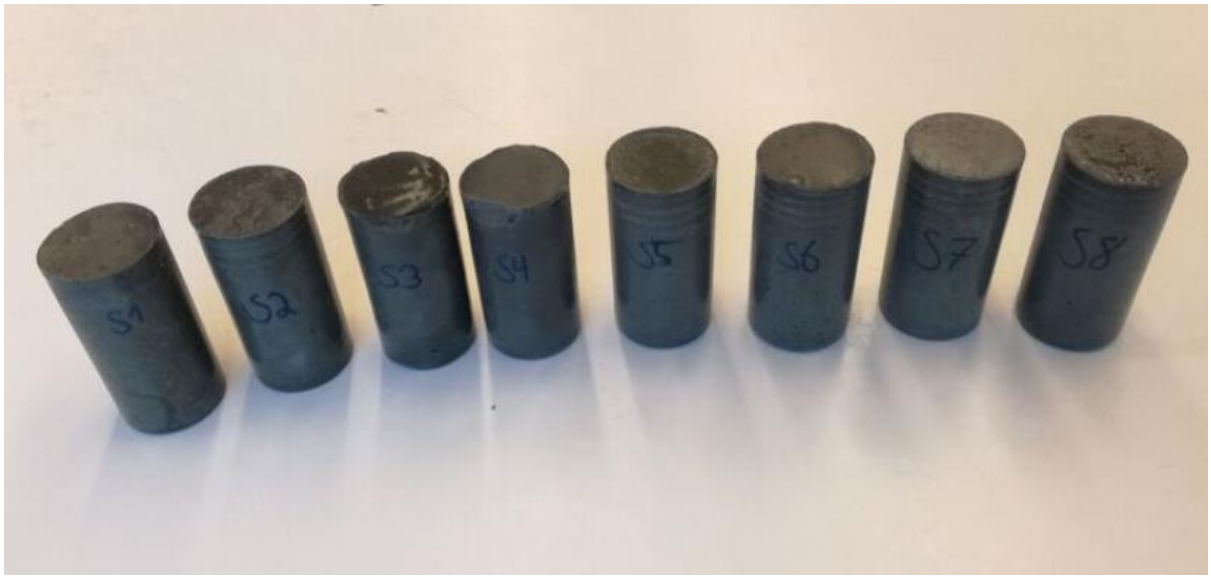

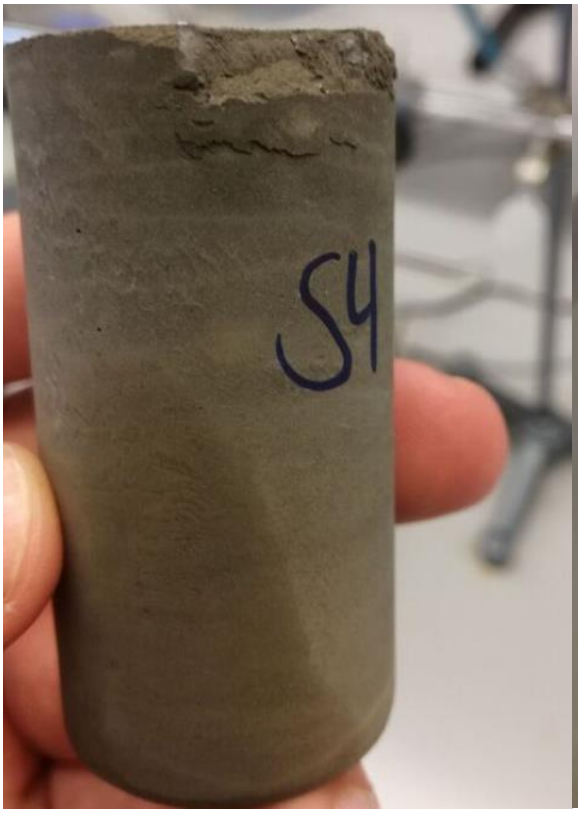

Plugs from TM#3 (plugs from de-ionized water ***not*** included in results)

Plugs from TM#4, TM#5 and TM#6

Plugs from TM#8 and TM#9

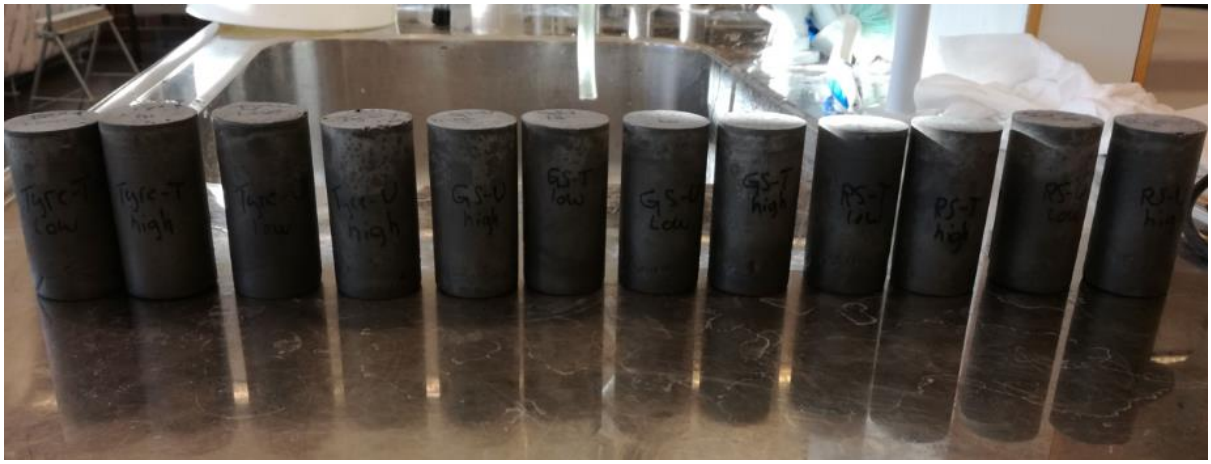

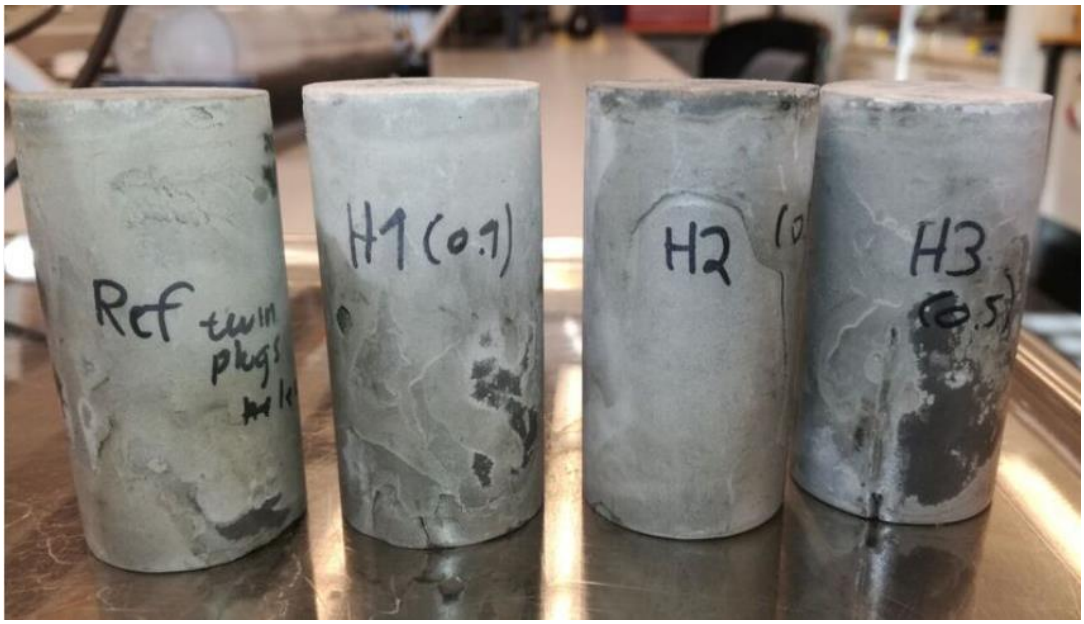

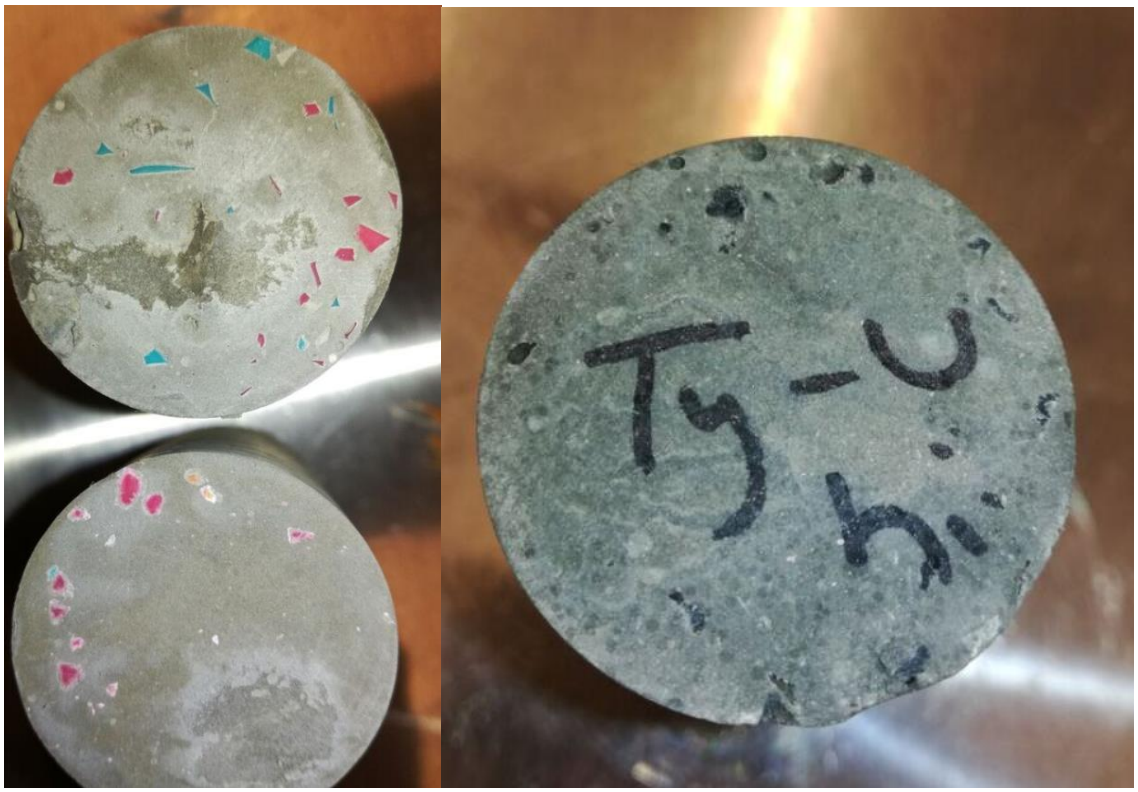

Dispersion of Rubber elements within cement structure

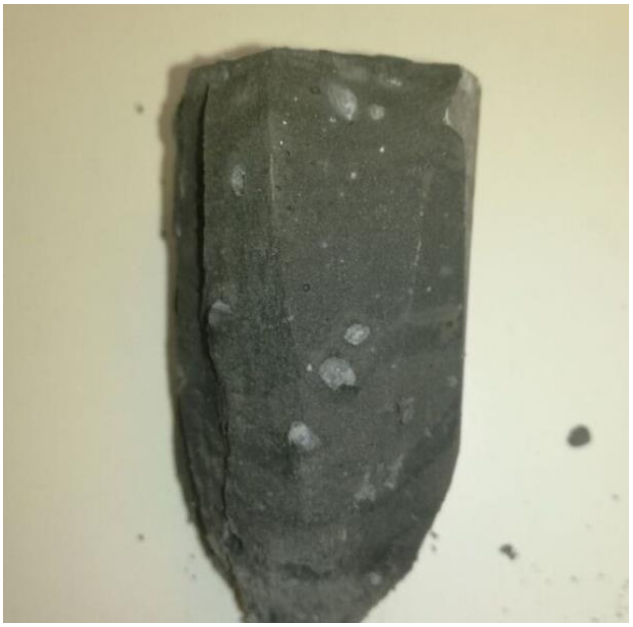

Appendix C: Force-deformation Diagrams

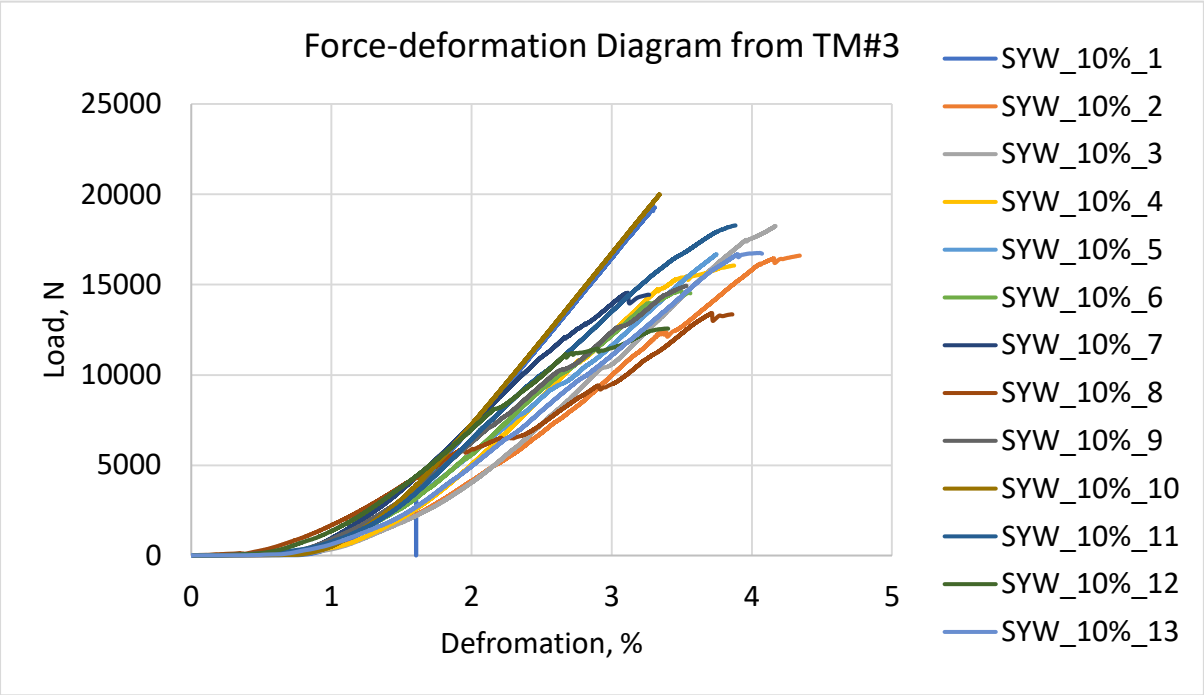

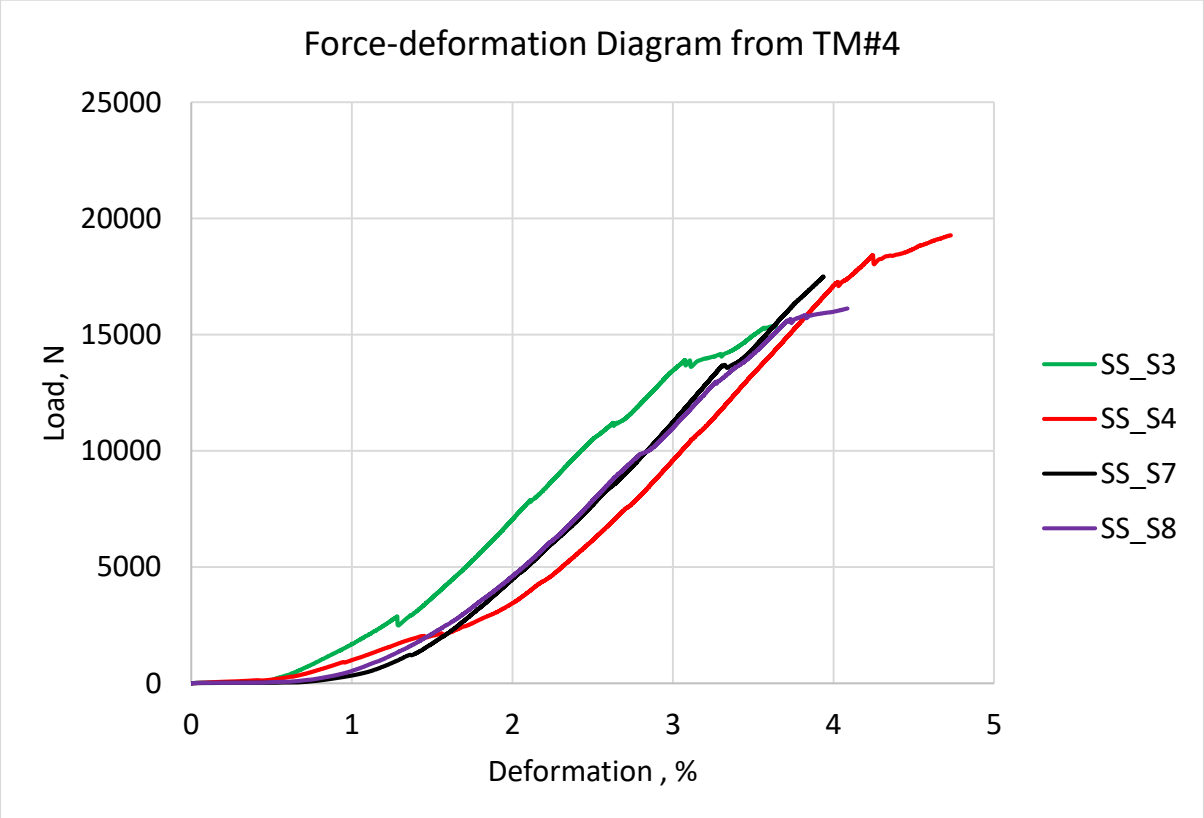

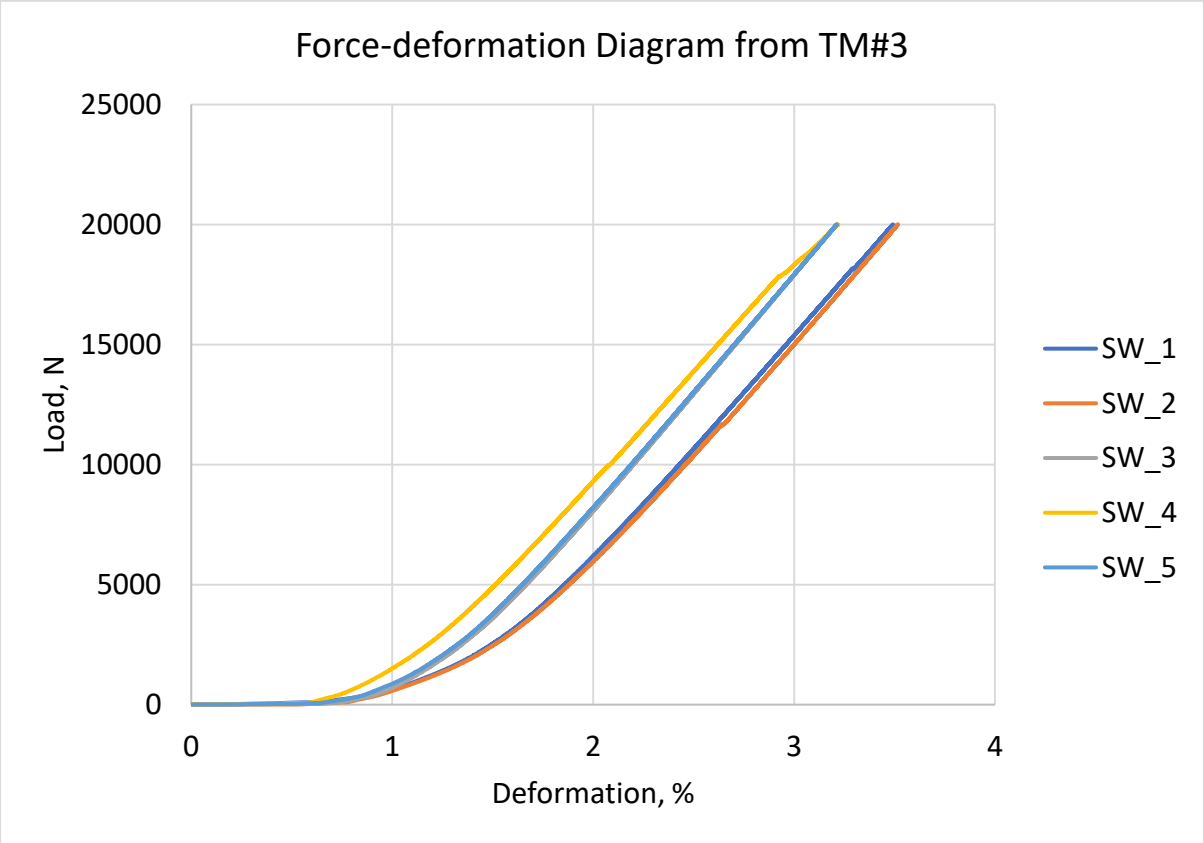
Force-deformation Diagram from TM#3
Load, N
25000
20000
15000
10000
5000
0
0
1
2
3
4
Deformation, %
SW_1
SW_2
SW_3
SW_4
SW_5

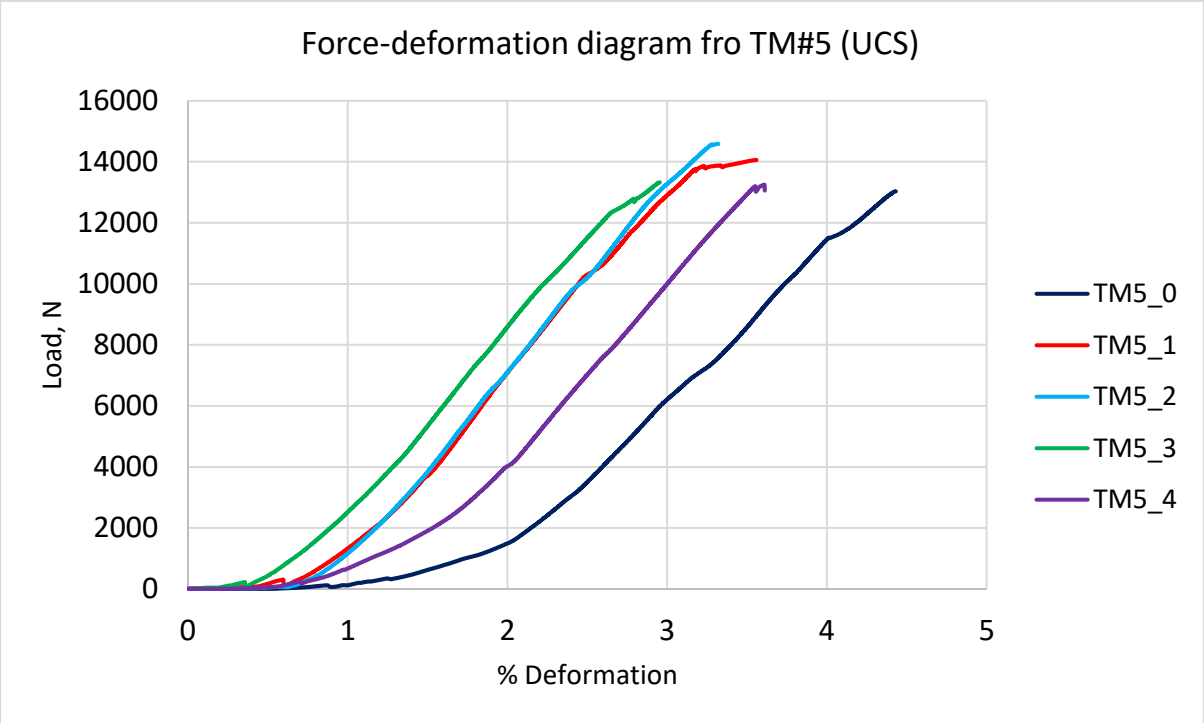
Force-deformation diagram fro TM#5 (UCS)
Load, N
16000
14000
12000
10000
8000
6000
4000
2000
0
0
1
2
3
4
5
% Deformation
TM5_0
TM5_1
TM5_2
TM5_3
TM5_4

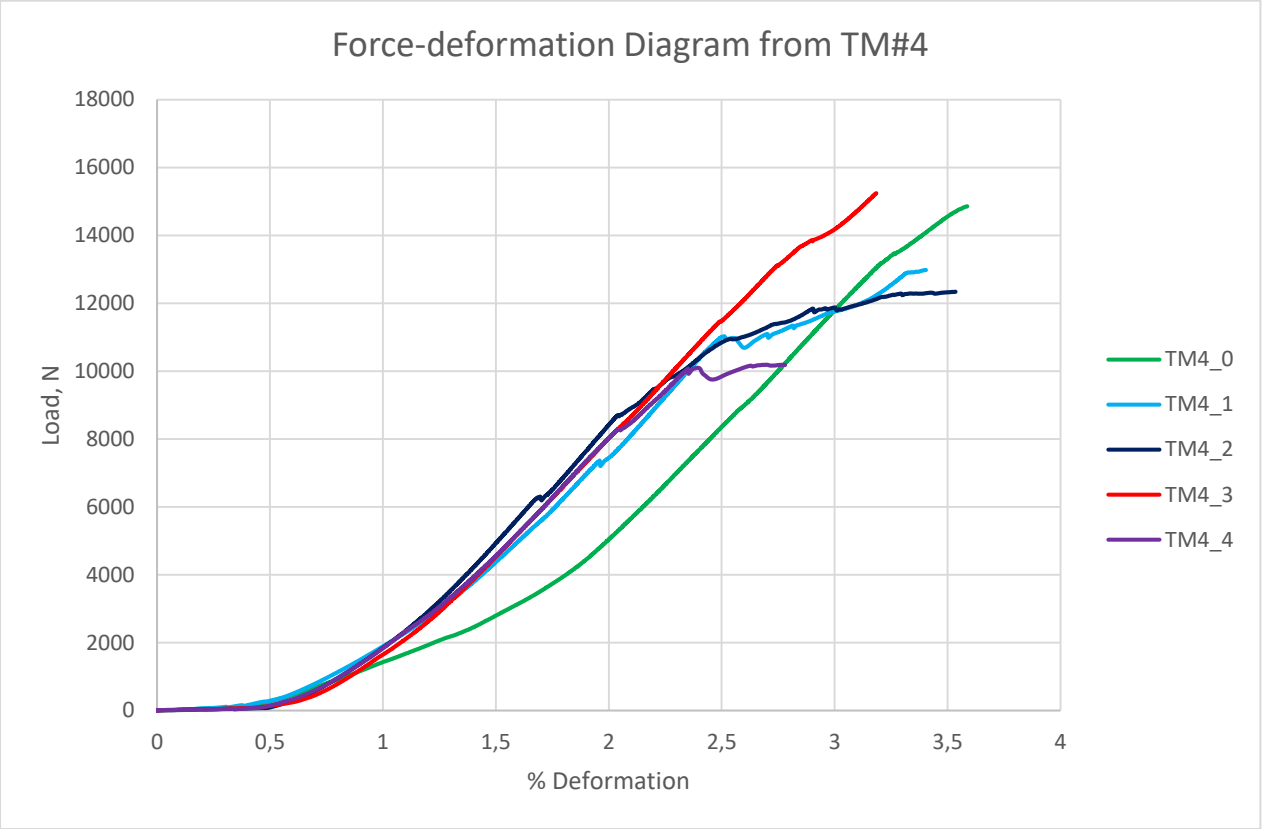
Force-deformation Diagram from TM#4
Load, N
18000
16000
14000
12000
10000
8000
6000
4000
2000
0
0
0,5
1
1,5
2
2,5
3
3,5
4
% Deformation
TM4_0
TM4_1
TM4_2
TM4_3
TM4_4

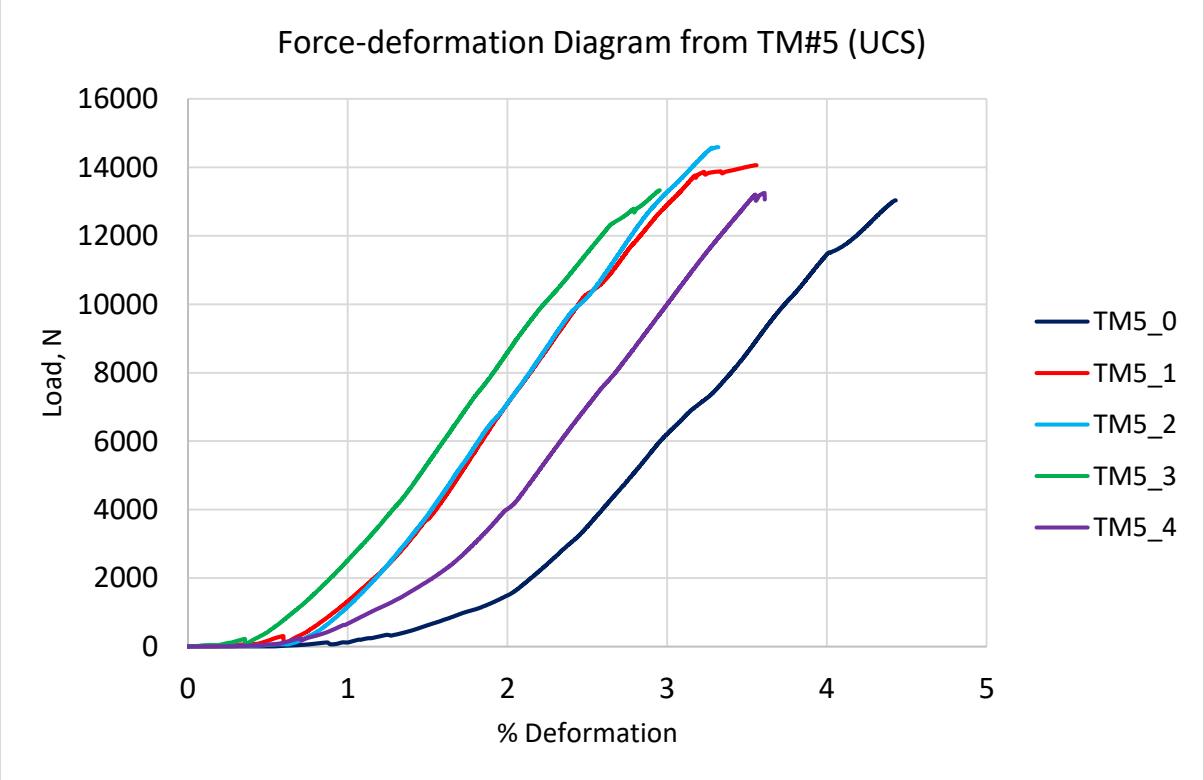
Force-deformation Diagram from TM#5 (UCS)
Load, N
16000
14000
12000
10000
8000
6000
4000
2000
0
0
1
2
3
4
5
% Deformation
TM5_0
TM5_1
TM5_2
TM5_3
TM5_4

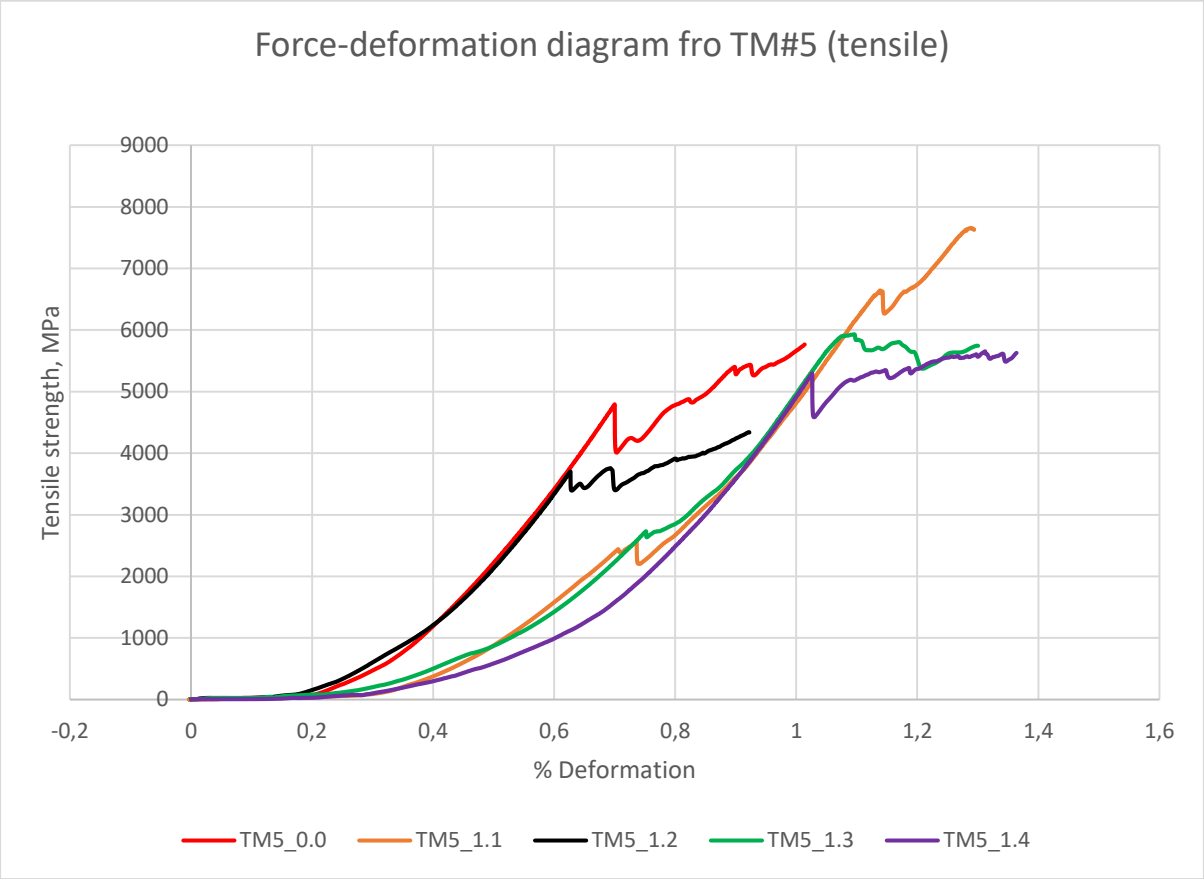
Force-deformation diagram fro TM#5 (tensile)
Tensile strength, MPa
9000
8000
7000
6000
5000
4000
3000
2000
1000
0
-0,2
0
0,2
0,4
0,6
0,8
1
1,2
1,4
1,6
% Deformation
TM5_0.0
TM5_1.1
TM5_1.2
TM5_1.3
TM5_1.4

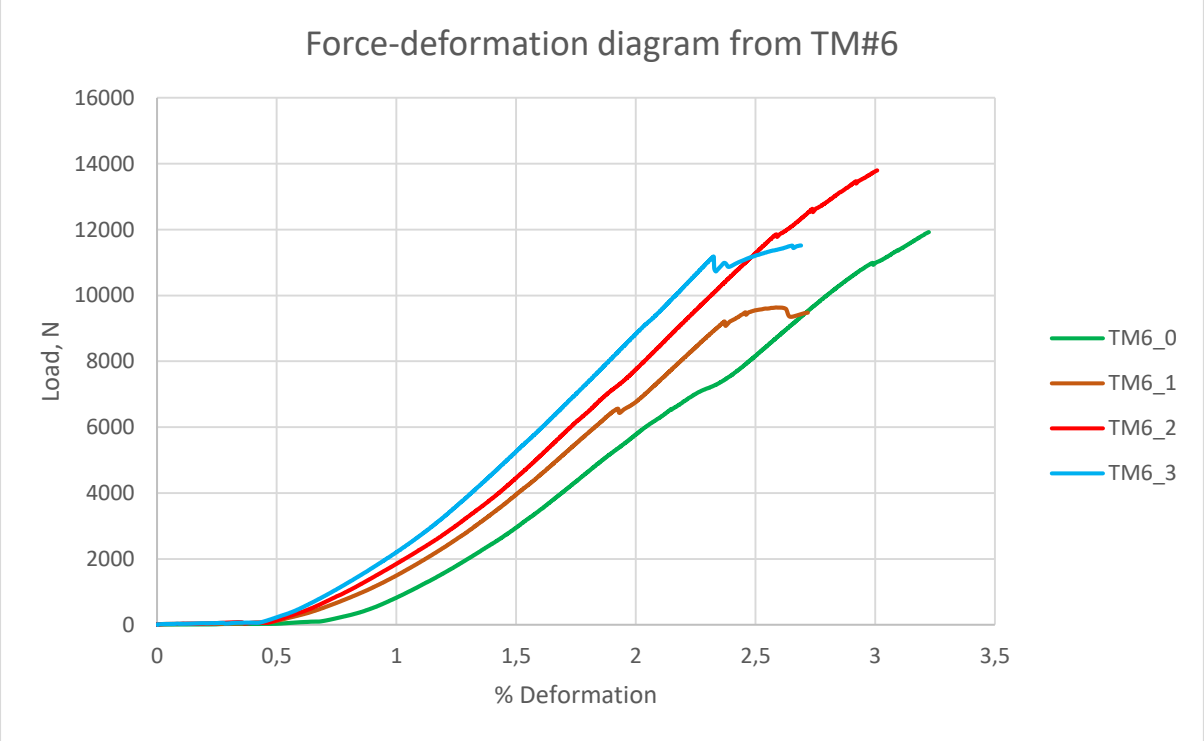
Force-deformation diagram from TM#6
Load, N
16000
14000
12000
10000
8000
6000
4000
2000
0
0
0,5
1
1,5
2
2,5
3
3,5
% Deformation
TM6_0
TM6_1
TM6_2
TM6_3

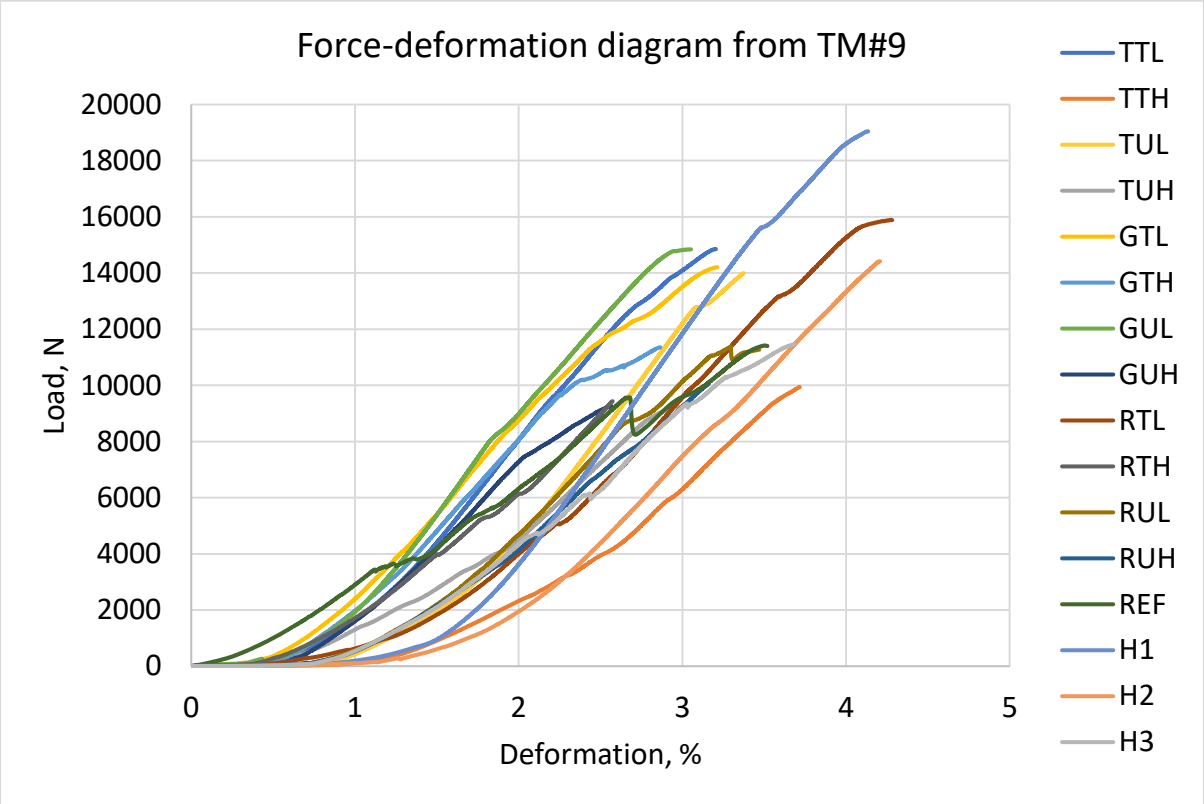
Force-deformation diagram from TM#9
Load, N
20000
18000
16000
14000
12000
10000
8000
6000
4000
2000
0
0
1
2
3
4
5
Deformation, %
TTL
TTH
TUL
TUH
GTL
GTH
GUL
GUH
RTL
RTH
RUL
RUH
REF
H1
H2
H3

Appendix D: Auxiliary Experimental Photos